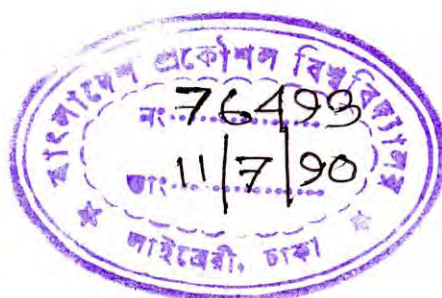


NON LINEAR ANALYSIS AND DESIGN OF GEOTEXTILE REINFORCED  
UNPAVED ROADS

Thesis  
by

GOUR PADO SAHA



Submitted to the Department of Civil Engineering, Bangladesh  
University of Engineering and Technology, Dhaka in partial  
fulfilment of the requirements for the degree

of

MASTER OF SCIENCE IN CIVIL ENGINEERING

April, 1989



BANGLADESH UNIVERSITY OF ENGINEERING AND TECHNOLOGY, DHAKA.

NON LINEAR ANALYSIS AND DESIGN OF GEOTEXTILE REINFORCED  
UNPAVED ROADS


Thesis  
by

GOUR PADO SAHA




Approved as to style and content by:


Chairman of the  
Committee

  
Dr. M. HUMAYUN KABIR  
Professor,  
Dept. of Civil Engineering

Member

  
Dr. M. ALEE MURTUZA  
Professor and Head,  
Dept. of Civil Engineering


Member

  
Mr. A.F.M. ABDUR RAUF  
Associate Professor,  
Dept. of Civil Engineering

Member

  
Dr. M. ZAKARIA  
Associate Professor,  
Dept. of Civil Engineering

Member  
(External)

  
Dr. M.H. KHAN  
Chairman,  
NODAK International Ltd.  
House No. 14, Road No.7  
Dhanmondi R/A, Dhaka 1205.

April, 1989

## ABSTRACT

A new non linear approach to analysis and design of unreinforced and reinforced unpaved roads on clay subgrade is developed. These are based on the non linear stress strain behaviour generally exhibited by the clay subgrade soils as well as geosynthetic and natural fibre reinforcing elements.

The newly developed design method is based on closed form solution of the plane strain analysis of the deformation track produced under wheel loading, which consider the compatibility of deformation (rutting) between the constituent materials, clay subgrade and reinforcing element.

Appropriate constitutive laws, for monotonic and repeated loading conditions, for the subgrade clay and reinforcing elements are developed and used to predict the behaviour under quasi-static and traffic loading conditions. The equivalent material approach is used to simulate the weakening of the system under traffic loading condition. Special test setup are fabricated and installed to establish these constitutive relations.

The settlement behaviour of clay subgrade is analysed using the fundamental approach suggested by Prakash, Sharan and Saran (1984), using non linear constitutive relation. The out of the plane load deformation behaviour of reinforcing elements are determined by assuming the deformation track to be of parabolic shape.

Design charts are produced to show the applicability of the new methodology for a silty clay subgrade and a woven tape polyethylene geotextile reinforcing element. A comparison of the proposed method with the conventional Giroud and Noiray (1981) method is also produced which show the latter method to yield unsafe results specially under low deformation (rutting) conditions.

As part of the research a number of computer program are developed in FORTRAN.



## ACKNOWLEDGMENTS

The author expresses his heartiest gratitude and sincerest indebtedness to his supervisor Dr. Muhammed Humayun Kabir Professor, Department of Civil Engineering for his constant encouragement, expert guidance and valuable suggestions at all stages of this research work.

The author tenders his best regards and profound gratitude to Dr. M. Alee Murtuza, Professor and Head, Department of Civil Engineering for his keen interest and granting permission to use soil mechanics laboratory facility.

The author is highly obliged to Dr. Mizanul Huq, Honorary General Secretary, Institution of Engineers, Bangladesh for granting permission to use Micro Computer for typing this thesis.

Thanks and appreciation are due to Mr. A.S.M. Nuruzzaman, M. Alamgir and Monoj Kanti Das for their inspiration and cooperation in the preparation of this thesis.

Finally, the author tenders his thankfulness to Mr. Habibur Rahman and Mr. Alimuddin for their help in various stages of laboratory investigation.

## CONTENTS

Subject	Page No.
ABSTRACT	(iii)
ACKNOWLEDGMENTS	(v)
LIST OF TABLES	(ix)
LIST OF PLATES	(ix)
LIST OF FIGURES	(x)
NOTATIONS	(xiii)
CHAPTER ONE	INTRODUCTION
1.1	General 2
1.2	Historical Development 4
1.3	Existing Design Methods 5
1.4	Statement of the Problem 6
1.5	Objective of Research 7
CHAPTER TWO	LITERATURE REVIEW
2.1	General 10
2.2	Axle Load and Contact Area 11
2.3	Mode of Failure 15
2.4	Concept of Compatibility 15
2.5	Beneficial Mechanisms Resulting from use of Reinforcement 16
2.5.1	Restraint Effect 16
2.5.2	Membrane Effect 17
2.5.3	Friction and Boundary Layer Effect 17
2.6	Design for Thicknesses of Aggregate and Reinforcement 19
2.6.1	Design Method Proposed by Giroud and Noiray (1981) 20
2.6.2	Design Method Proposed by Van den Berg and Kenter (1984) 36
2.7	Material Characterisation 43
2.7.1	Aggregate - Base Layer 43

2.7.2	Subgrade Soil - Clay	43
2.7.3	Reinforcement	53
2.8	Case Studies	60
2.8.1	Stanely Airfield, Falkland Island, U.K.	60
2.8.2	Lune Estuary, U.K.	61
2.8.3	Milngaive, U.K.	61
2.8.4	Kilanda, Sweden	61
2.9	Concluding Remarks	61
2.9.1	Material Behaviour	62
2.9.2	Design Method	63
CHAPTER THREE	PROPOSED DESIGN METHOD	
3.1	General	65
3.2	Design Consideration	66
3.3	Geometry of Unpaved Road	68
3.4	Loading Condition	68
3.5	Properties of Aggregates	68
3.6	Properties of Subgrade Soil	70
3.6.1	Constitutive Relation	70
3.6.2	Mathematical Formulation	71
3.7	Properties of Reinforcing Elements	74
3.7.1	Constitutive Relation	75
3.7.2	Mathematical Formulation	78
3.8	Analysis of Behavior of Road Structure	83
3.8.1	Load Distribution Through Aggregate Layer	83
3.8.2	Behaviour of Clay Subgrade	84
3.8.3	Geometry of Deformation	87
3.8.4	Unpaved Road without Reinforcement	88
3.8.5	Unpaved Road with Reinforcement	89
CHAPTER FOUR	CHARACTERISATION OF DESIGN PARAMETERS	
4.1	General	95
4.2	Clay Soils	95
4.2.1	Test Setup for Repeated Loading Triaxial Test of Clay Soils	95



	4.2.2	Test Procedure	96
	4.2.3	Test Results	97
4.3		Reinforcing Materials	100
	4.3.1	Repeated Loading Test Rig for Reinforcing Materials	100
	4.3.2	Preparation of Samples	100
	4.3.3	Test Procedure	104
	4.3.4	Test Results	106
4.4		Characterisation of Design Parameters	107
CHAPTER FIVE	DESIGN CHARTS		
	5.1	General	124
	5.2	Design Charts	124
	5.3	Design Example	127
	5.4	Load Sharing of Constituent Materials	127
CHAPTER SIX	DISCUSSION AND CONCLUSION		
	6.1	General	136
	6.2	Materials Behaviour	136
	6.3	Design Method	137
	6.4	Comparison	140
	6.5	Conclusions	142
	6.5.1	Existing Design Method	142
	6.5.2	Proposed Design Method	144
	6.5.3	Overall	144
		RECOMMENDATION FOR FUTURE RESEARCH	146
		REFERENCES	149
	APPENDIX - I	Test Results of Clay Soil	156
	APPENDIX - II	Test Results of Polyethylene Geotextile	160
	APPENDIX - III	Flow Chart of Computer Program	167



## LIST OF TABLES

Table	Description	Page No.
CHAPTER TWO		
2.1	Stresses Beneath a Uniformly Loaded Strip (after Jergenson, 1934)	51
CHAPTER FOUR		
4.1	Properties of Clay Soils	101
4.2	Properties of Reinforcing Materials	110
CHAPTER FIVE		
5.1	Design Parameters	125
5.2	Wheel Loading Parameters	126
CHAPTER SIX		
6.1	Refinements of Proposed Design Method over Giroud and Noiray (1981) Method	143

## LIST OF PLATE

CHAPTER FOUR		
4.1	Photograph of Repeated Loading Test Rig	103

## LIST OF FIGURES

Figure	Description	Page No.
<b>CHAPTER TWO</b>		
2.1	Wheel Contact Area	13
2.2	Geometrical Description of Wheel Contact Area	13
2.3	Beneficial Mechanism	18
2.4	Test Results from Lai and Robnett (1980)	18
2.5	Pyramidal Load Distribution	22
2.6	Load Distribution Factor vs. Number of Load Repetitions (after Giroud et. al, 1984)	22
2.7	Design Charts for Unreinforced Road(Quasi Static, after Giroud and Noiray, 1981)	24
2.8	Design Charts for Unreinforced Road(Traffic Loading, after Giroud and Noiray, 1981)	27
2.9	Deformation in Reinforcement	29
2.10	Relation Between Settlement and Rutting	31
2.11	Design Chart for Reinforced Road (Quasi Static, Giroud and Noiray, 1981)	34
2.12	Practical Design Chart(after Giroud and Noiray, 1981)	35
2.13	Free Body of a Road Section	38
2.14	Bi-Linear Soil Model	38
2.15	Location of Plastic Failure	41
2.16	Design Chart for Selection of Aggregate (after Celenese Fibre Marketing Company)	44
2.17	Hyperbolic Stress Strain Model	48
2.18	Effect of Rate of Loading on Strength of Soils (after Bjerrum et. al. 1958)	54
2.19	Repeated Loading Stress Strain Model (after Idriss et. al, 1978)	54
2.20	Mechanical Behaviour of Geosynthetic	56
2.21	Mechanical Behaviour of Geotextile GX5	57
2.22	Mechanical Behavior of Geotextile GX6	58

2.23	Effect of Confining Pressure on Hyperbolic Parameters	59
CHAPTER THREE		
3.1	Geometry of Unpaved Road	69
3.2	Definition of Single Wheel Geometry and Contact Areas	69
3.3	Qualitative Diagram of Constitutive Relation for Clay	72
3.4	Qualitative Diagram of Constitutive Relation for Reinforcing Material Type 1	77
3.5	Qualitative Diagram of Constitutive Relation for Reinforcing Material Type 2	79
3.6	Qualitative $p_o - \delta$ Formulation for Clay Subgrade	86
3.7	Deformed Shape of Reinforcement and Equilibrium	90
CHAPTER FOUR		
4.1	Repeated Loading Triaxial Test Apparatus	98
4.2	Graphical Representation of Repeated Loading Test Results of Clay Soil	99
4.3	Repeated Loading Test Rig	102
4.4	Schematic Diagram of Sample Preparation	105
4.5	Graphical Representation of Test Results of Polyethylene	108
4.6	Graphical Representation of Test Results of CANVAS (after Kabir et.al. 1988)	109
4.7	Constitutive Relation for Clay Soil	111
4.8	Constitutive Relation of Polyethylene Geotextile	114
4.9	Mechanical Behaviour of Clay Soil	117
4.10	Mechanical Behaviour of Polyethylene Geotextile	118
4.11	Mechanical Behaviour of Jute Fabric CANVAS (after Kabir et. al. 1988)	119
4.12	Mechanical Behaviour of Jute Fabric CBC (after Kabir et. al. 1988)	120
4.13	$P_o - \delta$ Plot of Clay Soil	121

## CHAPTER FIVE

5.1	Design Chart for Unreinforced Unpaved Road	128
5.2	Design Chart for Reinforced Road with Polyethylene Geotextile	129
5.3	Design Chart for Reinforced Unpaved Road with CANVAS (after Kabir et.al. 1988)	130
5.4	Design Chart for Reinforced Unpaved Road with CBC (after Kabir et.al, 1988)	131
5.5	Load Sharing by Clay Subgrade and Polyethylene Geotextile	133
5.6	Load Sharing by Clay Subgrade and Reinforcement Jute Fabric CBC(after Kabir et.al., 1988)	134

## CHAPTER SIX

6.1	Design by Proposed Method and Giroud and Noiray Method (1981)	138
6.2	Resistance Offered by Clay Subgrade	139
6.3	Resistance Offered by Reinforcement	139



## NOTATIONS

A	Track width
A', A''	Displaced soil areas
A	Contact area
B	Dimension of contact area along traffic direction
B'	Width of individual Tire
D	Stress strain characteristics parameter
E	Stress strain characteristics parameter
E <sub>u</sub>	Undrained modulus of elasticity of soil
F	Stress strain characteristics parameter
K	Modulus of stiffness of reinforcement at 2% of strain
K'	Constant parameter
L	Dimension of contact area perpendicular to traffic direction
N	Number of passages of vehicles
N <sub>c</sub>	Bearing capacity factor
N <sub>i</sub>	Number of passages of axle load other than 80 kN
N <sub>s</sub>	Number of passages of standard axle
P	Axle load
P <sub>e</sub>	Equivalent axle load
P <sub>i</sub>	Axle load other than 80 kN
R	Constant parameter
S <sub>u</sub>	Undrained shear strength of soil
Y	Location parameter of plastic zone of soil
a	Half length of loaded area for reinforced condition
a <sub>o</sub>	Half length of loaded area for unreinforced condition
b	Road width
b', b''	Half chord length
b <sub>f</sub>	Width of plastic zone
c <sub>u</sub>	Undrained shear strength of clay
c <sub>uN</sub>	Undrained shear strength of clay at N load repetitions
e	Distance between two wheels
h	Aggregate thickness for reinforced road
h <sub>o</sub>	Aggregate thickness for unreinforced road

$h'_o$	Aggregate thickness for unreinforced condition under traffic loading condition
$k$	Modulus of subgrade reaction
$n$	Number of tire
$p$	Stress at the base of aggregate for reinforced condition
$p_{ec}$	Equivalent tire pressure
$p_c$	Tire inflation pressure
$p_o$	Stress at the base of aggregate layer for unreinforced condition
$p_r$	Load shared by the reinforcement
$p_s$	Load shared by the soil
$r$	rutting
$r_e$	Radius of contact area
$t$	Tensile force in reinforcement
$t_o$	Horizontal component of tensile stress in reinforcement
$t_{max}$	Maximum tensile force in reinforcement
$x$	Horizontal distance to the centre of the vehicle
$z$	Load distribution factor
$\Delta z$	Element thickness of soil layer
$\alpha_o \alpha$	Load distribution factor
$\beta$	Inclination of deformed reinforcement with vertical
$\gamma$	Unit weight of soil, aggregate
$\epsilon$	Axial strain in soil
$\epsilon$	Axial strain in reinforcement
$\sigma$	Total axial stress in soil
$\bar{\sigma}$	Effective axial stress in soil

CHAPTER ONE





in rural areas, the role of rural unpaved road is of vital importance as a part of the overall transportation infrastructure. Also the forest areas in the North-East, South-East and South-West parts of the country lacks in sound road networks. Sound unpaved road network for low volume traffic in these areas are of paramount importance for boosting the agro-based and forest-based economy of this country. Traditionally unpaved and in most of the cases unsurfaced earth roads are used in the rural and forest areas. Moreover, this country is in the development stage of its infrastructure and therefore unpaved access roads are being used now and more will be used in near future. Unpaved roads may also play a vital role in emergency use after disasters like flood, cyclone etc., which are very prevalent in this country. It can be stated without reservation that as the price of paved constructions are going up all the time, unpaved roads of low cost and durable construction have a bright prospect in this country. If this new geoinclusion technology is judiciously used in unpaved road constructions it can revolutionise the concept of road networking in this country. Ofcourse as part of such a venture, the prospect of, using local natural materials like jute, bamboo etc., as well as production of geosynthetics materials locally, should be explored.

In a reinforced unpaved road structure geoinclusion layer is laid between the subgrade soil and the overlaying aggregate layer. The primary functions of the geoinclusion layer here are, Separation and Reinforcement. The secondary functions being

filtration and drainage to transport porewater and thereby relieving porewater pressure generating in the subgrade soil under wheel loading. A detailed description of the function of geoinclusions in different applications have been presented by Kabir (1984).

Although the art of construction of both reinforced and unreinforced unpaved roads are known to mankind from the earliest of times, the development of scientific design methods considering material behaviour and appropriate design parameters is very recent. However, almost all of the existing design methods are based on oversimplified and in some cases inaccurate assumptions. The traditional design methods are based on limit equilibrium theories and linear material behaviour. These do not take into account the nonlinear mechanical behaviour and compatibility of deformation amongst the constituting materials which dictate the degrees of mobilisation of resistances in these materials due to loading. Therefore, these methods may lead to erroneous designs especially for such complex systems as reinforced unpaved roads.

## 1.2 HISTORICAL DEVELOPMENT

The art of construction of reinforced unpaved roads, in some form or other, were known to man from very early times. The ancient Romans used woven reed mats to construct a road over soft ground. Like our present day technology, they used to lay down the mats over marshy ground and used stone aggregates on top of



this. Even before 2500 B.C., in the United Kingdom pathways were constructed over logs, as reported by Archaeological Department, (Rankilor, 1981). Brushwood mattresses made of birch and bundles of hazel branches was used from Polden Hills to the Mendips in Southern England. Several kilometers of track were built to testify the success of the technique. In some Southeast Asian countries like China, Indonesia and India roads on soft grounds were traditionally constructed using facines. The British used bitumen treated jute as a reinforcing element in unpaved road during the World War II as reported by Slim (1955). He reported satisfactory functioning of these roads even under high volume traffic and monsoon conditions.

### 1.3 EXISTING DESIGN METHOD

Traditionally (Terzaghi, 1943), stability analyses were performed using limit equilibrium theories. The design methods of reinforced unpaved roads proposed by Giroud and Noiray (1981), Sellmeijer et. al. (1983), Van den Berg and Kenter (1984) are basically based on the limit equilibrium theory.

Giroud and Noiray's design method is based on conventional limit state theory. They have presented two separate analyses, one is quasi static analysis for light traffic and the other is for heavy traffic. In case of unreinforced unpaved road they assumed the resistance offered by the subgrade soil equal to  $\pi c_u$  and for reinforced condition total stress (load) is shared by the subgrade soil  $((\pi + 2)c_u)$  and resistance developed in the

reinforcing element depending on the degrees of deformation (rutting). For traffic condition, they suggested to calculate the required aggregate thicknesses from an empirical equation, established from extensive full scale field tests data. Sellmeijer et.al. and Van den Berg and Kenter's design methods are almost similar to that of Giroud and Noiray method, except that they considered, the membrane theory to calculate the resistances developed in the reinforcement and bilinear soil model.

The limit equilibrium theory is not suitable especially in case of reinforced earth structures as they are composed of different constituent materials with different mechanical properties. In this type of design problem, the compatibility of deformation and respective mobilisation of resistances under external loading are the most vital considerations.

#### 1.4 STATEMENT OF THE PROBLEM

Almost all types of soft clay soils and reinforcing elements (geotextile, geogrid, jute fabrics etc.) show non linear load deformation behaviour under wide ranges of deformation conditions. Moreover, the reinforced road structure is a composite one, incorporating clay subgrade and reinforcement, having different load deformation behaviour and hence load transfer mechanisms, are involved here in sharing the pressure transmitted from the wheels. Therefore, a sound design method should take due consideration of these into design. Thus a sound



design method should consider the amounts as well as the degrees of mobilisation of resistances in the materials under compatible deformation conditions. In light of these, the considerations on which a sound design method should be based, may be stated as the followings.

- (1) non linear behaviour of both the subgrade soil and reinforcing materials under repeated loading conditions.
- (2) compatibility of rutting between subgrade soil and reinforcing elements under all serviceability conditions, thus establishing realistic mobilisation of respective resistances.

#### 1.5 OBJECTIVE OF RESEARCH

The research work reported here was undertaken to establish a sound design method, for reinforced unpaved roads on clay subgrades, which is based on realistic nonlinear behaviour as well as mobilisation of resistances under compatible deformation (rutting) conditions. For proper justification, development and portrayal of such a design method the objective of this work may be stated as the followings.

- (1) Review of literature to find inadequacies of existing design methods.
- (2) Set guide lines for an adequate and realistic design method and establish relevant design considerations.
- (3) Development of realistic constitutive relations, selection of design parameters and development of relevant test methods.
- (4) Development of design equations based on realistic material

behaviour and deformation compatibility.

(5) Design charts for portrayal of practical significance of the research work.

GOUR (PADA) SAHA.

Non linear anly. & desi. of geot 625.7

1989 1 76493

CHAPTER TWO

## CHAPTER TWO

### LITERATURE REVIEW

#### 2.1 GENERAL

Unpaved roads are in use from the earliest of civilisation. Although these types of road are mainly used as temporary access roads, these also find application in permanent type of constructions. Reinforced unpaved roads are particularly suitable in combating emergencies like military application. These are also cost effective compared with its plain counterpart. Synthetics and natural products like jute fabrics may be used as reinforcing elements.

A review of literature revealed that significant works have been done in the development of design methods. Nieuwenhuis (1977), Bakker (1977), Giroud and Noiray (1981), Perrier (1983), Sellmeijer et. al (1983), and Van den Berg and Kenter (1984) developed design methods. All these methods are based on limit state theory and material (Clay subgrade and reinforcing element) properties are not properly characterised.

Several researchers have produced mathematical models for cyclic stress strain behaviour of clay soils. Among them Idriss et. al (1978) and Yamanouchi and Yashuhara (1977) developed constitutive relations for stress strain and load repetitions behaviour. The non linear stress strain behaviour normally



exhibited by most of the clay soils and reinforcing materials has been modelled by hyperbolic constitutive laws (Kondner, 1963), parabolic functions (Berth et. al, 1973) and spline functions (Desai, 1971).

In this chapter an elaborate review on the existing design methods are produced to identify their limitations. Moreover, a review on an geometrical stress distribution and material characterisation aspects are also included.

## 2.2 Axle Load and Contact Area

The axle load of vehicles and their frequency of application is important factors in the design of unpaved road as well as paved road structures. According to AASHTO (American Association of State Highway and Transportation Officials) road test data, magnitude is more important than frequency of loading (AASHTO, Road Test, 1962). The most commonly used standard axle load is 80 kN. It is assumed that the contact pressure between the tire and the surface of the road is equal to tire pressure. It is also assumed that contact pressure are uniform over the imprint areas. Assuming circular tire imprints the radius of contact area may be expressed as the following.

$$r_e = \sqrt{\frac{P}{\pi p_c}} \quad \dots 2.1$$

where,

$r_e$  = radius of contact area

$P$  = total load on the tire

$p_c$  = tire pressure

Tire imprint is approximated by an area comprising rectangular and semicircular areas as shown in Figure 2.1.

Giroud and Noiray (1981) made a detailed description on this aspect. They assumed the axle load  $P$  to be equally carried by the four wheels. According to this assumption  $P$  may be expressed as:

$$P = 4 A_c . p_c \quad \dots 2.2$$

where,

$P$  = axle load

$A_c$  = contact area

$p_c$  = tire pressure

They replaced the double contact area as shown in Figure 2.2 by a rectangle  $LxB$  and from field test data they proposed an empirical relation defining this area as:

$$LB = 2 A_c \sqrt{2} \quad \dots 2.3$$

They introduced a term "equivalent tire pressure"  $p_{ec}$  (assumed uniformly distributed) over a rectangular surface area of  $LxB$  on the surface of the aggregate layer. Therefore:

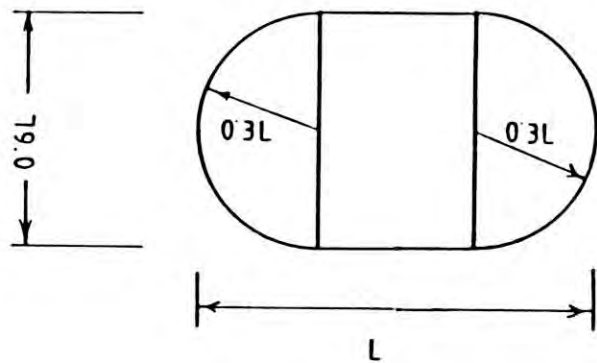
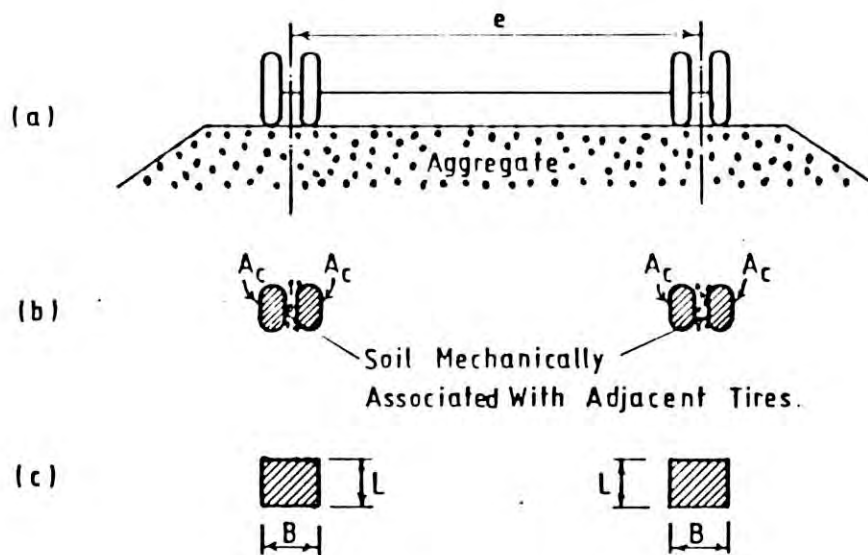


Figure 2.1 Wheel Contact Area



- a) Geometry of Vehicle Axle
- b) Tire Contact Areas
- c) Equivalent Contact Area

Figure 2.2 Geometrical Description of Wheel Contact Area

$$P = 2 L B p_{ec} \quad \dots 2.4$$

From Equations 2.2, 2.3 and 2.4 the equivalent contact pressure may be expressed as:

$$p_{ec} = \frac{P}{\sqrt{2} B} \quad \dots 2.5$$

From field test data they found that:

$$L = \frac{B}{\sqrt{2}} \quad \dots 2.6$$

for on highway trucks

$$L = \frac{B}{2} \quad \dots 2.7$$

for off highway trucks

Finally:

$$B = \sqrt{\frac{P}{p_{ec}}} \quad \dots 2.8$$

for on highway trucks

$$B = \sqrt{\frac{P \sqrt{2}}{p_{ec}}} \quad \dots 2.9$$

for off highway trucks



### 2.3 MODE OF FAILURE

Since the unpaved road is composed of three different types of materials, failure may occur in any one of the following modes:

- i) shear failure of base layer (aggregate)
- ii) shear failure of subgrade soil
- iii) excessive settlement of subgrade soil
- iv) tensile failure of reinforcing materials
- iv) slipping failure between reinforcing materials and the base and subgrade layer.

### 2.4 CONCEPT OF COMPATIBILITY

The last couple of decades have seen the advent and growth of geotextile and geogrids as new and economical construction materials. A number of design methods have been developed during this time but all are based on limit equilibrium method and simplified assumptions. In these methods of design, the importance of strain in materials is not properly incorporated. Roscoe (1970) first recognised the importance of strain in geotechnical designs. When a material possesses different stress strain behaviour then it is really impractical to design structure to carry load without considering strain. McGown et. al (1984) and Bonaparate et. al (1984) emphasised on the consideration of strain/deformation compatibility in the design of reinforced earth structures. Beech (1987) described the importance of stress strain relationship and the compatibility of strain/deformation in the design of reinforced soil system. In

this context he referred the design approach of deep foundation. In deep foundation, loads are carried by two independent load resisting mechanisms.

i) load taken by shearing resistance around the foundation.

ii) load taken by bearing resistance of the foundation.

Since soil shows two different stress strain behaviour for shearing and base resistance, limit equilibrium is not applicable as this method direct to superimpose of their ultimate values. Their ultimate resistances are mobilised at different strain/deformation conditions. Thus a sound design method should consider compatibility of strain/deformation and thereby mobilisation of resistances.

## 2.5 BENEFICIAL MECHANISMS RESULTING FROM USE OF REINFORCEMENT

Many researchers worked on mechanisms by which reinforcement inclusion in ARS (aggregate, reinforcement and soil) system reduces the rutting of roadway under repetitive vehicular loading. These mechanisms are described in the followings.

### 2.5.1 Restraint Effect

Two restraint effects are recognised on subgrade clay and/or aggregate due to the inclusion of reinforcement. The first is caused by the reinforcement induced normal stress developed in the reinforcement in the regions AB, CC' and B'A' (Figure 2.3). This downward normal stress is equivalent to an additional surcharge. This surcharge has the benefit of restricting the potential shear flow developed in the subgrade soil due to the



wheel loads. Laboratory results from Lai and Robnett (1981), support the concept of this mechanism. The second type is the confining effect. The upward normal stress around BC and B'C' regions in Figure 2.3 causes increase of confining stress in the aggregate. Similarly, the subgrade soil around AB, CC' and A'B' is also subjected to a higher confining stress. The effect of confining stress is described in the section on material characterisation.

#### 2.5.2 Membrane Effect

As the reinforcement in an ARS system undergoes large deformation under vehicular loading, as shown in Figure 2.3, the fabric is deformed and develops inplane tensile stress. The effect of this reinforcement induced normal stress will result in a reduction of the stress exerted on the subgrade soil between BC and B'C', the regions directly under the wheel loads. The net effect should be a reduction of the magnitude of rutting for a given number of repetitive loads. This phenomenon is termed as "membrane effect". Lai and Robnett confirmed the change of normal stress due to membrane effect and reduction in rate of rut formation with reinforcement inclusion by laboratory tests. Some experimental results are presented here directly from Lai and Robnett in Figure 2.4.

#### 2.5.3 Friction and Boundary Layer Effect

Friction developed along the interface between aggregate and reinforcement and friction/adhesion at the reinforcement subgrade

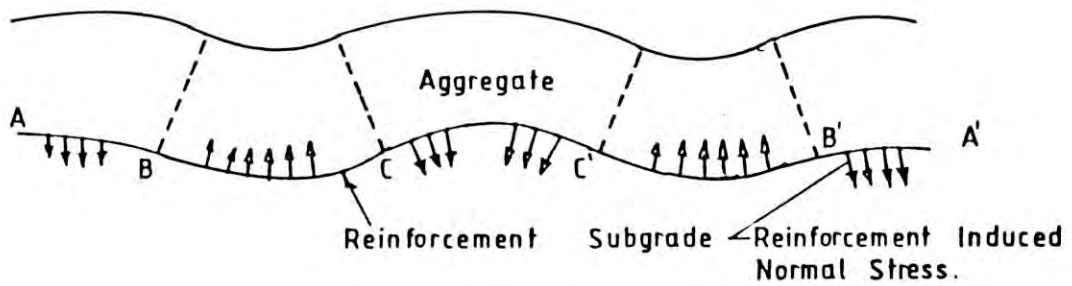


Figure 2.3 Beneficial Mechanism

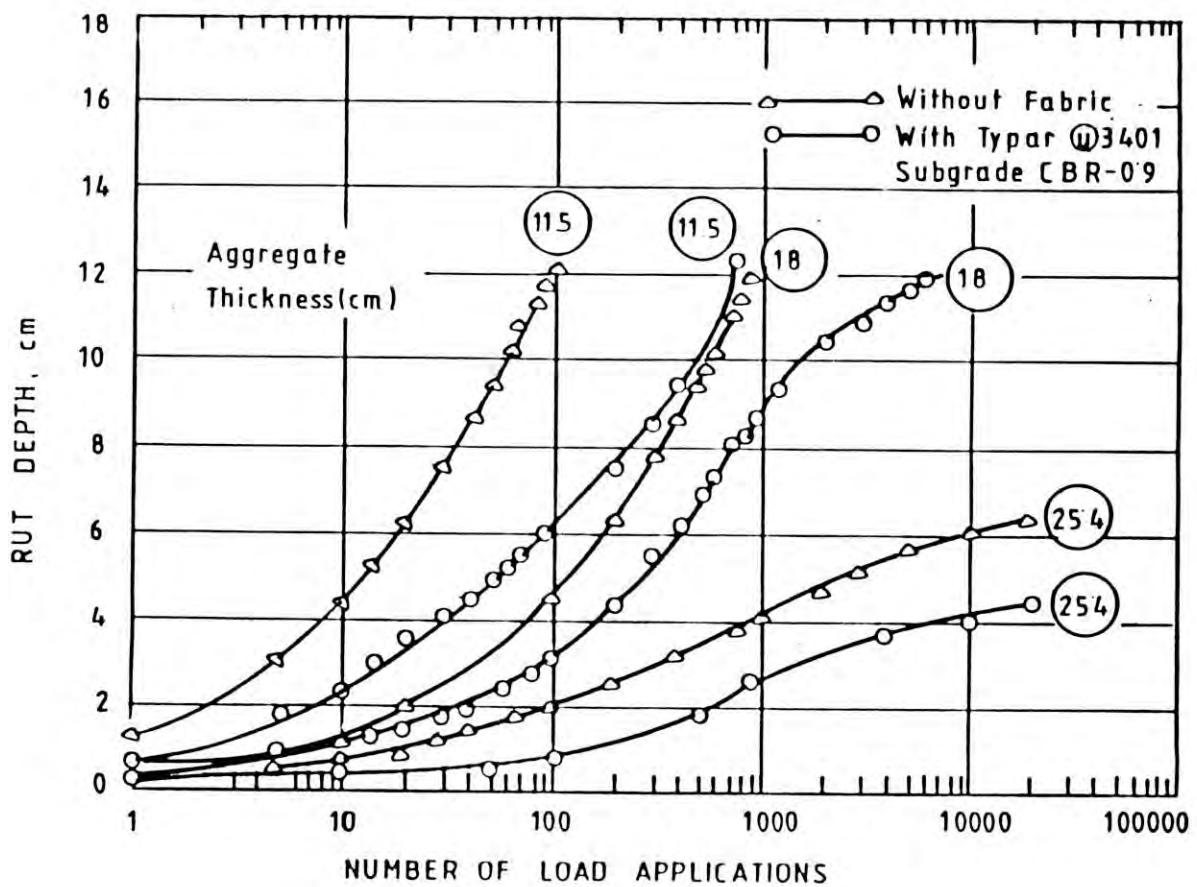


Figure 2.4 Test Result from Lai and Robnett (1980)



soil interface create a "boundary layer effect" whereby a layer of aggregate immediately above the reinforcement and a layer of the soil immediately beneath the reinforcement may act together with the reinforcement as a "composite material". This phenomenon was reported by Lai and Robnett as observed in the two dimensional model tests of the ARS system. They observed that soil and aggregate, within this region moved with the reinforcement in the same direction and any failure or cracks in the soil were observed to occur outside this zone. The composite behaviour as a result of the friction/adhesion and the "prestressing effect" from the reinforcement should possess more favourable properties such as more ductility and be less susceptible to the development of tension cracking.

## 2.6 DESIGN FOR THICKNESSES OF AGGREGATES AND REINFORCEMENT

Several researchers have proposed calculation methods for selection of reinforcement type and thicknesses of aggregates.

Nieuwenhuis (1977) is the first to quantify the reinforcement function. He considered the equilibrium of the reinforcement for several loadings, by taking modulus of subgrade reaction as soil design parameter. There are two drawbacks that encountered in Nieuwenhuis design. Firstly, as it is a large deformation problem the modulus of subgrade reaction is not a representative parameter. Secondly, he didn't consider the most conventional concept "ultimate bearing capacity". Bakker (1977) tried to overcome Nieuwenhuis's drawbacks. His design is based

on ultimate bearing capacity theory of soil. Ludwig(1978) presented similar calculation as Bakker in a different way. Giroud and Noiray (1981) presented an elaborate numerical treatment of the problem. Perrier (1983) consider the equilibrium of reinforcement but he didn't fulfill the equilibrium of the subsoil. Sellmeijer et.al (1983), Van den Berg and Kenter (1984) presented detail mathematical treatment considering membrane theory. Among all methods, Giroud and Noiray (1981) and Van den Berg and Kenter (1984) methods are discussed as these are the most elaborate.

#### 2.6.1 Design Method Proposed by Giroud and Noiray (1981)

The design methodology proposed by Giroud and Noiray is described in the followings.

##### Load Distribution System

Giroud and Noiray assumed a pyramidal load distribution pattern for cases without or with reinforcement as shown in Figure 2.5, from which the following equations could easily be established.

$$p_{ec} LB = (B + 2h_o \tan \alpha_o)(L + 2h_o \tan \alpha_o)(p_o - \gamma h_o) \quad \dots 2.10$$

without reinforcement

$$p_{ec} LB = (B + 2h \tan \alpha)(L + 2h \tan \alpha)(p - \gamma h) \quad \dots 2.11$$

with reinforcement

Now from Equations 2.4, 2.10 and 2.11:

$$p_o = \frac{P}{2(B + 2h_o \tan \alpha_o)(L + 2h_o \tan \alpha_o)} + \gamma h_o \quad \dots 2.12$$

without reinforcement

$$p = \frac{P}{2(B + 2h \tan \alpha)(L + 2h \tan \alpha)} + \gamma h \quad \dots 2.13$$

with reinforcement

In their calculation they assumed the value of  $\tan \alpha_o = \tan \alpha = 0.6$ . Giroud et. al (1984) showed that the load distribution factor decrease with increasing load repetitions as shown in Figure 2.6.

Unpaved roads without reinforcement: Giroud and Noiray suggested two separate analyses, the so called quasi static analysis for light traffic (1 to 10 passages of standard axle) condition and analysis for traffic loading for cases exceeding 10 passages but not greater than 10,000 passages.

Quasi-static analysis: According to Giroud and Noiray, if there is no reinforcing materials between subgrade soil and aggregate layer, the load applied on the subgrade soil by dual wheel and by the weight of aggregate layer is equivalent to a uniform pressure,  $p_o$ , over a width  $(B + 2h_o \tan \alpha_o)$ , and to a uniform lateral surcharge  $\gamma h_o$  (Figure 2.5). They considered the elastic



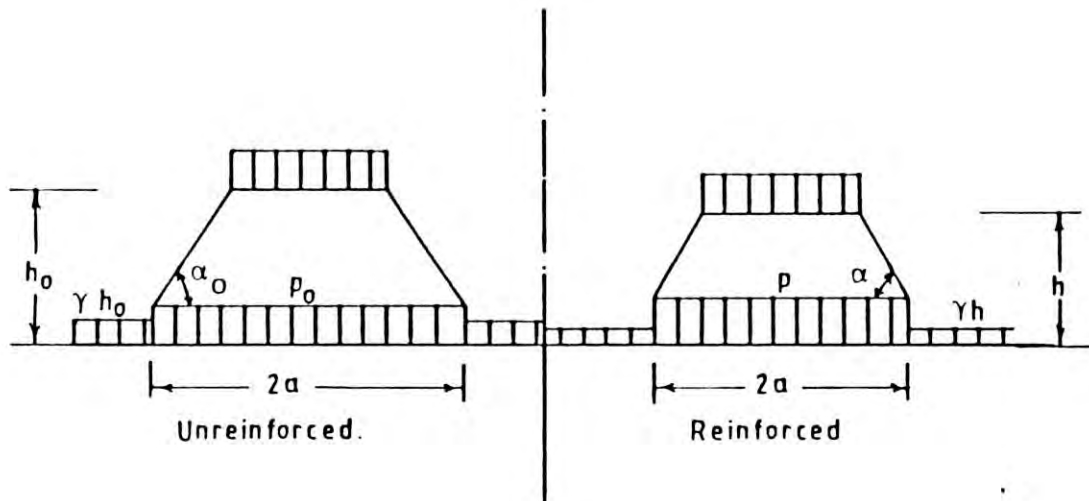


Figure 2.5 Pyramidal Load Distribution

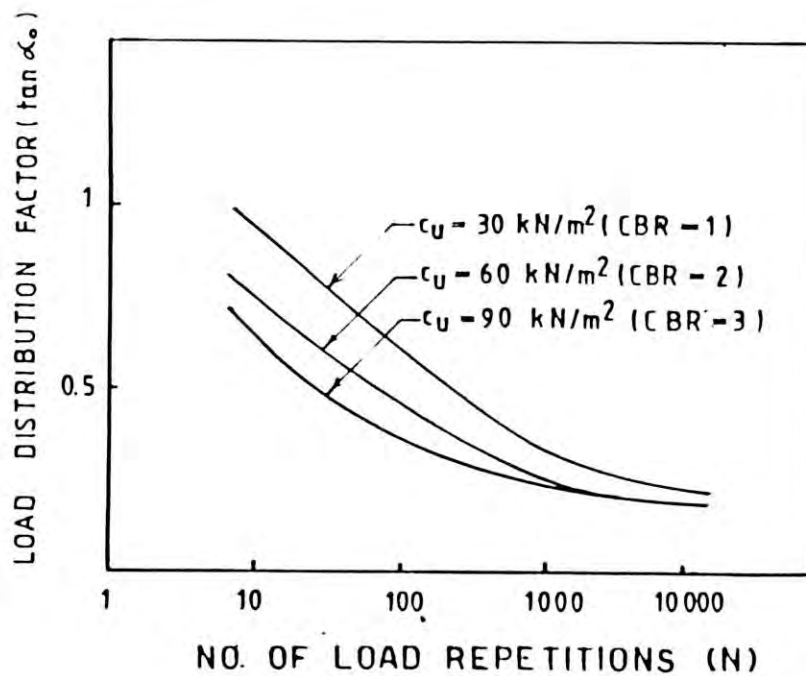


Figure 2.6 Load Distribution Factor Versus Number of Load Repetition (after Giroud et. al, 1984)

behaviour of soil only and pointed out that if  $p_o$  exceeds the elastic bearing capacity of the subgrade soil complete failure will occur because of large deflection due to several passages of wheel. On this basis, they suggested following equations:

$$p_o = \pi c_u + \gamma h_o \quad \dots 2.14$$

Again from Equations 2.12 and 2.14

$$\frac{P}{2(B + 2h_o \tan \alpha_o)(L + 2h_o \tan \alpha_o)} = \pi c_u \quad \dots 2.15$$

Replacing B and L from Equations 2.6 to 2.9 in Equation 2.15:

$$c_u = \frac{P}{2\pi (\sqrt{P/p_c} + 2h_o \tan \alpha_o)(\sqrt{P/2p_c} + 2h_o \tan \alpha_o)} \quad \dots 2.16$$

For on highway trucks

$$c_u = \frac{P}{2\pi (\sqrt{P\sqrt{2}/p_c} + 2h_o \tan \alpha_o)(\sqrt{P/2p_c\sqrt{2}} + 2h_o \tan \alpha_o)} \quad \dots 2.17$$

For off highway trucks

Using Equations 2.16 or 2.17 they established a set of curves shown in Figure 2.7 from which thickness of aggregates can be obtained for different values of axle load P.

Analysis for traffic loading: Giroud and Noiray based their

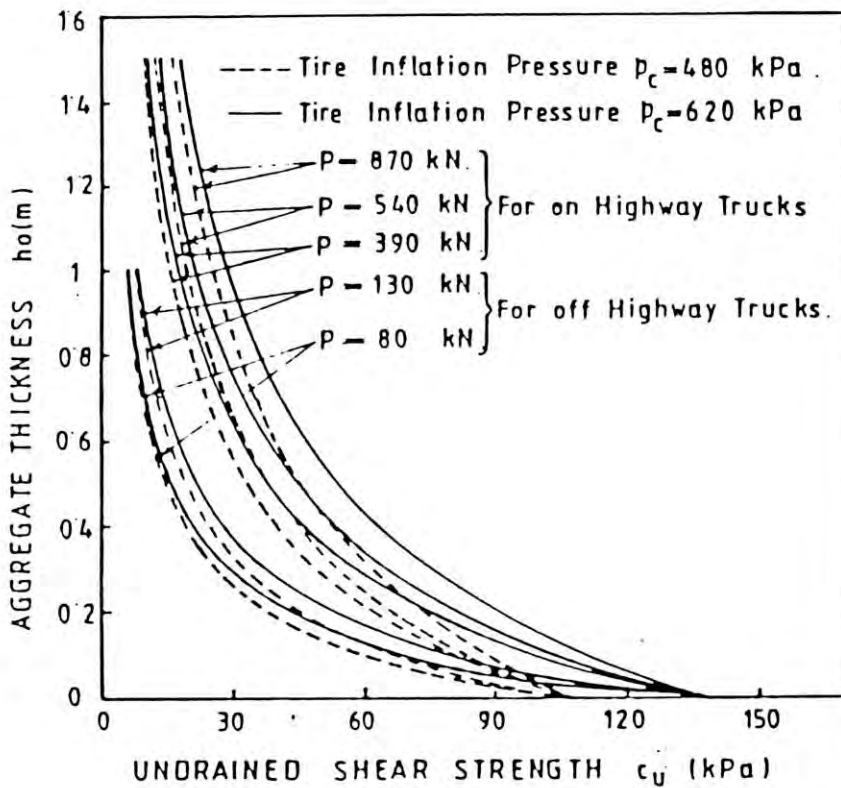


Figure 2.7 Design Charts for Unreinforced (Quasi-static) Road (after Giround and Noiray, 1981).



analysis on results from a large number of tests on unpaved roads conducted by the US Army Corps of Engineers (Hammit, 1970). In these tests the failure criterion was established at a rut depth of 0.075 m. Based on these results Webster and Alford (1978) presented a chart which gives the thickness of aggregate layer for different number of passages (N). Giroud and Noiray established a equation which was found to be in good agreement with Webster and Alford analysis and may be presented as follows:

$$h_o' = \frac{0.19 \log N_s}{(CBR)^{0.63}} \quad \dots 2.18$$

where  $h_o'$  is thickness of aggregate layer (m), N is number of passages of standard Axle (P = 80 kN). Equation 2.18 is valid for an axle loading of 80 kN and a rut depth of 0.075 m. For other values of axle loading and rut depths Giroud and Noiray proposed the following modifications. For axle loads,  $P_i$ , other than P:

$$N_s / N_i = ( P_i / P_s )^2 \quad \dots 2.19$$

where  $N_s$  is number of passages of standard axle ( $P_s = 80$  kN) and  $N_i$  is number of passages of axle transmitting  $P_i$ . Webster and Watkins (1977), based on extensive test results, remarked that increase of rut depth with number of passages is much more marked as soon as rut depth exceeds 0.075 m. They replaced  $\log N_s$  in Equation 2.18 by  $[\log N_s - 2.34(r - 0.075)]$  to get  $h_o'$  for rut depths other than 0.075 m. Now from Equations 2.18 and 2.19 and

replacing CBR by the relation  $c_u = 30,000 \text{ CBR}$ ,  $c_u$  in pascals,  $h_o'$  becomes:

$$h_o' = \frac{119.24 \log N + 470.98 \log P - 279.01 r - 2283.34}{(c_u)^{0.63}} \quad \dots 2.20$$

where  $P$  in Newtons;  $r$  in meters;  $c_u$  undrained shear strength of subgrade soil in Pascals. The Equation 2.20 should not be used when the number of passages exceeds 10,000. Giroud et. al. improved Equation 2.20 and presented as follows:

$$h_o' = \frac{125 \log N - 294(r - 0.075)}{(c_u)^{0.63}} \quad \dots 2.21$$

Following Equation 2.20 they produced design chart for traffic loading condition (Figure 2.8).

#### Unpaved roads with reinforcement

For reinforced condition Giroud and Noiray suggested quasi static analysis and analysis under traffic loading following similar philosophy as in case of unreinforced condition.

Quasi static analysis: Giroud and Noiray assumed that the subgrade soil is incompressible and settlement under the wheels causes heave in areas between and beyond the wheels as shown in Figure 2.3. Thus the reinforcement takes a wavy shape and thereby get stretched. As the reinforcement get stretched it will carry load, the equilibrium equation takes the form as:

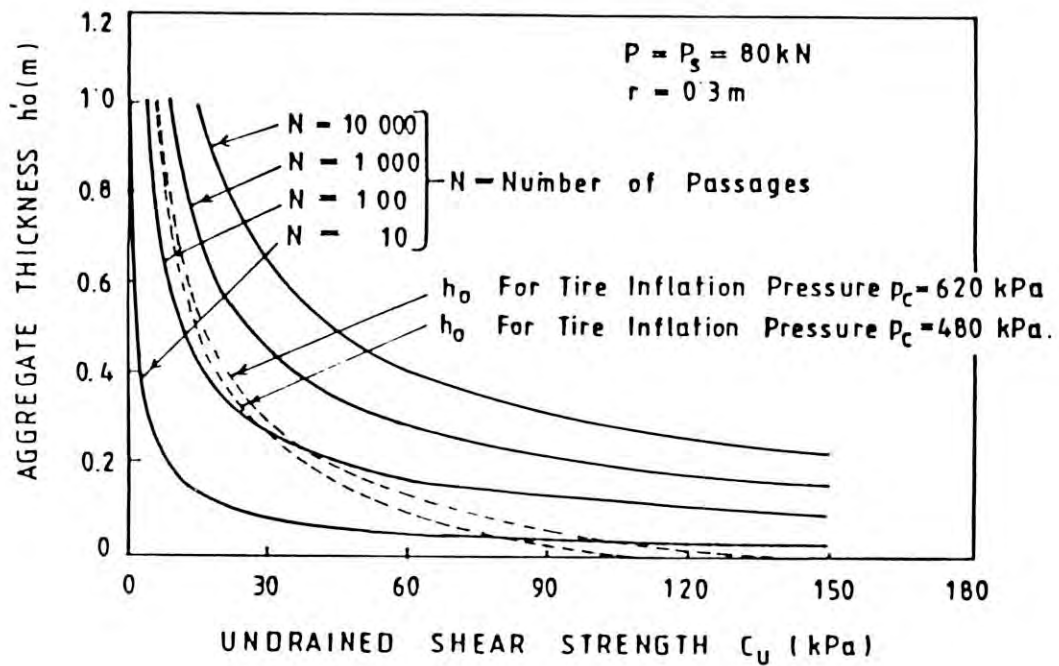


Figure 2.8 Design Charts for Unreinforced (traffic Loading) Roads (After Giroud and Noiray, 1981).



$$p = p_s + p_r \quad \dots 2.22$$

where  $p$  is the total pressure from wheel at the base of the aggregate layer,  $p_s$  is the load carried by subgrade soil and  $p_r$  is the load carried by the reinforcement.

Giroud and Noiray argued that because of the confinement provided by the reinforcement, deflection of the subgrade soil will be small for all level of loading less than the ultimate bearing capacity. Therefore:

$$p_s = (\pi + 2)c_u + \gamma h \quad \dots 2.23$$

From Equations 2.22 and 2.23

$$p - p_r = (\pi + 2)c_u + \gamma h \quad \dots 2.24$$

The wavy shape of the deformed reinforcement results from the incompressibility of the subgrade soil. The soil displaced downwards by settlement must be equal to the volume of the soil displaced upwards due to heaving. The shape of the deformed reinforcement is assumed to consist of portions of parabolas connected at A and B, points located on the initial plane of the reinforcements (Figure 2.9). It is also assumed that the subgrade soil deflection doesn't affect the aggregate layer significantly. Webster and Watkin's full scale test data confirm this assumption. Now from Figures 2.2, 2.5 and 2.9:

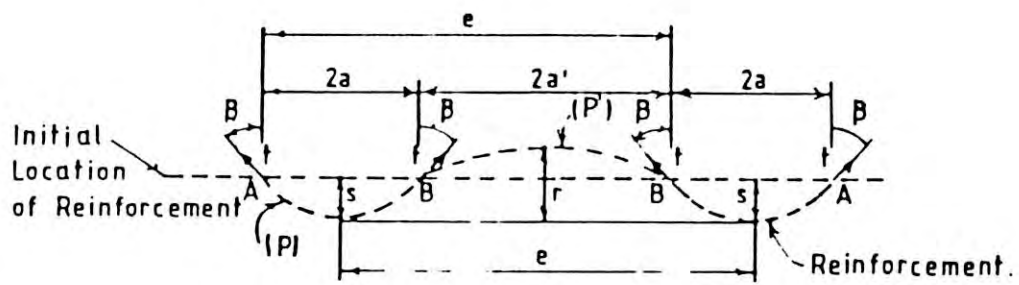


Figure 2.9 Deformation in Reinforcement.

$$2a = B + 2h \tan \alpha \quad \dots 2.25$$

$$2a = e - B - 2h \tan \alpha \quad \dots 2.26$$

Giroud and Noiray considered two types of geometry of deformation modes. In the first case, the central parabola is wider i.e  $a' > a$ . The relationship between settlement  $S$ , rut depth  $r$  can be found by equating areas  $A$  and  $A'$  as shown in Figure 2.10.a.

$$A = \frac{2aS}{3}, \quad A' = \frac{2a'(r - S)}{3}$$

Therefore:

$$S = \frac{ra'}{a + a'} \quad \dots 2.27$$

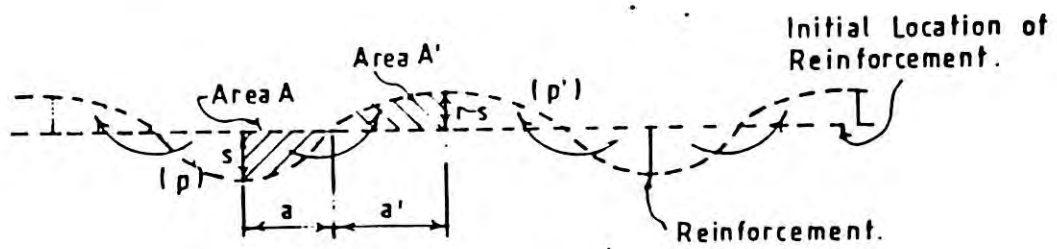
In the second case, when central parabola is smaller (Figure 2.10b), the relation takes the form:

$$S = \frac{2ra^2}{2a^2 + 3aa' - a'^2} \quad \dots 2.28$$

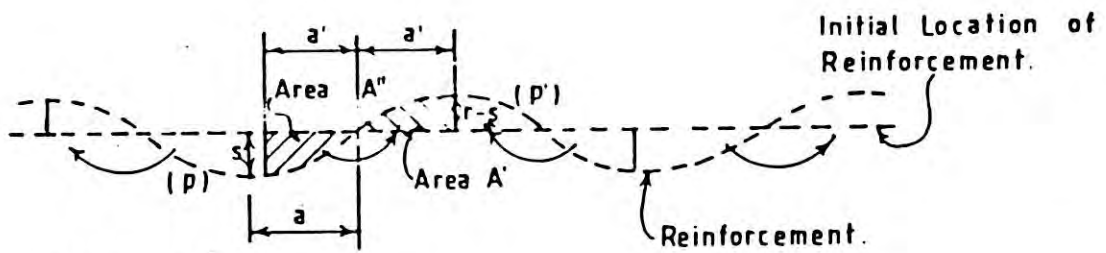
and when  $a = a'$ , any of Equations 2.27 or 2.28 may be used. Giroud and Noiray assumed, elongation as uniform along the entire length of reinforcement and in case of  $a' > a$  strain is given by:

$$\epsilon_r = \frac{b + b'}{a + a'} - 1 \quad \dots 2.29$$





(a)  $a' > a$



(b)  $a > a'$

Figure 2.10 Relation Between Settlement and Rutting.

Where  $\epsilon_r$  is strain in reinforcement;  $a, a'$  are half length of the chord subtended respectively by (P) and (P');  $b, b'$  are half length of (P) and (P'). The strain can be calculated using Equation 2.29 and the following relationship between an arc of parabola and subtended chord:

$$\frac{b}{a} - 1 = \frac{1}{2} \left[ \sqrt{1 + (2S/a)^2} + (a/2S) \ln \left\{ (2S/a) + \sqrt{1 + (2S/a)^2} \right\} - 2 \right] \quad \dots 2.30$$

$$\frac{b'}{a'} - 1 = \frac{1}{2} \left[ \sqrt{1 + \{2(r - S)/a'\}^2} + a' / \{2(r - S)\} \ln \{2(r - S)/a' + \sqrt{1 + \{2(r - S)/a'\}^2}\} - 2 \right] \quad \dots 2.31$$

when  $a > a'$ , the strain in reinforcement is given directly by Equation 2.30 because:

$$\epsilon_r = b/a - 1 \quad \dots 2.32$$

From Figure 2.9

$$a \cdot p_r = P_r \cos \beta \quad \dots 2.33$$

From properties of parabolas

$$\tan \beta = a/2S \quad \dots 2.34$$

As Giroud and Noiray assumed a linear relationship between load

and strain, thus:

$$P_r = K \epsilon_r \quad \dots 2.35$$

Now from Equations 2.33, 2.34 and 2.35

$$p_r = \frac{K \epsilon_r}{a \sqrt{1 + (a/2S)^2}} \quad \dots 2.36$$

where  $P_r$  is tension in reinforcement;  $K$  is the secant modulus at two percent of strain. Now from Equations 2.13, 2.24 and 2.36 and putting  $\tan \alpha = 0.60$  the following equations may be derived:

$$(\pi + 2)c_u = \frac{P}{2(B + 2h \tan \alpha)(L + 2h \tan \alpha)} - \frac{K \epsilon_r}{a \sqrt{1 + (a/2S)^2}} \quad \dots 2.37$$

Using Equations 2.6, 2.7, 2.8, 2.9 and 2.37 they developed a set of design charts as shown in Figure 2.11 for different modulus of stiffness of reinforcement. The practical design chart is provided in Figure 2.12.

Giroud and Noiray assumed that the difference of aggregate thickness between the reinforced and unreinforced condition is not affected by the traffic loading. This assumption may be valid if one ignores the contribution of reinforcement. Because in case of unreinforced condition (quasi static) the load is taken by soil is assumed to be  $(\pi c_u)$  and in case of reinforced condition (quasi static) that taken by soil is assumed as



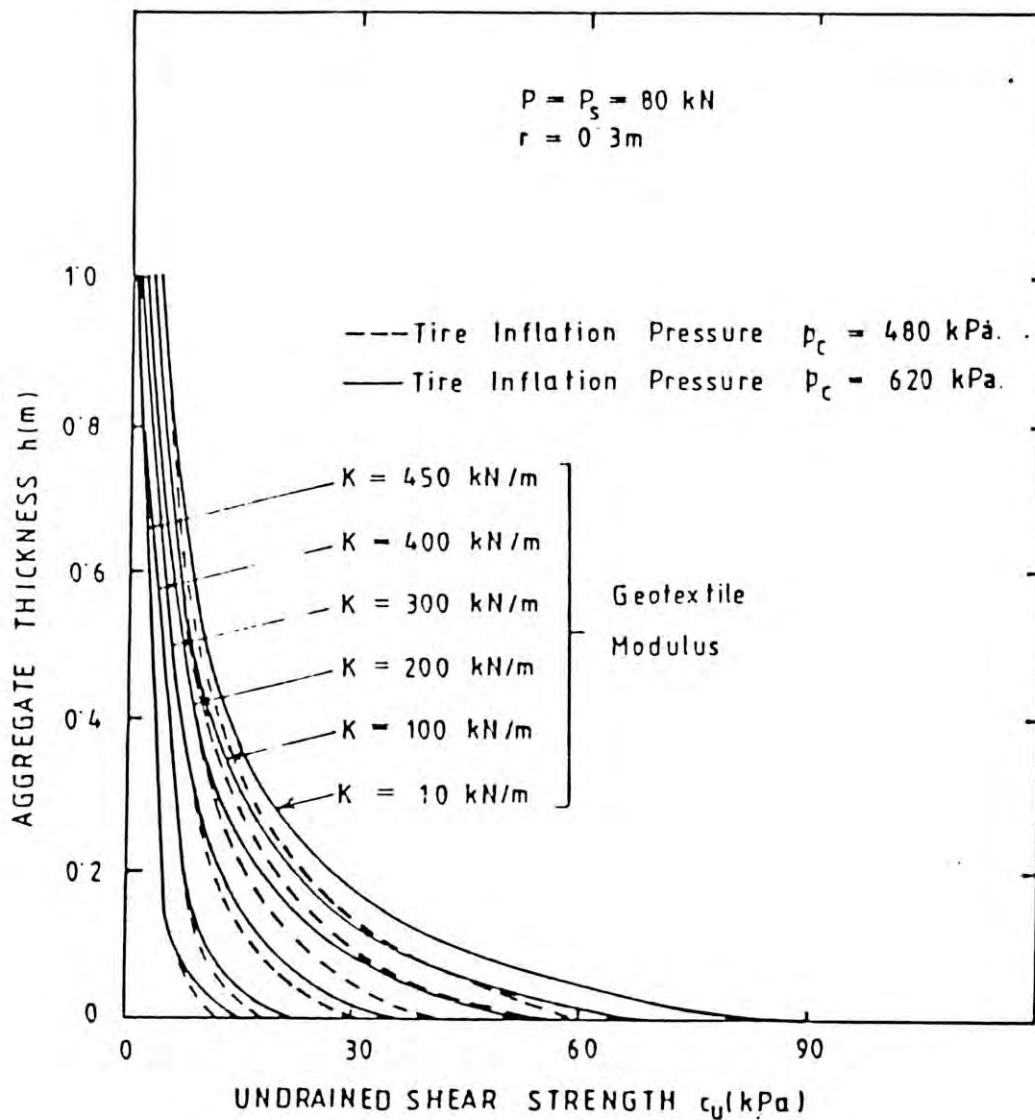


Figure 2.11 Design charts for Reinforced (Quasi-static) Condition (after Giroud and Noiray, 1981).

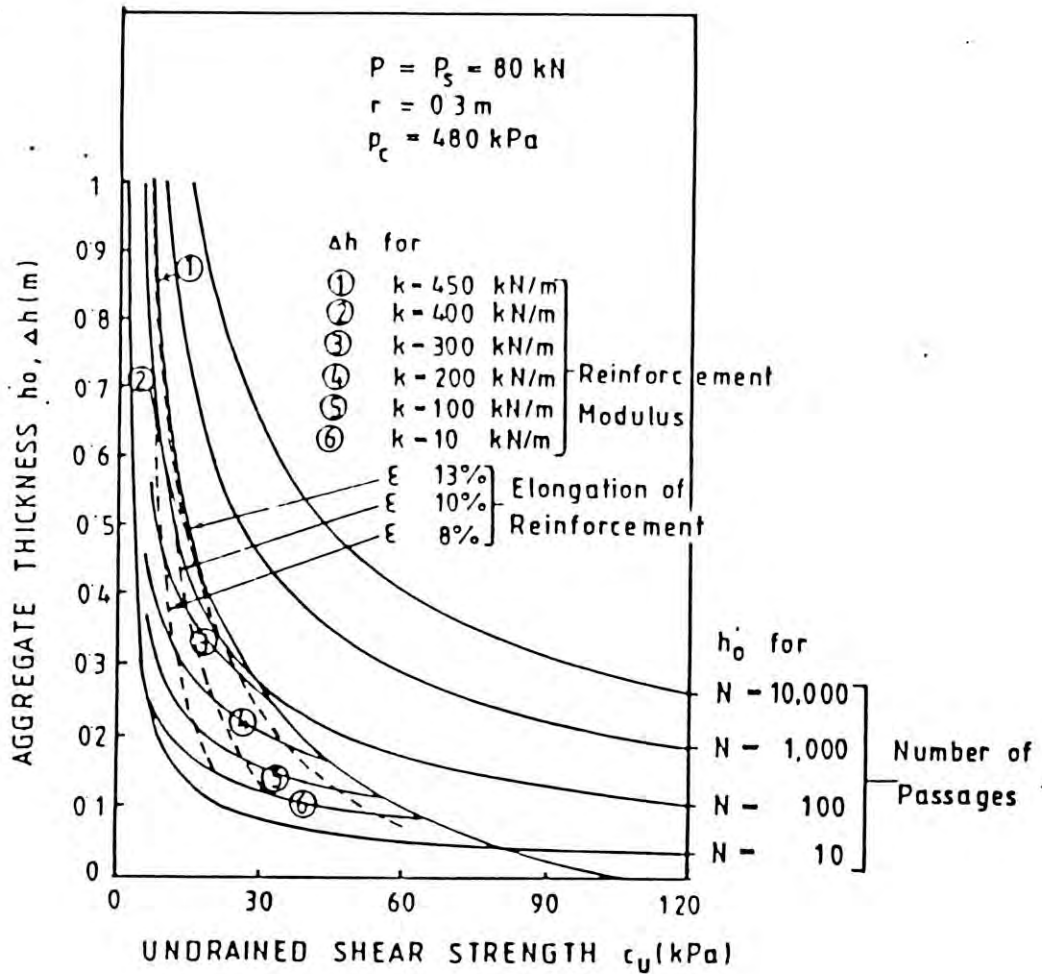


Figure 2.12 Practical Design Charts.  
(after Giroud and Noiray, 1981).

$((\pi + 2)c_u)$ . They suggested to evaluate the design thickness ( $h'$ ) by subtracting the reinforced quasi static thickness ( $h$ ) from unreinforced quasi static thickness ( $h_o$ ) and then subtract the difference of thickness ( $\Delta h = h_o - h$ ) obtained earlier, from the thickness ( $h_o'$ ) for unreinforced traffic condition.

### 2.6.2 Method Proposed by Van den Berg and Kenter (1984)

The design method proposed by Van den Berg and Kenter (1984) are described here. They established the design equations to calculate the aggregate thickness and the type of reinforcement considering the so called "membrane theory" and the equilibrium of the system. From equilibrium of the system (Figure 2.13):

$$t_o \left( \frac{d^2 S}{dx^2} \right) + p_s = - p_o - \gamma h \quad \dots 2.38$$

From membrane theory

$$t = t_o \sqrt{\left[ \left( \frac{dS}{dx} \right)^2 + 1 \right]} \quad \dots 2.39$$

where,

$t$  = tensile stress in reinforcement

$t_o$  = horizontal component of tensile stress ( $t$ )

$S$  = vertical displacement (settlement) of reinforcement

$x$  = horizontal distance to the centre of the vehicle

$\gamma$  = unit weight of aggregate

$h$  = thickness of aggregates



$p_s$  = load taken by subgrade soil

$p_o$  = pressure at the base of the aggregate layer

For subgrade soil they assumed a simplified bilinear representation of load deformation behaviour as shown in Figure 2.14. They also assumed that in the elastic phase, soil will show a linear load deformation behaviour from which they found:

$$p_s = kS \quad \dots 2.40$$

where  $k$  is the modulus of subgrade reaction of the subgrade soil. For plastic phase they used Brinch Hansen bearing capacity equation:

$$p_s = N_c (c_u + 3/4 b \bar{\gamma} \tan \phi) \quad \dots 2.41$$

where,

$c_u$  = cohesion of subgrade soil

$\phi$  = angle of internal friction of the subgrade soil

$\bar{\gamma}$  = effective unit weight of the subgrade soil

$b$  = road width

$N_c$  = bearing capacity factor

Like Giroud and Noiray, they assumed a uniform pressure  $p$  transmitted from the wheel at the base of the aggregate layer, but they present it in a different way:

$$p = \frac{P}{2(nB' + 2zh)(B' + 2zh)} \quad \dots 2.42$$

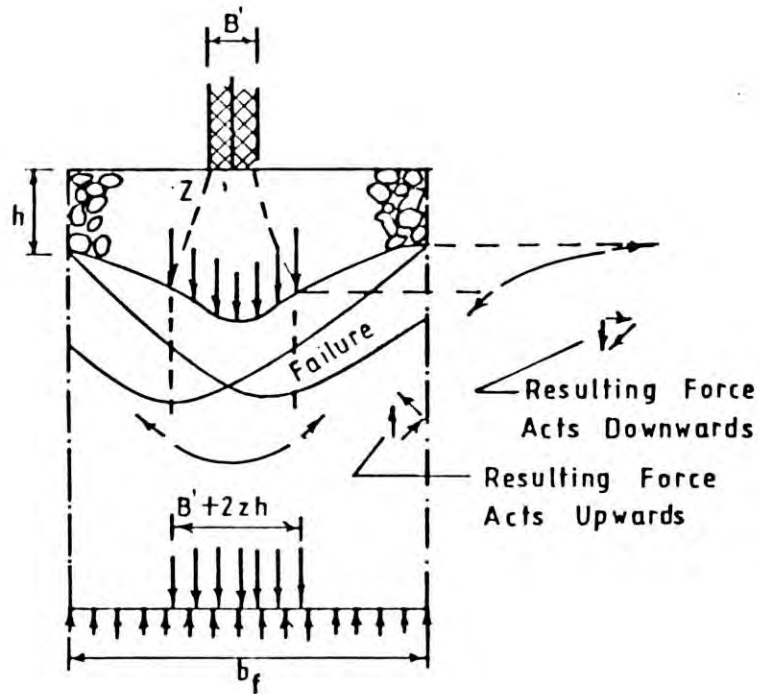


Figure 2.13 Free Body of a Road Section  
(after Van den Berg and Kenter, 1984)

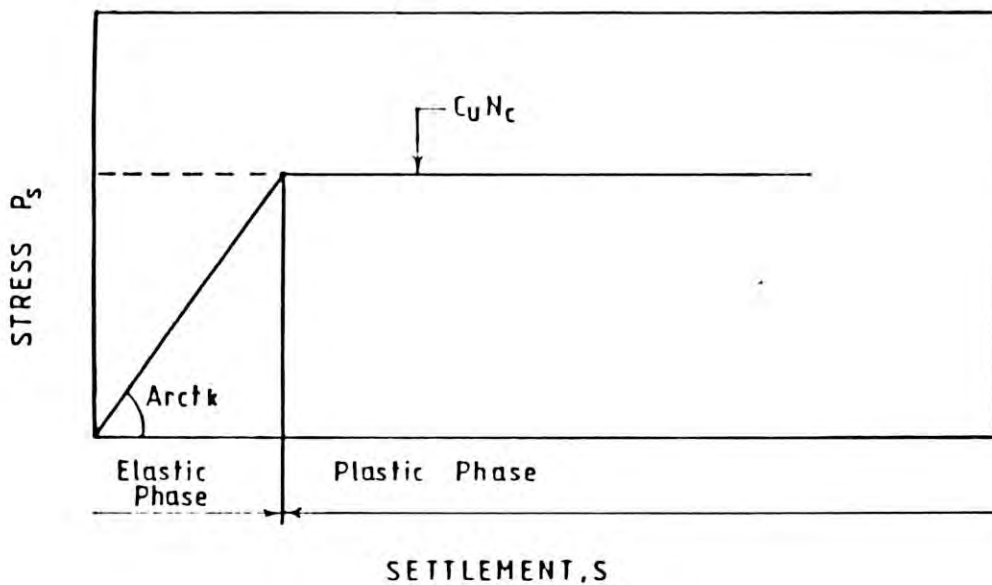


Figure 2.14 Bilinear Soil Model

where,

P = axle load

B' = tire width

n = number of tires

z = load distribution factor of aggregate

They solved the equilibrium Equation 2.38 for elastic phase of the subgrade soil with the help of Equation 2.40:

$$kS/p = 2\cosh(\beta_1 - \alpha_1)\cosh\xi \sinh\eta / \sinh\beta_1 \quad \dots 2.43$$

$$kS/p = 2\cosh(\beta_1 - \alpha_1)\cosh\xi \sinh\eta / \sinh\beta_1 + 1 - \cosh(\xi - \alpha_1 + \eta) \quad \dots 2.44$$

$$kS/p = 2\cosh\alpha_1 \cosh(\xi - \beta_1) \sinh\eta / \sinh\beta_1 \quad \dots 2.45$$

where

$$\alpha_1 = 1/2 A (k/t_0)$$

$$\beta_1 = 1/2 b (k/t_0)$$

$$\eta = 1/2(nB' + 2zh) (k/t_0)$$

$$\xi = x (k/t_0)$$

A = track width

Equation 2.43 is valid for  $0 < \xi < \alpha_1 - \eta$ , i.e. for the area between the centre of the road and the area loaded by uniform load p. Equation 2.44 is true for  $\alpha_1 - \eta < \xi < \alpha_1 + \eta$ , i.e. in the area loaded by p. The Equation 2.45 holds for  $\alpha_1 + \eta < \xi < \beta_1$ , i.e. for the area between the area loaded by p and edge of the road.



In the above Equations (2.43, 2.44 and 2.45) the parameter  $k/t_0$  has a considerable influence. The practical value of this parameter is relatively high, even for a strong reinforcement and very soft subgrade soil. The vertical displacements are very negligible outside the area  $\alpha l - \eta < \alpha l + \eta$ . Therefore, the state of stress is hardly influenced by the reinforcement inclusion. This phenomenon is also found in the present study. Van den Berg and Kenter considered the aggregate weight as a driving load. From vertical equilibrium they found that:

$$b_f = \frac{P}{2(p - \gamma h)(B' + 2zh)} \quad \dots 2.46$$

where  $b_f$ , is the width of the plastic zone. They considered three possible cases for which the plastic failure of the subgrade soil may occur. These are shown in Figure 2.15. Among these three cases, the first is most frequent to occur. Van den Berg and Kenter solved Equation 2.38 with Equations 2.41 and 2.46 for different location of plastic failure (Figure 2.15). They satisfied the condition of compatibility and established the following equations:

$$r = \frac{b_f - nB' - 2zh}{4} \quad \dots 2.47$$

$$\lambda^3 = \frac{2k((b_f - nB' - 2zh)^2 + 3Y^2)}{3pb_b b_f^2} \quad \dots 2.48$$

CASE

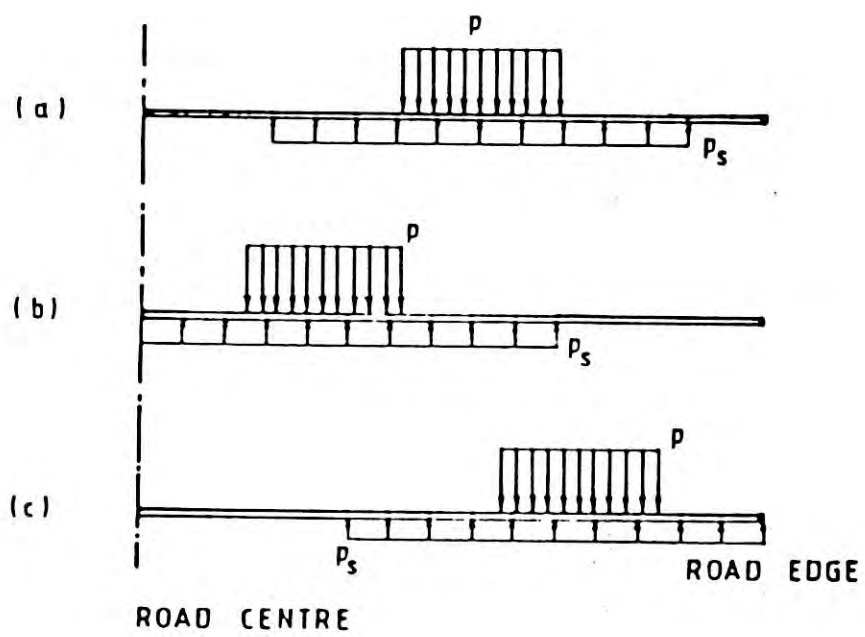


Figure 2.15 Location of Plastic Failure (after Van den Berg and Kenter, 1984).

$$t_{\max} = 0.5pbf \sqrt{[ \{ (bf - nB' - 2zh + |Y|) / bf \}^2 + \lambda^2 ]} \quad \dots 2.49$$

where,

$r$  = total (elastic and plastic) rut depth

$K$  = modulus of stiffness of reinforcement

$t_{\max}$  = maximum tensile stress in the reinforcement

$Y$  = location parameter of the plastic zone

$Y = 0$  if  $bf < A$ ;  $bf < b - A$  (case a)

$Y = b - A$  if  $bf > A$ ;  $bf < b - A$  (case b)

$Y = b - A - bf$  if  $bf > b - A$  (case c)

Van den Berg and Kenter considered the traffic loading by taking the bearing capacity factor  $N_c = 5.0$  instead of 5.14. They mentioned that for traffic loading the bearing capacity factor  $N_c^*$  should be equal to  $2/3N_c$ . Because of lateral restraint provided by the reinforcement, they assumed larger value ( $N_c^* = 5$ ). Van den Berg and Kenter also introduced a new concept of equivalent axle load. They defined the equivalent axle load as "the equivalent load has the same effect in one load cycle as the actual load in many cycles". From test results they set up an empirical equation:

$$P_e = P^{6.2} \sqrt{N} \quad \dots 2.50$$

where,

$P_e$  = equivalent axle load



P = real axle load

N = number of load repetitions

## 2.7 MATERIAL CHARACTERISATION

The characterisation of design parameters of the constituent materials (aggregate, geotextile and subgrade soil) is described in the following sections.

### 2.7.1 Aggregate - Base Layer

The base layer is used to provide adequate distribution of applied load. Most of the researchers consider the base layer as only a load transfer media. Giroud and Noiray pointed out that the CBR value of aggregate should be greater than 80 for effective load distribution. Celenese Fiber Marketing Company (1975) provides a curve for selecting aggregate size as shown in Figure 2.16. The strength parameter of granular materials that contribute in bearing the surface load is solely the frictional contact between the granular particles. The maximum frictional force can be attained if the granular materials possesses the following properties:

- 1) the particle should be dry and clean
- 2) the particles should be in firm contact with one another
- 3) the particles should be angular in shape and well graded

### 2.7.2 Subgrade Soil - Clay

Among all other geotechnical materials, clay soils are most complicated in their engineering behaviour. The stress strain

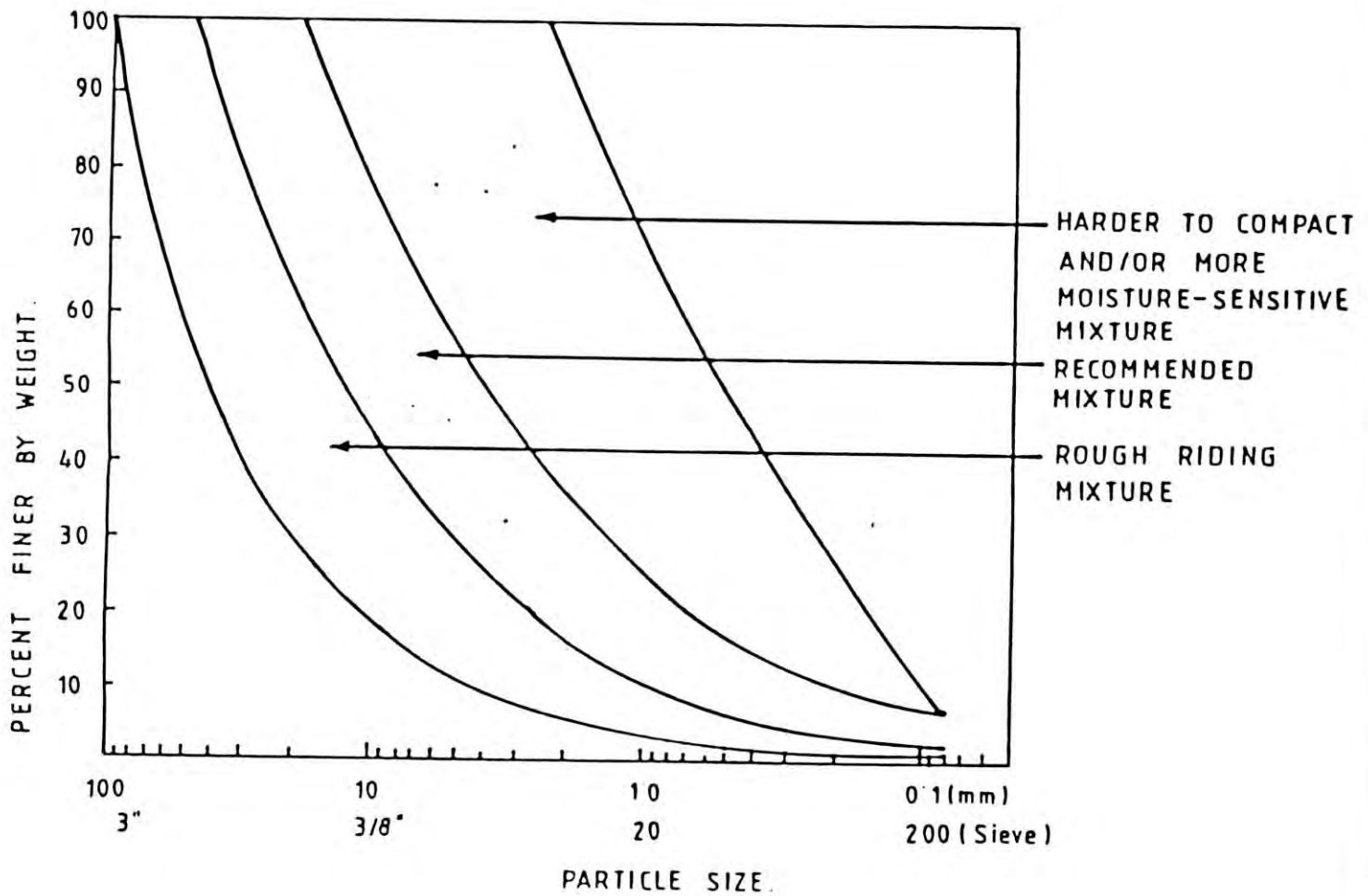


Figure 2.16 Design Charts for Selection of Aggregates (after Celenese Fibres Marketing Company, 1975).

properties is the vital consideration in the design of bearing problem.

### Stress Strain Behaviour

Most of the clay soils exhibit non linear stress strain behaviour. However majority of the engineering problems assume linear behaviour of clay and initial or tangent modulus is a well known design parameter. The conventional way to determine the stress strain modulus is from unconsolidated undrained triaxial compression tests. Ladd (1965) found that the undrained modulus is a function of initial consolidation pressure. Research done by Berre and Bjerrum (1973), Vaid and Campanella (1974) also support Ladd's findings. The variation of modulus with confining pressure at which the sample is consolidated were reported by Janbu (1963). Ladd (1964), Varadarajan (1973) and Yudhir (1975). Ladd (1964), Berre and Bjerrum (1973) observed the modulus to decrease with increase in stress level.

There are several empirical equations from which the undrained modulus can be obtained. Cooling and Skempton (1942). Skempton and Henkel (1957) have found that undrained strength could be related to modulus of elasticity of the soil by the relation:

$$E_u = k' S_u \quad \dots 2.51$$

They suggested the value of  $k$  as 140. But Bjerrum (1964)



suggested different values of  $k$  as 250 to 500. Duncan and Buchigani (1976) established that undrained elastic modulus of a soil does not depend only on the undrained shear strength but also on the plasticity index and stress history.

### Mathematical Approximation of Stress Strain Behaviour

A number of non linear stress strain model have been established by several researchers. Kondner (1963) first approximated the non linear stress strain behaviour by hyperbolic equation using two parameters. The equation is expressed as:

$$\sigma_1 - \sigma_3 = \frac{\epsilon}{a + b \epsilon} \quad \dots 2.52$$

Here  $\epsilon$  is axial strain,  $\sigma_1$ ,  $\sigma_3$  are major and minor principal stresses respectively,  $a$  and  $b$  are two constants known as hyperbolic parameter. From Equation 2.52

$$\sigma_{ult} = \lim_{\epsilon \rightarrow \infty} \sigma = \frac{1}{b} \quad \dots 2.53$$

and

$$\left( \frac{d\sigma}{d\epsilon} \right)_{\epsilon=0} = \frac{1}{a} \quad \dots 2.54$$

Thus  $a$  is the reciprocal of the initial tangent modulus ( $E_i$ ) and  $b$  is the reciprocal of the asymptotic value of stress difference,

when the stress strain curve approaches at infinite strain as shown in Figure 2.17. The Equation 2.53 does not exist in almost all cases. It is better to express the equation in the following way:

$$\text{Lit } \lim_{\epsilon \rightarrow \infty} (\sigma_1 - \sigma_3) = \frac{1}{b} = R(\sigma_1 - \sigma_3)_f$$

Where  $(\sigma_1 - \sigma_3)_f$ , is the ultimate or failure value of the deviator stress and R is a correlation coefficient. Brinch Hansen (1963) prescribed three types of equations with some modifications from Kondner depending on the initial and final nature of the stress strain curve. When the curve starts linearly then the deviator stress  $\sigma_1 - \sigma_3$  is related to axial strain and constants a and b as Equation 2.52. When the curve starts with parabolic nature, then:

$$\sigma_1 - \sigma_3 = \sqrt{\frac{\epsilon}{a + b\epsilon}} \quad \dots 2.55$$

and the last one, when the actual stress strain curve shows a decrease after a maximum value:

$$\sigma_1 - \sigma_3 = \frac{\sqrt{\epsilon}}{a + b\epsilon} \quad \dots 2.56$$

Prakash, Sharan and Saran (1984) observed that the hyperbolic parameters a and b are independent of confining pressure. Although the inverse of hyperbolic parameters a and b should

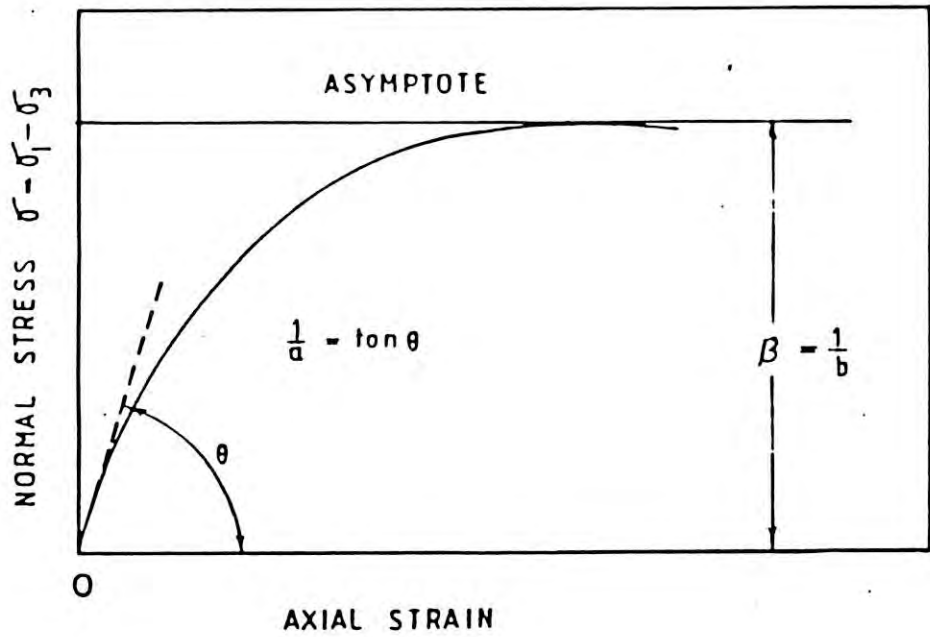
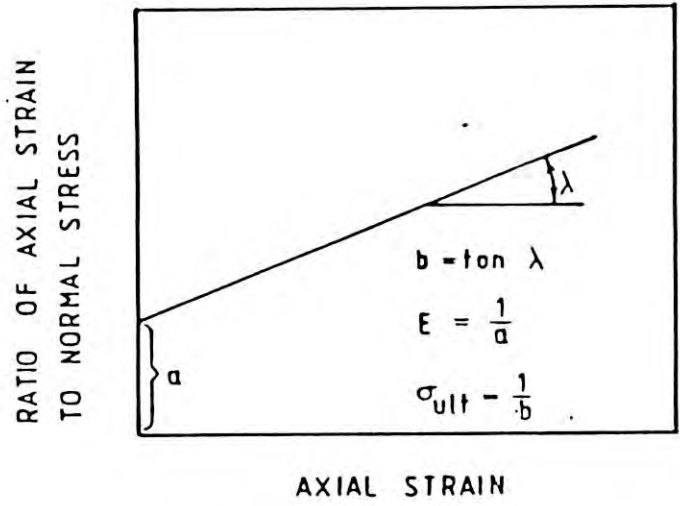


Figure 2.17 Hyperbolic Stress-Strain Model.



represent the initial modulus and undrained shear strength but it is not actually found as reported by many researchers. Berth et. al (1973) suggested a parabolic function of the type:

$$\varepsilon(r) = a' + \frac{b'}{r - r_f} + \frac{c'}{(r - r_f)^2} + \dots \quad \dots 2.57$$

where  $\varepsilon(r)$  is the strain at any stress ratio,  $r = \sigma_3 / \sigma_1$ ,  $r_f = r$  at failure, and  $a'$ ,  $b'$ ,  $c'$  are parameters depending on the observed stress strain characteristics of the material. Desai (1971) proposed the use of cubic spline function to represent a set of stress strain data.

#### Settlement Analysis

The excess stress caused by the load from structures in the soil will always be accompanied by some strain which in turn causes settlement of the structure. In general the total settlement is cumulative effect of (i) immediate settlement (ii) primary settlement (iii) secondary settlement. Immediate settlement results from the constant volume distortion of the loaded soil mass. When a saturated soil mass is subjected to rapid loading, e.g. traffic loading, the low permeability of the clay retards drainage of water out of the pores and the clay deforms in the undrained or constant volume mode.

There are so many equations and graphs to calculate stresses caused by imposed loads developed by different authors. Among

them Newark (1942), Janbu et. al (1956) are most commonly used. Jurgenson (1934) developed a set of equations to evaluate principal stresses. These are shown in Table 2.1. The equation developed by Jurgenson has been used in this study.

Settlement calculation normally done by using linear elastic theory, this method used undrained Young's modulus. Prakash, Sharan and Saran developed a constitutive model for evaluating settlement using non linear stress strain behaviour of clay. They proposed the following equations to calculate settlement:

$$\epsilon_1 = \frac{a(\sigma_1 - \sigma_3)}{1 - b(\sigma_1 - \sigma_3)} \quad \dots 2.58$$

$$\epsilon_2 = \frac{\sigma_2 - \nu(\sigma_1 + \sigma_3)}{\sigma_1 - \nu(\sigma_1 + \sigma_3)} \epsilon_1 \quad \dots 2.59$$

$$\epsilon_3 = \frac{\sigma_3 - \nu(\sigma_1 + \sigma_3)}{\sigma_1 - \nu(\sigma_1 + \sigma_3)} \epsilon_1 \quad \dots 2.60$$

The strain in the vertical direction for each layer is:

$$\epsilon_z = \epsilon_1 \cos^2 \theta_1 + \epsilon_2 \cos^2 \theta_2 + \epsilon_3 \cos^2 \theta_3 \quad \dots 2.61$$

The vertical settlement of any layer may be obtained by:

$$S = \epsilon_z \Delta Z \quad \dots 2.62$$

Table 2.1 Stresses Beneath a Uniformly Loaded Strip  
(after Jergenson, 1934)

x/b	z/b	$\sigma_z/p$	$\sigma_x/p$	$\tau_{xy}$	$\beta$	$\tau_{max}/p$	$\sigma_1/p$	$\sigma_3/p$
0	0.0	1.0000	1.0000	0	0	0.0000	1.0000	1.0000
	0.5	0.9594	0.4498	0	0	0.2548	0.9594	0.4498
	1.0	0.8183	0.1817	0	0	0.3183	0.8183	0.1817
	1.5	0.6678	0.0803	0	0	0.2937	0.6678	0.0803
	2.0	0.5508	0.0410	0	0	0.2546	0.5508	0.0410
	2.5	0.4617	0.0228	0	0	0.2195	0.4617	0.0228
	3.0	0.3954	0.0138	0	0	0.1908	0.3954	0.0138
	3.5	0.3457	0.0091	0	0	0.1683	0.3457	0.0091
	4.0	0.3050	0.0061	0	0	0.1499	0.3050	0.0061

$\beta$  is angle between direction of  $\sigma_1$  and the vertical.



The total settlement along any vertical axis is:

$$S_t = \int_0^n \epsilon_z \, dz \quad \dots 2.63$$

In the above Equations (2.58 to 2.63),  $a$  and  $b$  are hyperbolic parameters of the clay soil,  $\sigma_1$ ,  $\sigma_2$  and  $\sigma_3$  are principal stresses,  $\epsilon_1$ ,  $\epsilon_2$  and  $\epsilon_3$  are major, intermediate and minor principal strains.  $\theta_1$ ,  $\theta_2$  and  $\theta_3$  are direction's cosines of the principal strains with respect to the vertical axis and  $\Delta Z$  is the individual layer thickness.

#### Strength and Rate of Loading

Bjerrum, Simons and Torbolaa (1958) showed that the greater the time to undrained failure the lower will be undrained strength. This argument is also supported by Crawford (1959). Richardson and Whitman (1963) and Berre and Bjerrum (1973). Some typical data are shown in Figure 2.18.

#### Repeated Loading Behaviour

Laboratory tests have been done by different researchers to model stress strain behaviour of clay soils under repeated loading condition. Among them, some researchers proposed equation encountering the degradability of modulus of elasticity with load repetitions. The study indicates the following which is very important in the design consideration under repeated loading condition. The degradation of stress strain behaviour and the

strength reduction increased with number of load repetitions. Idriss et. al(1978), Yamanouchi and Yasuhara made details study on this aspect. Idriss et. al. have draw some conclusions from their study on normally consolidated clay. (1) Cyclic loading caused significant loss of modulus of soil (2) Cumulative generation of pore pressure (3) Monotonic tests indicate that the static modulus decreased significantly more than the peak static undrained strength. They found a good straight line fitting between the degradation ratio and cycle number on a logarithmic plot. Idriss et. al proposed a qualitative stress strain and load repetition model for clay soil which is shown in Figure 2.19. Giroud et. al proposed an empirical relation of clay soils as:

$$C_{uN} = \frac{1000 c_u}{1 + (\log N)^{1.5} c_u} \quad \dots 2.64$$

### 2.7.3 Reinforcement

Geotextile reinforcements are new constructional materials in civil engineering especially in geotechnical engineering construction. There was a confusion about the term Geotextile among the beginners. They thought that geotextile is a material like cloth but made of soil. In reality, geotextiles are fabrics made from polymers or natural fibres. It may be stated that within a couple of decades there will be no geotechnical solution without geotextile materials. Giroud (1984) described geotextiles as "the muscles, the veins and the skin of the earth when it is used for reinforcing, drainage or lining purpose".

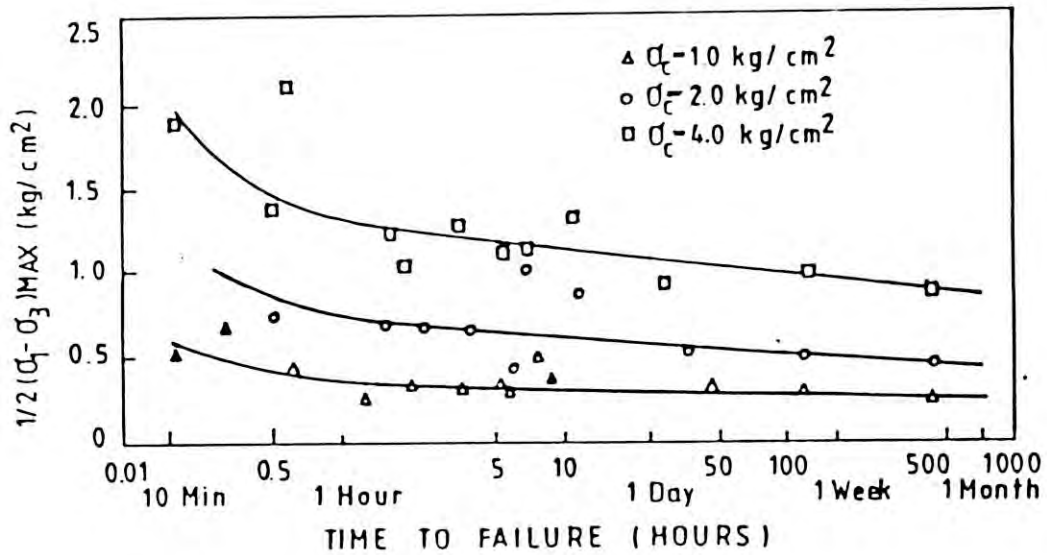


Figure 2.18 Effect of Rate of Loading on Strength .  
(after Bjerrum Simons and Torbolla, 1958).

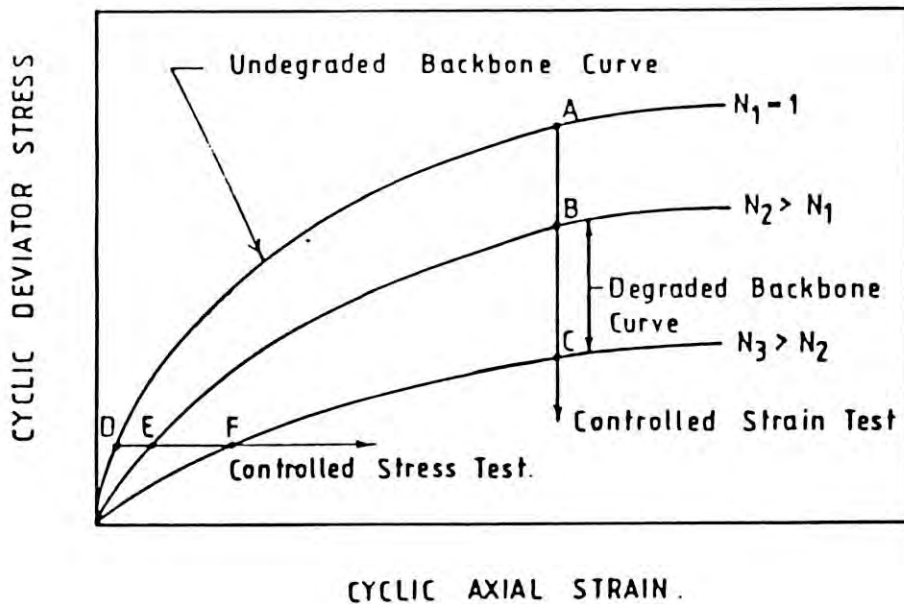


Figure 2.19 Repeated Loading Stress Strain Model  
(after Idriss et. at, 1978).

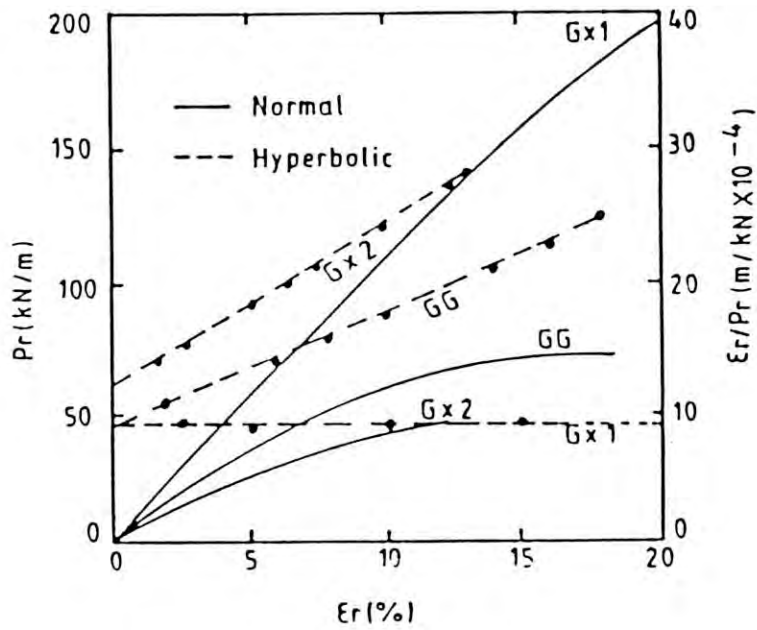


There are many types of geotextiles now available in the market. Among them, Kabir (1984) identified ten types of geotextiles. These are Knitted geotextile. Woven geotextile, Nonwoven geotextile, Composite geotextile, Web or Webbing, Mats, Nets, Grids, Formed plastic sheets and prefabricated composite structures.

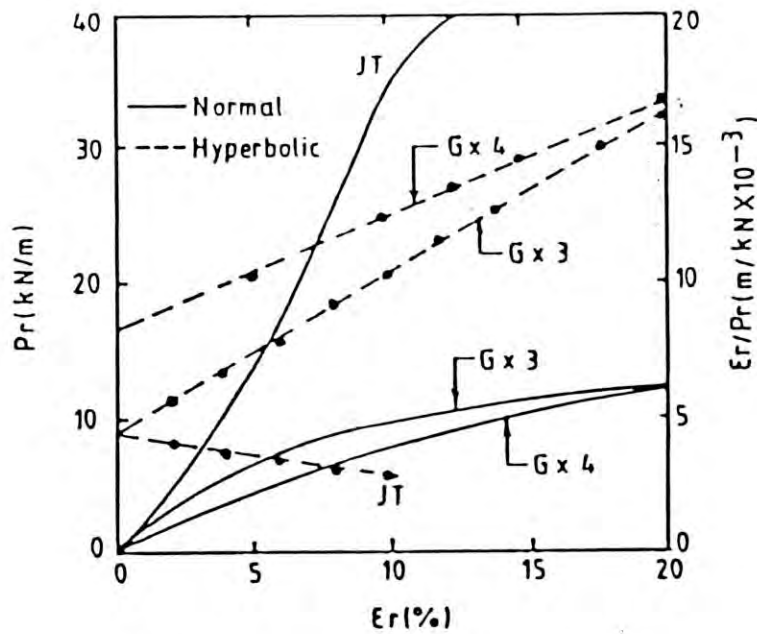
Most of the geotextile materials show non linear elasto visco plastic load strain behaviour. Since the reinforcing materials (geosynthetics) are fabricated from polymer structure, their load strain behaviour is affected by temperature, nature of confining media and the confining pressure and humidity. Like soil, Fahmy (1981) approximated the load strain behaviour of reinforcing materials by mathematical functions like polynomials, hyperbolic functions, spline functions etc. In this study, hyperbolic function has been used to model the load strain and load repetition behaviour of geosynthetics materials because of simplicity of the model. Some test data which follow this law with reasonable degree of accuracy is shown in Figures 2.20, 2.21 and 2.22. Effect of confining pressure on the hyperbolic parameters and on load strain behaviour is shown in Figure 2.23 for two types of woven type geotextile.

A number of testing techniques have been developed to date to quantify load strain behaviour of the reinforcing materials. These are, Strip tensile test, Plane strain test, Grab tensile test, Mullen burst test, Uniaxial loading test, Biaxial loading



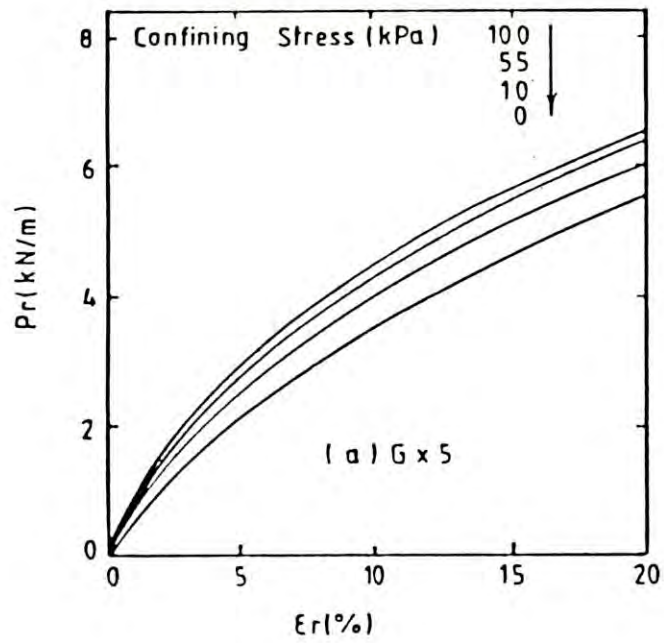


(a) Relatively Strong geosynthetic

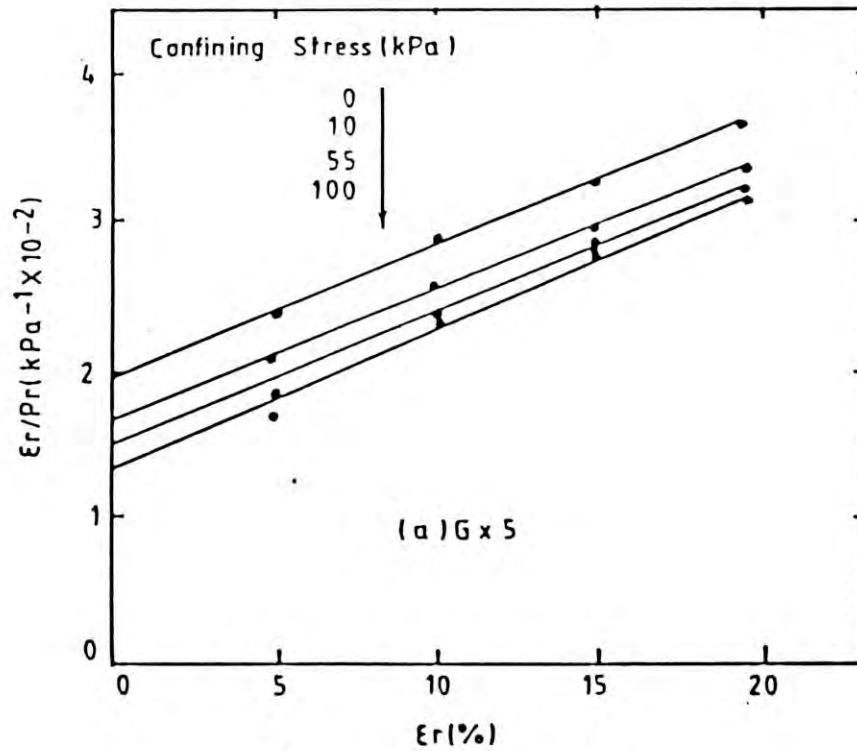


(b) Relatively Weak Geosynthetic

Figure 2.20 Mechanical Behaviour of Geosynthetic.

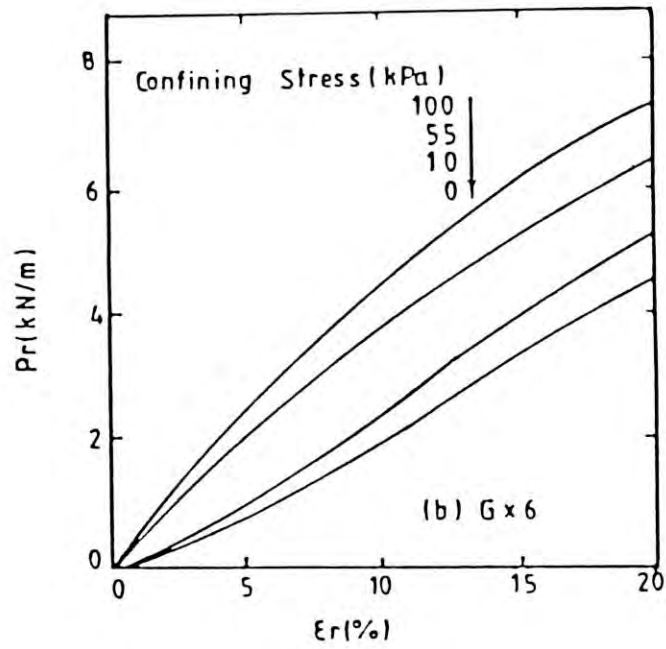


(a) Normal Presentation

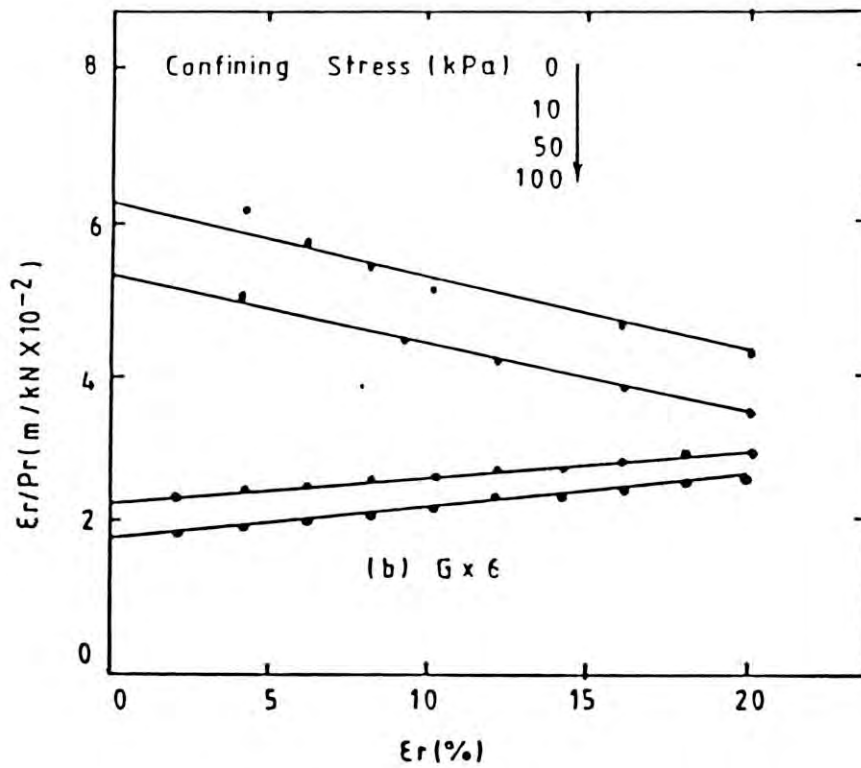


(b) Hyperbolic Presentation

Figure 2.21 Mechanical Behaviour of Geotextile GX5.



(a) Normal Presentation



(b) Hyperbolic Presentation

Figure 2.22 Mechanical Behaviour of Geotextile GX6.



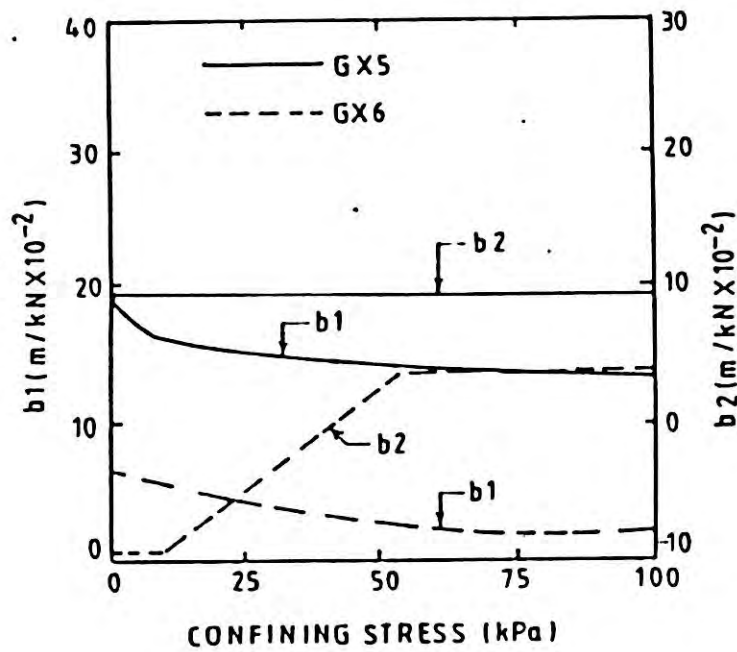


Figure 2.23 Effect of Confining Pressure on Hyperbolic Parameters.

test etc. Rankilor (1981) and Kabir (1984) have made detailed description of these tests. Kabir indicated that the repeated loading test of reinforcing materials may be done by creep test rig with slight modifications. Raumann(1979) has done hydraulic tensile test under repeated loading condition.

## 2.8 CASE STUDIES

Starting from the earlier time geosynthetics are being used to solve a number of geotechnical problems. Construction of unpaved road occupied significant portion of total road construction work worldwide. The pioneering countries are United Kingdom, Sweden, Japan. United States etc. Several examples are described below.

### 2.8.1 Stanley Airfield, Falkland Islands, U.K.

During the war between Britain and Argentina in 1982 which is well known as "Falkland War", the Stanley airfield received important attention because of war strategy. The extension work of the run ways became get top priority for landing large number heavy fighter aircrafts. But the soil conditions were very unfavourable. The main soil types were fine peaty sand having CBR value less than 3% as reported by Kennedy (1984). Flat level and poorly drained conditions were found in almost all extension areas. The water table was very high. Netlon CE 121 grid was used as reinforcement. After construction the run way was used for landing purpose satisfactorily.

### 2.8.2 Lune Estuary, England, U.K.

The type of construction was access road for vehicles and plant and pile driving rig. The main construction was tower for 400 KV overhead power lines near North West coast of England. The subsurface was very soft comprising dark grey clayey silts and silty clays. The type of reinforcement materials used in this project with 100 mm down crushed limestone aggregate was TERRAM 140, a meltbonded nonwoven geotextile.

### 2.8.3 Milngavie, Scotland, U.K.

Type of construction was access road across a settlement lagoon. The lagoon was a filled of 6 m soft slurry. TERRAM 140 was also used as reinforcement.

### 2.8.4 Kilanda, Sweden

It was a 400 KV power lines erection project. There was vast bog areas between the switching station and the Borguik Stenkullen power line. The depth of bog was about 1 to 6 m over a firm stratum. The road was designed for traffic of 700 passages of vehicles weighing between 1.5 and 4 tonnes and 500 heavy 15 to 300 tonnes vehicle trips in each direction. The road was reinforced by polyester fabric (Type 8650).

## 2.9 CONCLUDING REMARKS

From above review work the following remarks could be made:



### 2.9.1 Material Behaviour

Although most of the clay soils exhibit non linear stress strain behaviour, all researchers (Nieuwenhuis, Bakker, Giroud and Noiray, Sellmeijer et. al, Van den Berg and Kenter) defined it by two state, elastic limit and plastic limit., which is normally done in conventional soil mechanics. In case of a structure like unpaved road, where state and degrees of deformation is of paramount consideration, the limit state description of the materials behaviour is unrealistic. None of the authors considered the degradation of mechanical behaviour under repeated loading condition in their design methods from fundamental understanding of the material behaviour. Giroud and Noiray used an empirical relation based on extensive filed tests for a particular condition of rutting. Van den Berg and Kenter considered it by allowing a reduction in bearing capacity factor.

Giroud and Noiray and Van den Berg and Kenter defined the load strain behaviour of reinforcing materials by a single parameter, the modulus of stiffness at two percent of strain. This type of representation is not adequate as most of the reinforcing material exhibit non linear load strain behaviour. They didn't consider the degradation in modulus of stiffness under repeated loading condition. This is a very important factor, as most geotextiles are very susceptible to this type of degradation.



### 2.9.2 Design Method

All design methods described earlier are based on limit state condition of clay subgrade and single valued modulus of stiffness of reinforcing materials. Giroud and Noiray assumed elastic strength ( $\pi c_u$ ) in case of unreinforced condition and plastic strength ( $(\pi + 2)c_u$ ) in case of reinforced condition, without considering the degrees of mobilisation of resistances with accompanying deformation. Moreover, in case of reinforced condition these didn't satisfy the compatibility of deformation. The design method developed by Van den Berg and Kenter is based on membrane theory. They modelled the stress strain behaviour of subgrade soil by two straight lines which is little better representation than limit states.

76493

**CHAPTER THREE**

## CHAPTER THREE

### PROPOSED METHOD OF DESIGN

#### 3.1 GENERAL

A newly developed method of design applicable for the cases of, both reinforced and unreinforced unpaved roads on clay subgrade is presented in this chapter. The design methods developed so far by other researchers (Chapter Two), did not consider the non linear behaviour generally exhibited by most clay subgrade soils and reinforcing materials. The real load sharing mechanism of the constituent, clay subgrade and reinforcing materials under the compatible deformation is not also taken into account. A sound design method should take into account the degrees as well as the amounts of mobilisation of resistances in the materials under compatible conditions of deformation. Plane strain situation of the deformation developed under wheel loading is assumed in this study. The design method is based on a closed form solution of governing equations. These equations are developed by considering non linear behaviour of both subgrade clay soils and reinforcing materials as well as compatibility of rutting between them under all serviceability conditions.

To take into account the degradation of strength properties of the constituent materials under traffic loading, the so called "equivalent material" concept is used in developing the design



equations. These are modelled by using newly developed appropriate constitutive relations.

### 3.2 DESIGN CONSIDERATION

Many researcher published tests results of both model and prototype tests showing the beneficial effects of reinforcing on performance of unpaved roads(Chapter Two). Amongst them, Giroud and Noiray (1981) have presented detailed description of the problem considering parameters representing the subgrade soil, reinforcement, base aggregate, loading and geometry. However, their design method is based on the so called "elastic" and "ultimate" limiting states of the subgrade clay soil, which is assumed to be mobilised without considering the state of the accompanying strains and displacements. The only soil parameter which is used in their design is the undrained shear strength ( $c_u$ ). Further, they used single valued modulus of reinforcing materials which normally exhibit non linear load strain behaviour. The road system is composed of two materials, clay subgrade and reinforcement, with different characteristic properties and mechanisms of load transfer from the wheels. Therefore, a realistic design method should consider the amounts as well as the degrees of mobilisation of resistances in the materials under compatible deformation (rutting) conditions. These are considered in developing the design method presented in this chapter and are based on the following two fundamental and realistic considerations.

(1) Non linear behaviour of both the subgrade soil and

reinforcing material under repetitive loading conditions.

(2) Compatibility of rutting between subgrade soil and reinforcing element under all serviceability conditions.

To develop the design equations, a plane strain situation of the deformation of clay subgrade under wheel loading is assumed. This is done by using an analytical scheme, incorporating the true deviator stress strain behaviour of subgrade clay, suggested by Prakash, Saran and Sharan (1984). The hyperbolic model (Kondner, 1963) is used to characterise the stress strain load repetition behaviour of both subgrade clays and reinforcing materials. Most clayey soils and reinforcing materials were found to obey this law to a satisfactory level of accuracy.

Instead of the two approaches considering quasi static and traffic loading conditions used by Giroud and Noiray, a generalised design approach considering the non linear mechanical behaviour of, clayey subgrade soils and reinforcing elements under repetitive loading condition is established and presented. Analysis of behaviour under repeated traffic loading condition is achieved by using the equivalent material concept. This assumes the subgrade soils and reinforcing elements to be new (equivalent) materials possessing degraded mechanical behaviour which is appropriate for the number of load repetitions under consideration. These are represented by a series of curves each is appropriate for a number of load repetitions (N). Any point on



these curves depicts the final state of the mechanism without indicating the loading path.

### 3.3 GEOMETRY OF UNPAVED ROAD

Typical cross sections of reinforced and unreinforced unpaved road are presented in Figure 3.1. The notations used in this figure are,  $h_0$  = thicknesses (m) of aggregate layer required under unreinforced condition;  $h$  = thicknesses (m) of aggregate layer required under reinforced condition;  $\Delta h = h_0 - h$ , reduction in thicknesses (m) of aggregates due to presence of reinforcement.

### 3.4 LOADING CONDITION

The proposed method of analysis is mainly subjected to light buses, trucks, minibuses and Light Cross Country Vehicle (LCCV). A field survey was conducted to establish the average values of loadings and geometry of wheel contact areas of these vehicles. A general geometrical description of wheel configuration and contact area of a typical double wheel axle has been presented in section 2.2 (Figure 2.2). Those appropriate for single wheel axle is shown here in Figure 3.2. Average values of loadings and geometry of wheel contact areas were established from about fifty observations and are presented in chapter five.

### 3.5 PROPERTIES OF AGGREGATES

In this study the aggregates are assumed to be well graded, to provide sufficient interlock and effective load distribution.

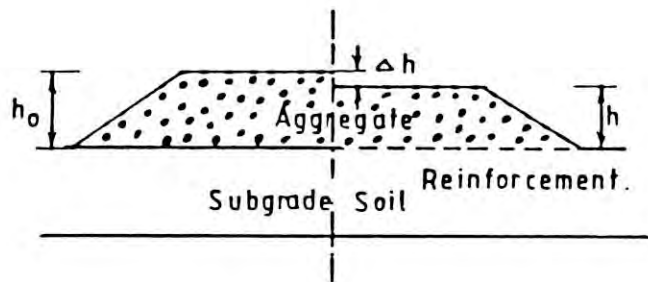
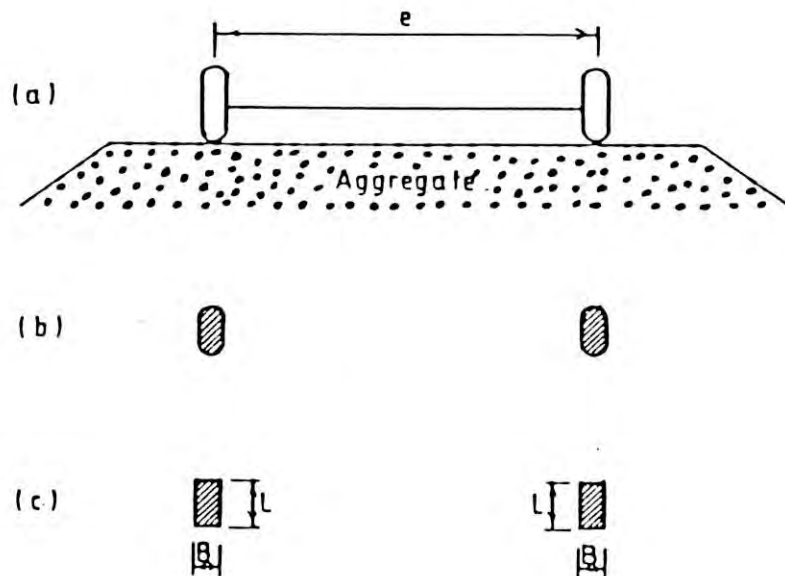


Figure 3.1 Geometry of Unpaved Road.



- (a) Geometry of Vehicle Axle
- (b) Tire Contact Areas
- (c) Equivalent Contact Area

Figure 3.2 Definition of Single Wheel Geometry and Contact Area.



The aggregates are assumed to be acting as a load distributing media only without the possibility of shearing type of failure within the aggregates. These should have California Bearing Ratio (CBR) larger than 80. To select proper type of aggregate size and gradation, DuPont chart (Celenese, 1975) should be used (Figure 2.16). The CBR value of brick aggregate normally found in Bangladesh fall in the range of 50 to 65 (Zakaria, 1982).

### 3.6 PROPERTIES OF SUBGRADE SOILS

Since clayey subgrade soils show non linear stress strain behaviour under wide ranges of deformation condition, a single limiting value description, using either undrained shear strength ( $c_u$ ) or California Bearing Ratio (CBR) for the subgrade clay soils is not sufficient. Moreover, a realistic representation of behaviour of clay soils under repeated wheel loading can only be modelled through properties and parameters obtained from representative repeated loading triaxial tests. Therefore, a new test setup was developed for this purpose. Tests were performed on a silty clay soil under representative confining condition to model its behaviour as well as to develop a generalised characterisation procedure. The newly developed non linear constitutive relation representing stress ( $\sigma$ ) - strain ( $\epsilon$ ) - and number of load repetitions ( $N$ ) behaviour is described in the next section.

#### 3.6.1 Constitutive Relation

The new non linear constitutive relation representing

stress-strain-load repetition behaviour for both clay subgrade and reinforcing elements is developed using the hyperbolic model forwarded by Kondner (1963). To establish the constitutive relation, the following steps are recommended. These are also explained in Figure 3.3 which should be used as ready reference.

- (1) Plot stress vs. strain upto failure strain or any other strain level for different load repetitions (Figure 3.3(a)).
- (2) Select a normalising strain  $\epsilon_n$  (e.g.  $\epsilon_n = \epsilon_f$ ).
- (3) Read off the stresses ( $\sigma_{nN}$ ) corresponding to the normalising strain ( $\epsilon_n$ ) for all load repetitions.
- (4) Plot normalised stress ( $\sigma_r = \sigma / \sigma_{nN}$ ) versus strain ( $\epsilon_r = \epsilon / \epsilon_n$ ) curves. All curves will pass through point (1,1) (Figure 3.3(b)).
- (5) Plot normalised curves in hyperbolic form ( $\epsilon_r / \sigma_r$ , versus  $\epsilon_r$ , Figure 3.3(c)).
- (6) Find the hyperbolic parameters  $a_N$  which are the intercepts on the ordinate axis.
- (7) Plot  $a_N$  vs.  $N$  on a semi log paper which is normally found to trace a straight line (Figure 3.3(d)).
- (8) Find the intercept of the straight line (corresponding to  $N=1$ ) and slope of the line (Figure 3.3(d)).
- (9) Plot  $\log N / (\sigma_1 - \sigma_{nN})$  vs.  $\log N$  on a plain paper (Figure 3.3(e)). This plot was also found to trace a straight line.
- (10) Find the intercept and slope of the line (Figure 3.3(e)).

### 3.6.2 Mathematical Formulation

The constitutive relation can be formulated as follows:

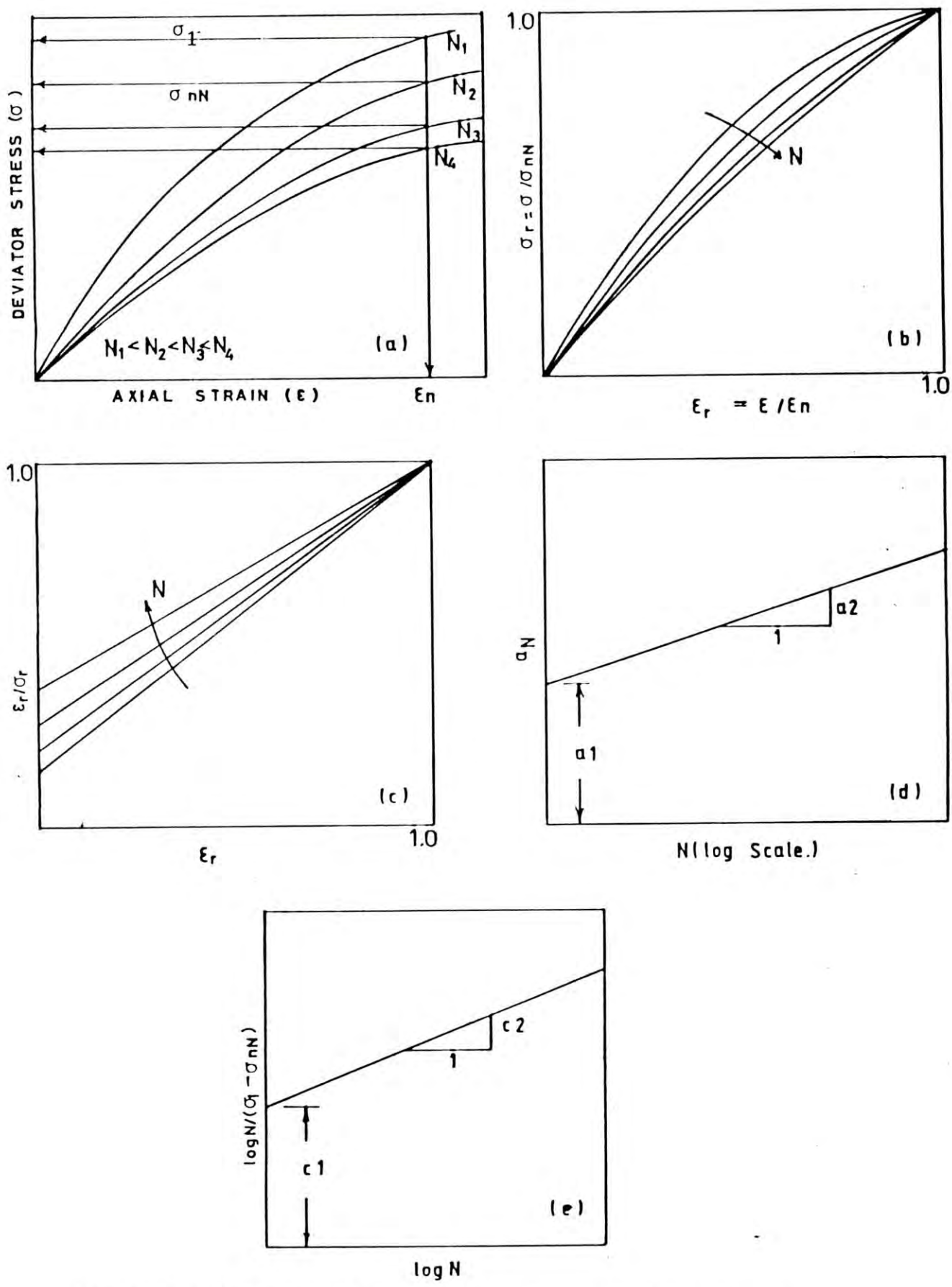


Figure 3.3 Qualitative Diagram of Constitutive Relation for Clay



$\epsilon_n$  = Normalising strain

$\sigma_{nN}$  = Normalising stress

From Figure 3.3(c)

$$\sigma_r = \frac{\epsilon_r}{a_N + (1 - a_N) \epsilon_r} \quad \dots 3.1$$

Now putting  $\sigma_r = \sigma/\sigma_{nN}$ ,  $\epsilon_r = \epsilon/\epsilon_n$  in Equation 3.1

$$\sigma = \frac{\sigma_{nN} \epsilon}{a_N \epsilon_n + (1 - a_N) \epsilon} \quad \dots 3.2$$

From Figure 3.3(d)

$$a_N = a_1 + a_2 \log N \quad \dots 3.3$$

From Figure 3.3(e)

$$\frac{\log N}{\sigma_1 - \sigma_{nN}} = c_1 + c_2 \log N$$

After rearranging

$$\sigma_{nN} = \sigma_1 - \frac{\log N}{c_1 + c_2 \log N} \quad \dots 3.4$$

Now from Equations 3.3 and 3.4 putting the value of  $a_N$  and  $\sigma_{nN}$  in Equation 3.2:

$$\sigma = \frac{(\sigma_1 - \log N / (c_1 + c_2 \log N)) \epsilon}{(a_1 + a_2 \log N) \epsilon_n + (1 - a_1 - a_2 \log N) \epsilon} \quad \dots 3.5$$

Where  $\sigma_1$ ,  $\epsilon_n$  and  $c_1$  are limiting values and  $a_1$ ,  $a_2$  and  $c_2$  are calibration factors.

Equation 3.5 can be modified to most well known hyperbolic form:

$$\sigma = \frac{\epsilon}{A_1 + A_2 \epsilon} \quad \dots 3.6$$

where,

$$A_1 = \frac{(a_1 + a_2 \log N) \epsilon_n}{(\sigma_1 - \log N / (c_1 + c_2 \log N))}$$

$$A_2 = \frac{1 - a_1 - a_2 \log N}{(\sigma_1 - \log N / (c_1 + c_2 \log N))}$$

$A_1$  and  $A_2$  may termed as modified hyperbolic parameters which may be readily used to establish the  $p_0 - \delta$  relation appropriate for the load repetition ( $N$ ).

### 3.7 Properties of Reinforcing Elements

Most of the reinforcing materials (geotextiles, geogrids and jute fabrics) exhibit non linear load strain behaviour under wide ranges of strain levels. If the working level of strain is at low strain level (say less than 2 percent) then the single modulus

treatment (normally taken at 2 percent strain level) will not produce considerable error for reinforcing elements which show concave downward load strain curves. But for reinforcements which show concave upward load strain curve like jute fabrics, may induce considerable error in the analysis. If the working level of strain is higher than 2%, the design will be on the unsafe side for first type of reinforcing element (described above) and on the conservative side for later type of reinforcing element. Therefore a single modulus representation (at 2 percent strain level) will not be a true representation of the actual behaviour. Load ( $P_r$ ) strain ( $\epsilon_r$ ) number of load repetitions ( $N$ ) relations similar to those suggested for clays is also developed using hyperbolic representation. Testing techniques to evaluate the design parameters of load strain behaviour of reinforcing elements, have been suggested by McGown, et. al. (1982,1984). A testing technique similar to these, having modification for performing tests under repeated loading was developed for this study.

### 3.7.1 Constitutive Relation

In general, reinforcing materials show two types of load strain pattern. The first type shows decrease in stiffness with increasing strain and this trend is continued upto failure strain. The second type show increase in stiffness with increasing strain upto a level of strain depending on the type of material and after that the stiffness values decreases. For these two types of materials, different approach is proposed to



formulate the constitutive relation.

Materials type 1:

- (1) Plot load( $P_r$ ) vs. strain( $\epsilon_r$ ) upto failure or any other working strain level for different load repetitions (Figure 3.4(a)).
- (2) Select a normalising strain  $\epsilon_{rN}$  (e.g.  $\epsilon_{rN} = \epsilon_{r1}$ )
- (3) Read off the loads ( $P_{rN}$ ) corresponding to the normalising strain ( $\epsilon_{r1}$ ) for all load repetitions.
- (4) Plot normalised load ( $P_{rN} = P_r / P_{rN}$ ) versus normalised strain ( $\epsilon_{rN} = \epsilon_r / \epsilon_{r1}$ ) curves. All curves will pass through the point (1,1) (Figure 3.4(b)).
- (5) Plot normalised curves in hyperbolic form (Figure 3.4(c)).
- (6) Find the hyperbolic parameter  $a_{rN}$  which are the intercepts on the ordinate axis.
- (7) Plot  $a_{rN}$  vs.  $N$  on a semilog paper which is normally found to trace a straight line (Figure 3.4(d)).
- (8) Find the intercept of the straight line (corresponding to  $N=1$ ) and slope of the line (Figure 3.4(d)).
- (9) Plot  $\log N / (P_{r1} - P_{rN})$  vs.  $\log N$  on a plain paper (Figure 3.4(e)). This plot was also found to trace a straight line.
- (10) Find the intercept and slope of the line (Figure 3.4(e)).

Materials Type 2:

- (1) Plot load( $P_r$ ) vs. strain( $\epsilon_r$ ) upto failure or any other

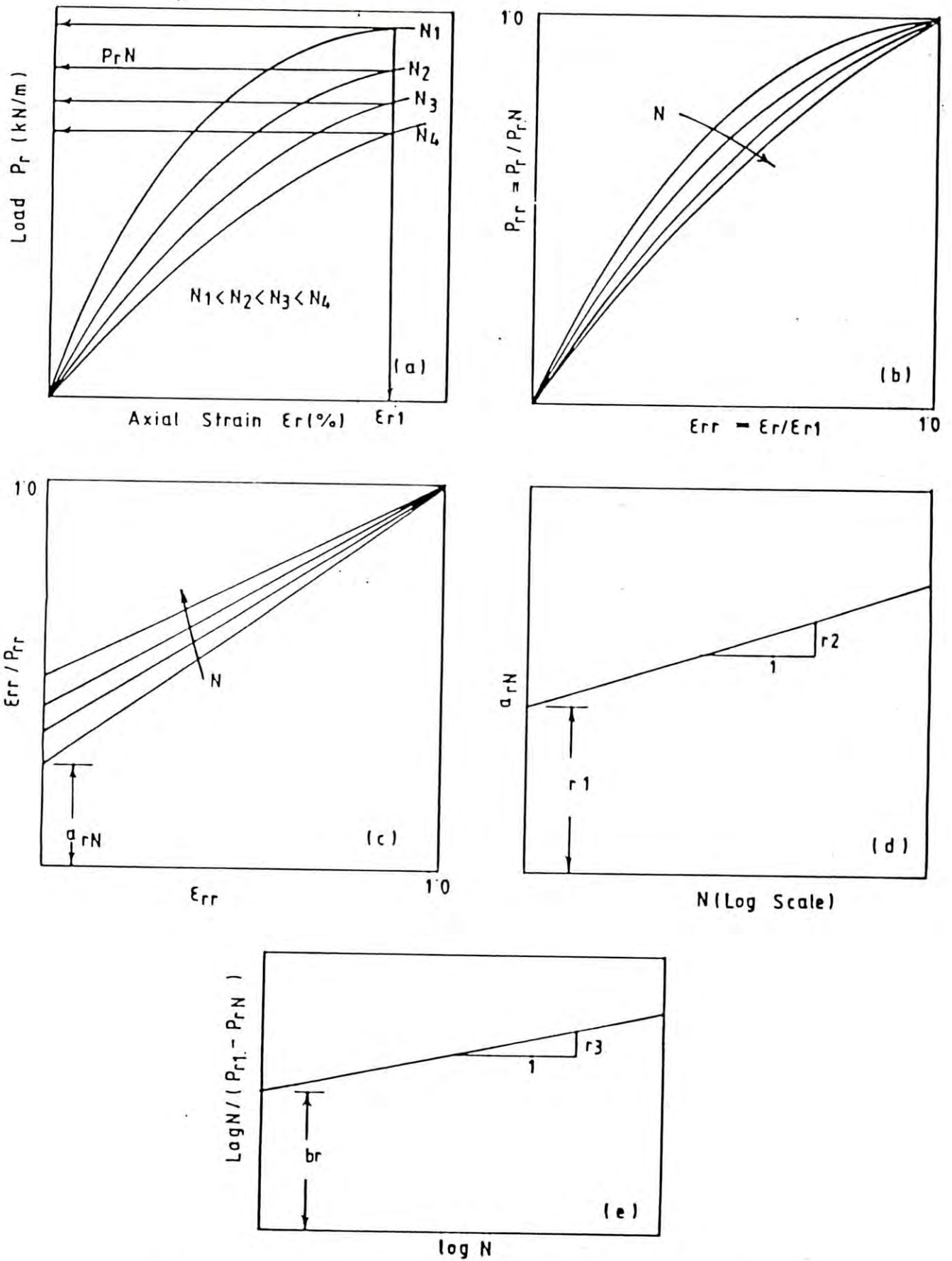


Figure 3.4 Qualitative Diagram of Constitutive Relation For Reinforcing Material Type-1.

working level of strain for different load repetitions (Figure 3.5(a)).

(2) Select a normalising load  $P_{rN}$  (e.g.  $P_{rN} = P_{r1}$ ).

(3) Read off normalising strains ( $\epsilon_{rN}$ ) corresponding to the normalising loads ( $P_{r1}$ ) for each load repetitions.

(4) Plot normalised load ( $P_{rR}$ ) versus normalised strain ( $\epsilon_{rR}$ ) curves. All curves will pass through the point (1,1) (Figure 3.5(b)).

(5) Plot normalised curves in hyperbolic form ( $P_{rR}/\epsilon_{rR}$  vs.  $P_{rR}$ , Figure 3.5(c)).

(6) Find the hyperbolic parameters  $a_{rN}$  which are the intercepts on the ordinate axis.

(7) Plot  $a_{rN}$  vs.  $N$  on a semilog paper which is normally found to trace a straight line (Figure 3.5(d)).

(8) Find the intercept of the straight line (corresponding to  $N=1$ ) and slope of the line (Figure 3.5(d)).

(9) Plot  $\epsilon_{rN}$  vs.  $N$  on a semilog paper (Figure 3.5(e)).

(10) Find the intercept and slope of the line.

### 3.7.2 Mathematical Formulation

The constitutive relations can be formulated as follows:

$\epsilon_{rN}$  = Normalising strain

$P_{rN}$  = Normalising load

Like clay (Section 3.6.2) the  $P_r - \epsilon_r - N$  relation of the reinforcing elements may be established as follows:



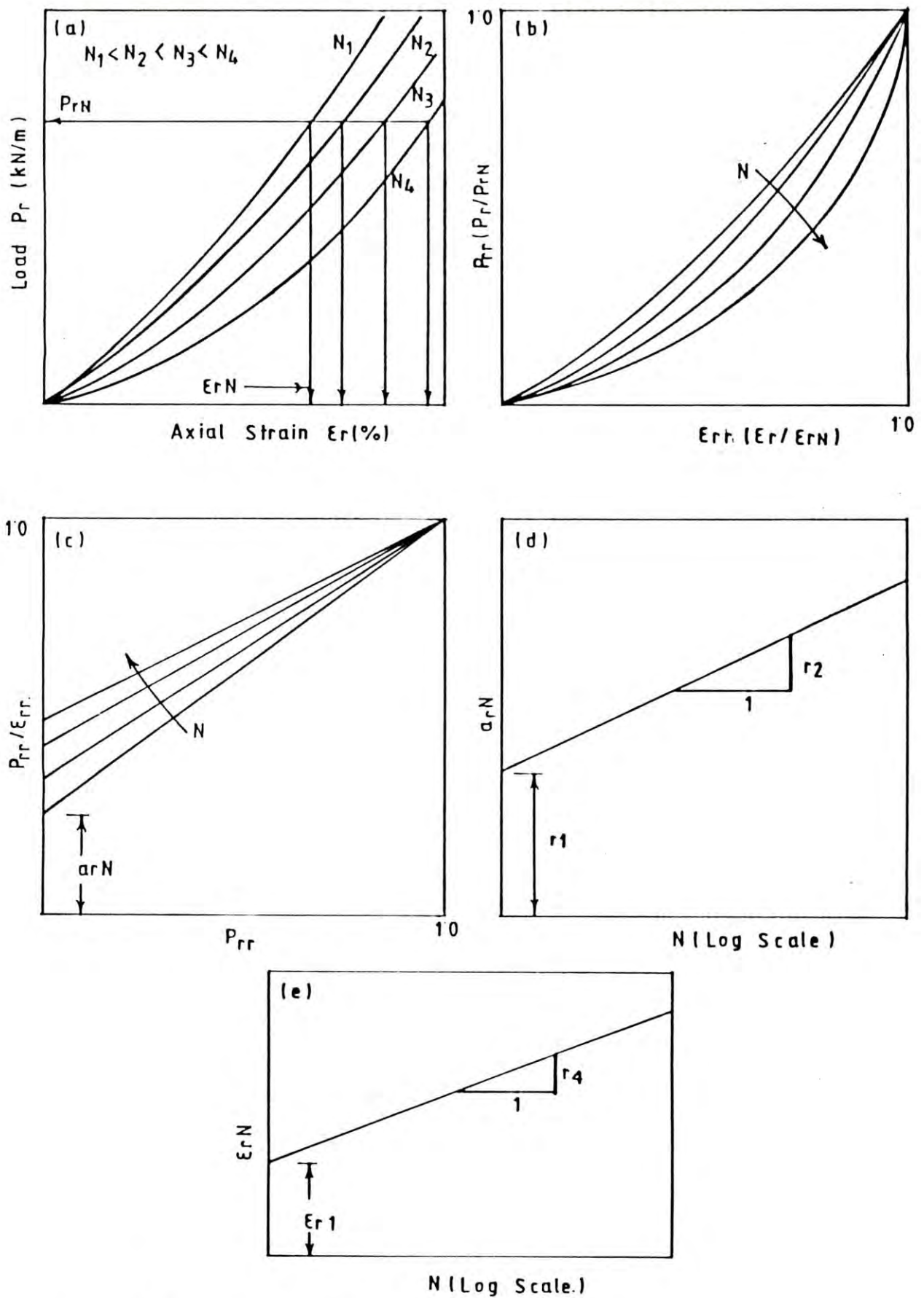


Figure 3.5 Qualitative Diagram of Constitutive Relation for Reinforcing Material Type-2

For material type 1

From Figure 3.4(c)

$$P_{rr} = \frac{\epsilon_{rr}}{a_{rN} + (1 - a_{rN}) \epsilon_{rr}} \quad \dots 3.7$$

Now putting  $P_{rr} = P_r/P_{rN}$  and  $\epsilon_{rr} = \epsilon_r/\epsilon_{r1}$  in Equation 3.7

$$P_r = \frac{\epsilon_r \cdot P_{rN}}{a_{rN} \epsilon_{r1} + (1 - a_{rN}) \epsilon_r} \quad \dots 3.8$$

From Figure 3.4(d)

$$a_{rN} = r_1 + r_2 \log N \quad \dots 3.9$$

From Figure 3.4(e)

$$\frac{\log N}{P_{r1} - P_{rN}} = b_r + r_3 \log N$$

After rearranging

$$P_{rN} = P_{r1} - \log N / (b_r + r_3 \log N) \quad \dots 3.10$$

Now from Equations 3.9 and 3.10 putting the values of  $a_{rN}$  and  $P_{rN}$  in Equation 3.8:

$$P_r = \frac{\epsilon_r (P_{r1} - \log N / (b_r + r_3 \log N))}{(r_1 + r_2 \log N) \epsilon_{r1} + (1 - r_1 - r_2 \log N) \epsilon_r} \quad \dots 3.11$$

For material type 2

From Figure 3.5(c)

$$P_{rr} = \frac{a_{rN} \epsilon_{rr}}{1 - \epsilon_{rr}(1 - a_{rN})} \quad \dots 3.12$$

From Figure 3.5(d)

$$a_{rN} = r_1 + r_2 \log N \quad \dots 3.13$$

From Figure 3.5(e)

$$\epsilon_{rN} = \epsilon_{r1} + r_4 \log N \quad \dots 3.14$$

Now from Equations 3.12, 3.13 and 3.14 and using  $P_{rr} = P_r/P_{r1}$  and

$\epsilon_{rr} = \epsilon_r / \epsilon_{rN}$ ,  $P_r$  becomes:

$$P_r = \frac{P_{r1}(r_1 + r_2 \log N) \epsilon_r}{\epsilon_{r1} + r_4 \log N - (1 - r_1 - r_2 \log N) \epsilon_r} \quad \dots 3.15$$

Where  $P_{r1}$ ,  $\epsilon_{r1}$  and  $b_r$  are limiting values and  $r_1$ ,  $r_2$ ,  $r_3$  and  $r_4$  are calibration factors. Test was done on one non woven tape polyethylene geotextile and two grades of jute fabrics (Kabir, et. al,1988) to show the applicability of the relations.

After rearrangement Equations 3.11 and 3.15 take the most



well known Hyperbolic form like clay subgrade as:

$$P_r = \frac{\epsilon_r}{b_1 + b_2 \epsilon_r} \quad \dots 3.16$$

where,

$$b_1 = \frac{(r_1 + r_2 \log N) \epsilon_{r1}}{P_{r1} - \log N / (b_r + r_3 \log N)}$$

For material type 1

$$b_1 = \frac{\epsilon_{r1} + r_4 \log N}{P_{r1} (r_1 + r_2 \log N)}$$

For material type 2

$$b_2 = \frac{1 - r_1 - r_2 \log N}{P_{r1} - \log N / (b_r + r_3 \log N)}$$

For material type 1

$$b_2 = \frac{-(1 - r_1 - r_2 \log N)}{P_{r1} (r_1 + r_2 \log N)}$$

For material type 2

$b_1$  and  $b_2$  may be termed as modified hyperbolic parameters which may be readily used in Equation 3.35 appropriate for the number

of load repetitions.

### 3.8 ANALYSIS OF BEHAVIOUR OF ROAD STRUCTURE

Giroud and Noiray (1981), in their design method used two separate analyses. One is for very light traffic (1 to 10 passages) and the other is for heavy traffic (not more than 10,000 passages of standard axle). The so called "Quasi-Static" analysis is used for cases under light traffic. The design parameters for soil and reinforcing elements are determined from monotonic test results. They used empirical equation given by Webster and Alford (1978) based on insitu test data produced by Hammit (1970) as described earlier, to develop analysis for heavy traffic loading in conjunction with the results obtained from quasi static analysis. In contrast, in this study an unified method of analysis for any intensity of traffic loading is established. The analysis method is based on newly developed constitutive relations appropriate for soil and reinforcement obtained from repeated loading tests which has been described in sections 3.6 and 3.7.

#### 3.8.1 Load Distribution Through Aggregate Layer

Like Giroud and Noiray, a pyramidal load distribution from the wheels through aggregate layer is assumed. The salient features of load distribution and the geometry of the problem for cases with or without reinforcement has been presented earlier in Figure 2.5. The pressure at the bottom of the aggregate layer, due to wheel loading from traffic, may be represented as follows

(Figure 2.5).

For cases without reinforcement, the pressure is:

$$p_o = \frac{P}{2(B + 2h_o \tan \alpha_o)(L + 2h_o \tan \alpha_o)} + \gamma h_o \quad \dots 3.17$$

For cases with reinforcement, the pressure is:

$$p = \frac{P}{2(B + 2h \tan \alpha)(L + 2h \tan \alpha)} + \gamma h \quad \dots 3.18$$

Like Giroud and Noiray recommendation it is assumed that  $\tan \alpha_o = \tan \alpha = 0.6$ . These values are used in all subsequent calculation presented here.

### 3.8.2 Behaviour of Clay Subgrade

The clay subgrade is assumed to be semi infinite, homogeneous and isotropic. The load deformation behaviour of clay subgrade under loading from wheels transferred through the aggregate layer is obtained by using the calculation scheme suggested by Prakash, Saran and Sharan. The method utilizes two parameter hyperbolic deviator stress strain relationship for clay soils. These are obtained from the constitutive relations  $\sigma - \epsilon - N$  described earlier. In this method following steps are taken:

(1) The clay layer beneath the loaded area is divided into a number of horizontal slices which is usually done in settlement calculation (Figure 3.6(a)). The influence of stresses are



considered upto a depth of three times the width of loading area.

(2) The major and minor principal stresses along the center line of the loaded area in each slice is calculated using theory of elasticity (Table 2.1, Figure 3.6(b)).

(3) The strain in the two directions are calculated using the hyperbolic stress strain relation and theory of elasticity (Equations 2.58 to 2.63, Figure 3.6(c)).

(4) The strain in the vertical direction, for each slice, is then determined from the strains in the principal directions using appropriate direction cosines.

(5) The deformation of each slice is the product of the strain in the vertical direction at the centre of the slice and its thickness.

(6) The total settlement is then obtained as the summation of deformations of each slice which is denoted as "S".

(7) The steps through one to six are repeated for different pressure ( $p_0$ ) on loaded area (2a).

(8) The steps through one to seven are repeated for different values of pressure ( $p_0$ ) on loaded area and width of loaded area (2a). The load settlement curve for different width of foundation is shown in Figure 3.6(d). The plot of pressure,  $p_0$  and the ratio ( $\delta = S/2a$ ) is normally found to trace a unique curve which is obtained by normalising the different load settlement curves by their respective width of loading. Prakash, Saran and Sharan found good agreement amongst results obtained from, this method, finite element analysis and test data.

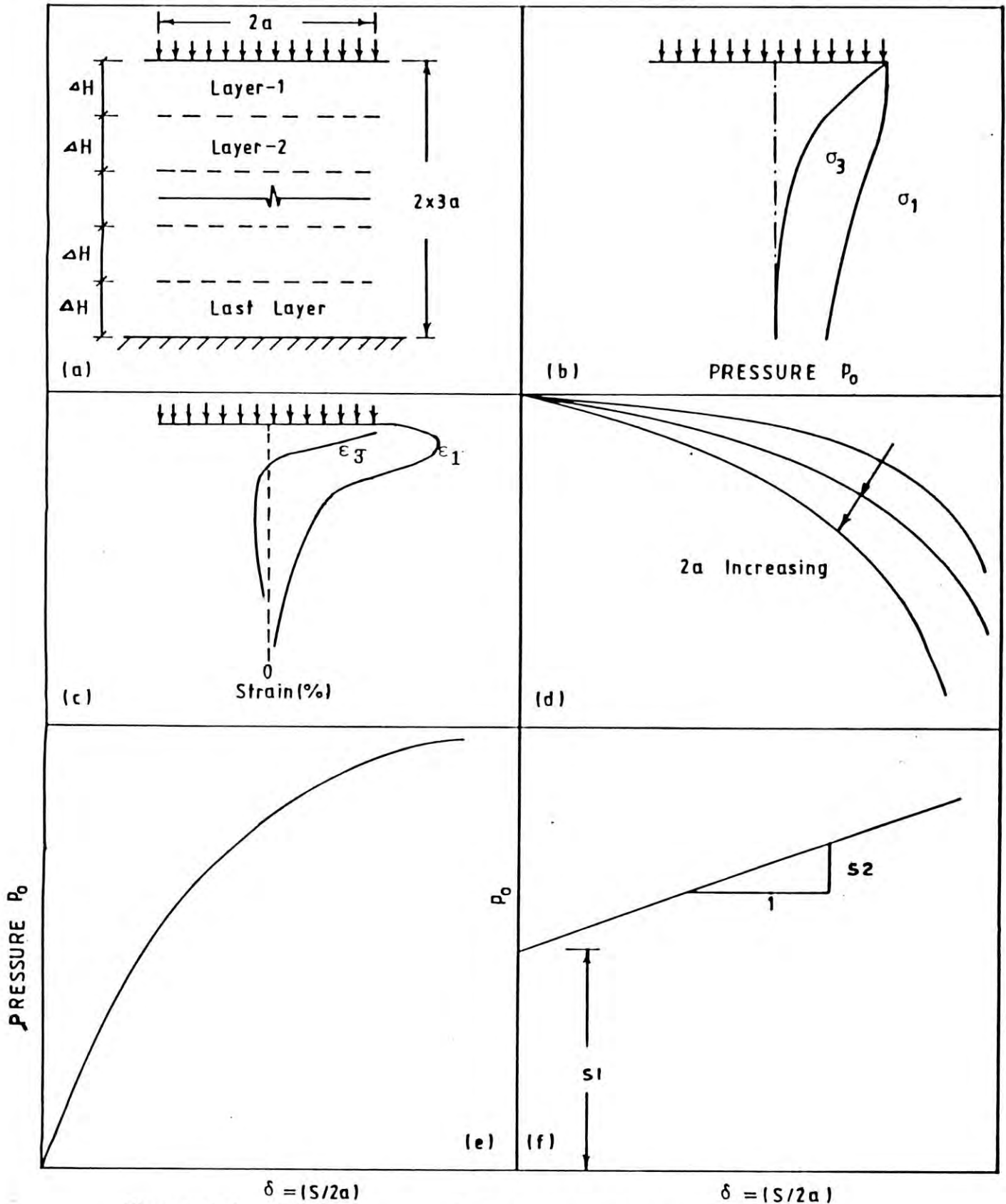


Figure 3.6 Qualitative  $p_0 - \delta$  Formulation for Clay Subgrade

The  $p_0 - \delta$  curves for clays, under investigation are shown in Figure 4.13 for different intensity of traffic. The hyperbolic representation of the  $p_0 - \delta$  relations are also presented in Figure 4.13. The design parameters, obtained from hyperbolic representation of  $p_0 - \delta$  relation of soil under investigation are provided in Table 5.1.

### 3.8.3 Geometry of Deformation

As the soil is assumed incompressible, the loading from the wheels causes the unpaved road to deform in the wavy manner. Thus the volume of soil displaced downwards due to wheel loading must be equal to that displaced upward due to heaving. Schematic diagrams of both unreinforced and reinforced unpaved road structures have been presented in Figure 3.1. Like Giroud and Noiray, three possible modes of deformation with respective equation and diagrams have been shown in Equations 2.27 and 2.28 and Figure 2.9. These equations can be transformed into a single equation through a single parameter  $C$  i.e.  $S = Cr$

where,

$$C = \frac{a'}{a + a'} \quad \text{Case I} \quad \dots 3.19$$

$$C = \frac{2a^2}{2a^2 + 3aa' - a'^2} \quad \text{Case II} \quad \dots 3.20$$

$$C = 1/2 \quad \text{Case III} \quad \dots 3.21$$



The strain in the reinforcement corresponding to the modes of deformation are shown in Equations through 2.29 to 2.32.

#### 3.8.4 Unpaved Road Without Reinforcement

The design of unpaved road without reinforcement involve determination of thickness of aggregate layer for different degrees of rutting. It has been discussed earlier that  $p_o - \delta$  relation for clay subgrades may be represented by hyperbolic functions. Therefore, the resistances,  $p_o$ , of the clay subgrade may be represented as:

$$p_o = \frac{\delta}{s_1 + s_2 \delta} + \gamma h_o \quad \dots 3.22$$

where,  $s_1$  and  $s_2$  are hyperbolic parameters (Figure 4.13 and Table 5.1) for clay subgrade appropriate for the number of load repetition (N). Now from Equations 3.17 and 3.22:

$$\frac{P}{2(B + 2h_o \tan \alpha_o)(L + 2h_o \tan \alpha_o)} = \frac{\delta}{s_1 + s_2 \delta} \quad \dots 3.23$$

Putting the value of  $\tan \alpha_o$  and  $\delta$  as defined earlier:

$$\frac{P}{2(B + 1.2h_o)(L + 1.2h_o)} = \frac{S}{(2a_o s_1 + s_2 S)} \quad \dots 3.24$$

Values of "S" as a function of "r" may be obtained from Equations 3.19, 3.20 and 3.21 depending on the mode of deformation. Design

charts giving thicknesses ( $h_0$ ) of aggregate layer for different degrees of rutting may now be produced from Equation 3.24 and using appropriate soil parameters  $s_1$  and  $s_2$ . Such charts for unpaved roads on a clay subgrade is produced in chapter five.

### 3.8.5 Unpaved Road With Reinforcement

The subgrade, saturated clay soil is assumed to be incompressible. Therefore, settlement under the wheels will be accompanied by heave between and beyond the wheels. Consequently, the reinforcing element, shown in Figure 3.7, takes a wavy shape, thereby getting stretched. In the zone AB (Figure 3.7) the stretching of the reinforcing element will relieve the underlying clay subgrade of some pressure transmitted from the wheels through the aggregates. Similar effects will produce additional confining of the soil in the zones BB and AC. Therefore, the use of reinforcement in an unpaved road structure may be described as producing three beneficial effects as described earlier. In this analysis, like that by Giroud and Noiray, the pressure relieving effect is only considered.

From equilibrium consideration, the pressure  $p$ , transmitted from the wheels through the aggregates on part AB (Figure 3.7) of the reinforced road is shared by clay subgrade and reinforcing element and should equal to:

$$p = p_s + p_r$$

... 3.25

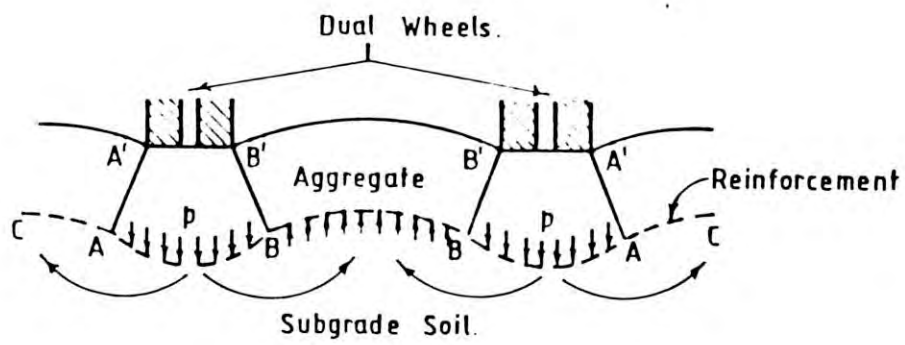


Figure 3.7 Deformed Shape of Reinforcement and Equilibrium



where,  $p_s$  and  $p_r$  are mobilised reactions (pressure) in the clay subgrade and reinforcement respectively appropriate for the intensity of traffic loading ( $N$ ), under the same degree of rutting. Therefore, determination of  $p_s$  and  $p_r$  should be based on analysis of the kinematics of the deformation produced due to wheel loading.

In reinforced unpaved road, for a known degree of rutting, the pressure shared by the clay subgrade may be determined from the following equation:

$$p_s = \frac{\delta}{s_1 + s_2 \delta} + \gamma h \quad \dots 3.26$$

where  $\delta = S/2a$  and the values of "S" as a function of rut depth may be obtained from Equations 3.19, 3.20 and 3.21.

The force due to pressure,  $p_r$  acting on zone AB (Figure 3.7) is equivalent to the vertical component of the tension  $p_r$  in the reinforcing element acting at points A and B. Therefore:

$$a.p_r = P_r \cos \beta \quad \dots 3.27$$

From property of parabolas

$$\tan \beta = a/2S = 1/(4(S/2a)) = 1/4\delta \quad (\delta = S/2a)$$

Thus

$$\cos\beta = \frac{1}{\sqrt{1 + 1/16 \delta^2}} = 4 \sqrt{\delta^2 / (16 \delta^2 + 1)} \quad \dots 3.28$$

Again from hyperbolic load strain representation of reinforcing elements, using parameters b1 and b2:

$$P_r = \frac{\epsilon_r}{b1 + b2 \epsilon_r} \quad \dots 3.29$$

The parameters b1 and b2, are dependent on the characteristics of reinforcing element and intensity of traffic loading (N). Values of b1 and b2 may be readily determined from equation 3.16. Now putting the values of cosβ and Pr from Equations 3.28 and 3.29 in Equation 3.27:

$$a. p_r = \frac{4 \epsilon_r}{(b1 + b2 \epsilon_r)} \left( \sqrt{\delta^2 / (16 \delta^2 + 1)} \right) \quad \dots 3.30$$

From the assumption of parabolic deformation, the strain in the reinforcing element is:

$$\epsilon_r = .5 [ \sqrt{1 + (2S/a)^2} + (a/2S) \ln \{ (2S/a) + \sqrt{1 + (2S/a)^2} \} - 2 ] \quad \dots 3.31$$

Now substituting the value of  $\delta = S/2a$  in Equation 3.31:

$$\epsilon_r = .5 [ \sqrt{1 + 16 \delta^2} + (1/4\delta) \ln(4\delta + \sqrt{1 + 16 \delta^2}) - 2 ] \quad \dots 3.32$$

From Equations 3.30 and 3.32, it is clear that  $p_r$  may be expressed as a function of  $\delta$  only for different values of  $N$ . The pressure  $p_r$  may be obtained from Equation 3.30 as:

$$p_r = \frac{4 \epsilon_r \delta}{a(b_1 + b_2 \epsilon_r) \sqrt{(16 \delta^2 + 1)}} \quad \dots 3.33$$

Now from Equations 3.18 and 3.25

$$\frac{P}{2(B + 2h \tan \alpha)(L + 2h \tan \alpha)} = p_s + p_r \quad \dots 3.34$$

Now putting the value of  $\tan \alpha$ ,  $p_s$  and  $p_r$  as defined earlier:

$$\frac{P}{2(B + 1.2h)(L + 1.2h)} = \frac{\delta}{s_1 + s_2 \delta} + \frac{4 \epsilon_r \delta}{a(b_1 + b_2 \epsilon_r) \sqrt{(16 \delta^2 + 1)}} \quad \dots 3.35$$

The parameters  $\epsilon_r$  and  $\delta$  are functions of the degrees of rutting. Design charts giving required thicknesses of aggregates, "h" due to different degrees of rutting, may now be produced from solution of Equation 3.35. The design charts for the reinforcing elements on the clay subgrades for different intensities of traffic loading ( $N$ ) are presented in chapter five.



**CHAPTER    FOUR**

## CHAPTER FOUR

### CHARACTERISATION OF DESIGN PARAMETERS

#### 4.1 GENERAL

In this chapter the method of characterisation, of design parameters of the constituent materials are presented. These are based on laboratory tests, some of which are newly developed as part of this study. The materials include a subgrade clay and a geotextile reinforcing element. The relevant laboratory test methods are also described briefly.

#### 4.2 CLAY SOILS

A soft silty clay soil obtained from the outskirts of Dhaka city was chosen for this study, as this type of soil occurs abundantly in Bangladesh. Tests on remoulded samples of this soil were performed to establish design parameters. The test program included a number of routine as well as special type of test. The latter types were specially developed for this study. The routine tests included Atterberg limits and unconsolidated undrained triaxial test. The repeated loading triaxial test method especially developed for the characterisation of design parameters is described in the following sections.

##### 4.2.1 Test Set up for Repeated Loading Triaxial Test of Soils

With fabrication of some small components, the conventional triaxial test apparatus was made ready for repeated loading

triaxial test. The test setup is shown in Figure 4.1. The method of preparation of soil samples is routine in nature and therefore, is not described here.

#### 4.2.2 Test Procedure

To simulate the field behaviour, appropriate amount of confining pressure was applied. To establish stress strain behavior at different load cycles, three levels of load were chosen. These were done by performing conventional triaxial tests. From these test results the back bone curve of the soil was established. The loads were chosen in such a way so that the final load doesn't incur any failure in the sample before 1000 cycles of loading and unloading.

The test procedure is described in the following steps, which should be read in conjunction with Figure 4.1.

- (1) A 1.4 inch diameter by 2.8 inch long cylindrical sample was taken and enclosed in a membrane by using a membrane stretcher.
- (2) Weight of the membrane enclosed sample was taken to 0.1g.
- (3) The base of the triaxial cell and its accessory lines were deaired properly by flushing with preboiled deaired water.
- (4) Two deaired porous stone was placed at top and bottom of the sample and the sample was placed on the base of the cell.
- (5) To fill up the cell with water valve 'w' was kept open until the cell is completely full of water.
- (6) Valves 'T' and 'B' in the top and bottom lines respectively were kept closed throughout the test.



- (7) Adjusting the manometer level, a cell pressure of 20.8 kPa was built up which was maintained throughout the the test.
- (8) The deformation dial gauge was clamped with the fixed vertical rod and initial reading was taken.
- (9) The cell pressure was then applied by opening valve 'p' and simultaneously appropriate counterweight, amounting to 0.45kg in this case, was placed on the hanger.
- (10) At this stage deformation dial gauge reading was taken.
- (11) The appropriate deviator stress was then applied through a direct hanger loading system and it was maintained for 15 seconds afterwhich the deformation dial gauge reading was recorded.
- (12) The deviator stress was then released, by removing the hanger weight, and this state was maintained for the next 15 seconds. The deformation dial gauge reading was then recorded.
- (13) Steps 11 and 12 were repeated upto 1000 times.

In the operations described in steps 11 and 12, the load (dead weight) was applied and released in sequence by using the base frame of triaxial machine (Figure 4.1).

#### 4.2.3 Test Results

The test results obtained from repeated loading triaxial tests on the silty clay soil are shown in Appendix I and a typical graphical representation is shown in Figure 4.2. The test results indicate that the stress strain behaviour of the soil under investigation show considerable degradation in stress strain behaviour with cycles of loading which occurred at a

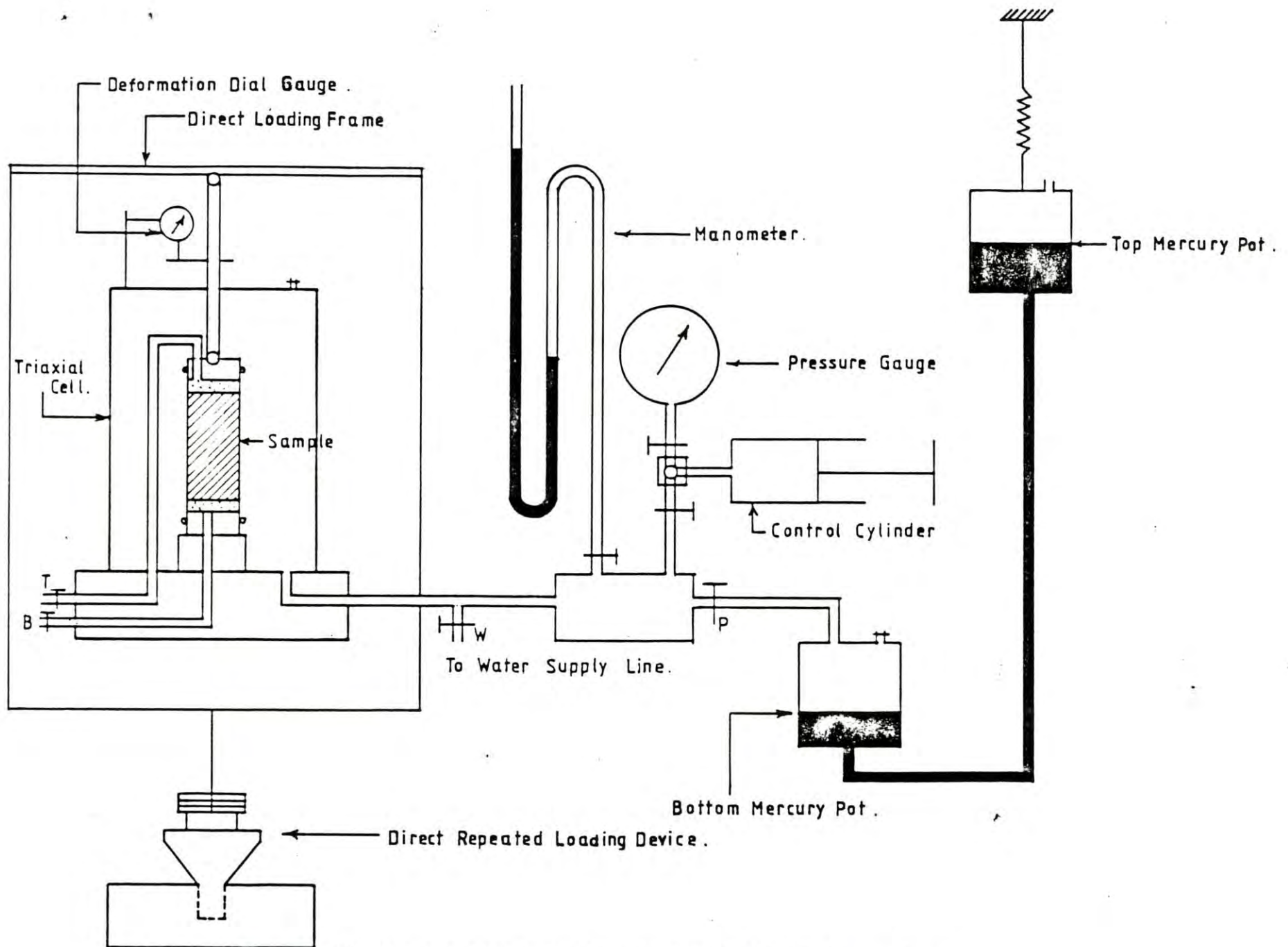


Figure 4.1 Repeated Loading Triaxial Test Apparatus

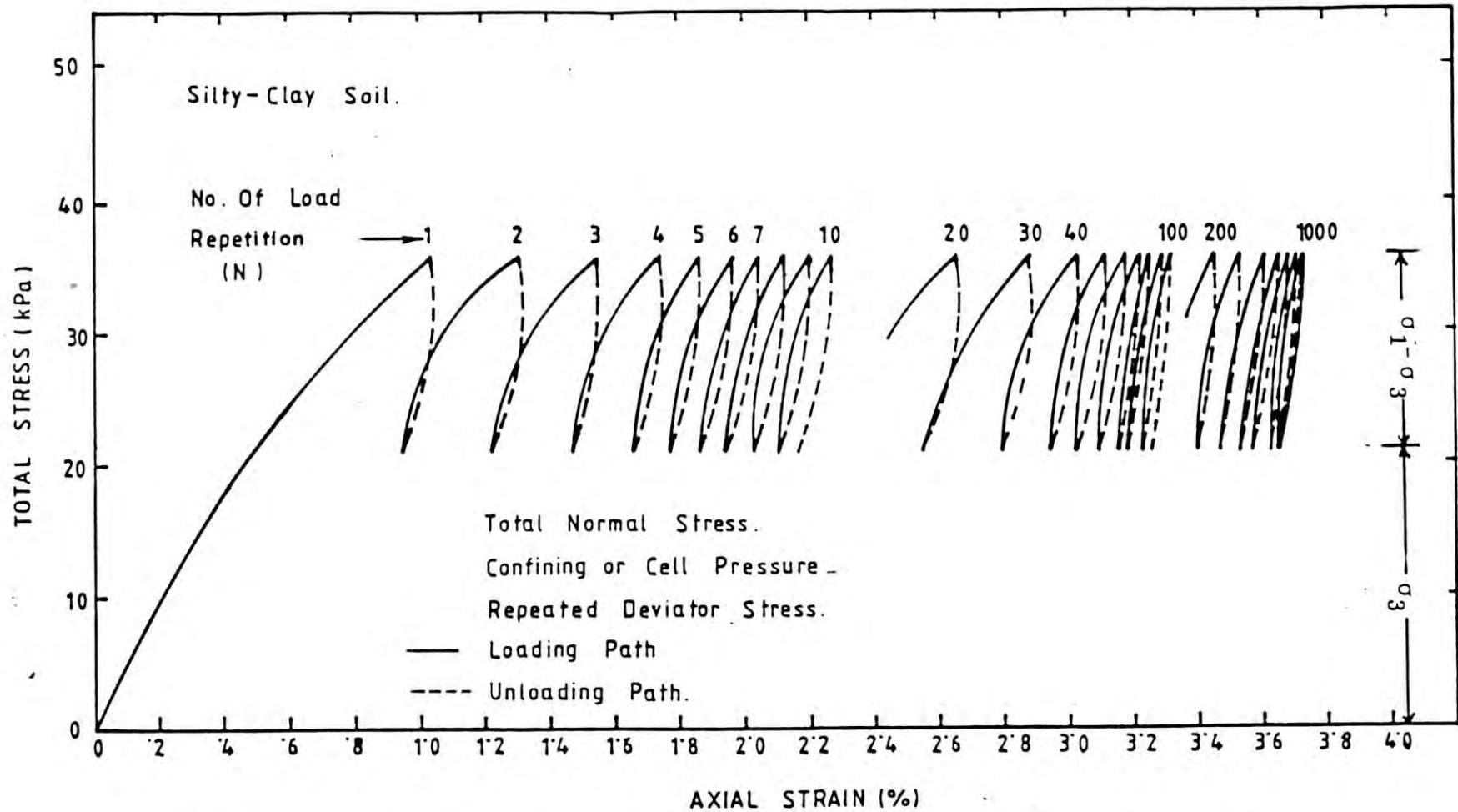


Figure 4.2 Graphical Representation of Repeated Loading Test Results of Clay Soil



diminishing rate. The physical properties along with the relevant design parameters are shown in Table 4.1.

#### 4.3 REINFORCING MATERIALS

To demonstrate the development of the newly conceived constitutive relations for reinforcing materials, which have been described in chapter three, a woven tape polyethylene material was chosen. The uniaxial repeated loading tensile test was conducted on samples of this material. This type of test may be adopted as a universal method which has been demonstrated, by the work of Saha and Kabir(1988) and Kabir et. al. (1988), for two grades of jute fabrics namely CANVAS 36X16 and CBC 72X12.

##### 4.3.1 Repeated Loading Test Rig for Reinforcing Materials

A repeated loading test rig, with some modifications from the creep test rig developed by Kabir (1984), was locally fabricated and installed. The rig along with the relevant test attachments are shown in Figure 4.3 and Plate 4.1. The test rig houses a loading hanger, two deformation dial gauges having appropriate seating arrangements, extension rods and shaddale mechanisms.

##### 4.3.2 Preparation of Samples

The size of the samples were taken 100 mm in gauge length and 200 mm in width conforming to ASTM Standard. Initially 100 mm X 300 mm samples were taken. Both top and bottom 100 mm were reinforced with fibre glass fabric tapes together with polyester

Table 4.1 Properties of Clay Soil

Liquid Limit		60.0
Plastic Limit		23.0
Natural Moisture Content(%)		34.0
Limiting Values	$\sigma_1$ (kPa)	40.0
	$\epsilon_n$ (%)	20.0
	a1	0.198
Calibration Factors	c1 (kPa <sup>-1</sup> )	0.105
	c2 (kPa <sup>-1</sup> )	0.1098
	a2	0.02228

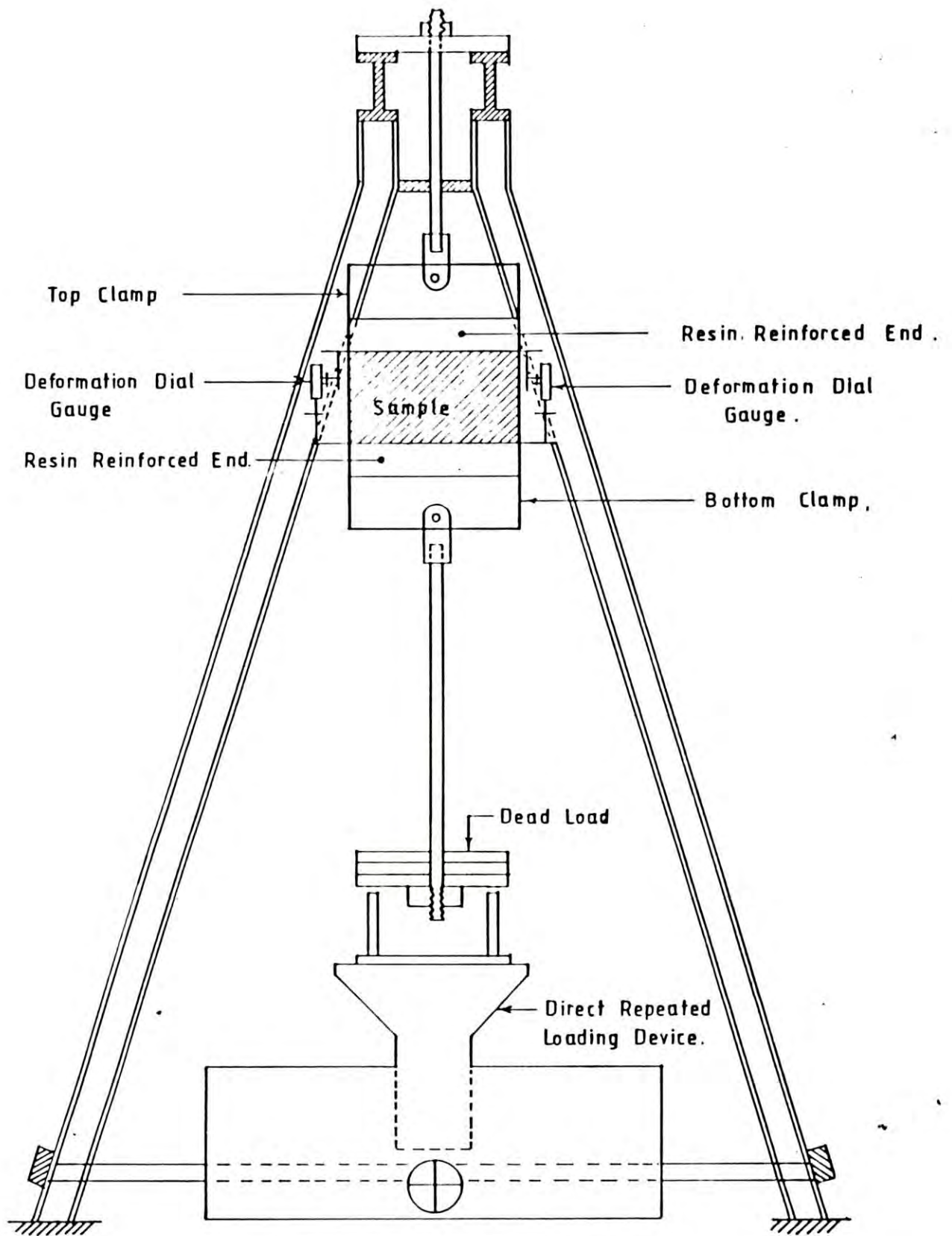


Figure 4.3 Repeated Loading Test Rig





Plate 4.1 Photograph of Repeated Loading Test Rig

resin. This provided the very stiff reinforced end sections required for suitable clamping. A catalyst, methyl keaton peroxide was used to accelerate the setting time as well as to control the chemical reaction. At least 24 hours were allowed for curing time. After that holes were drilled in the prepared reinforced ends of the specimen. Each half of the end clamps was then fitted at each end of the specimen, by a set of six cap screws. Coarse sand paper was placed between the specimen and the clamps, which were themselves serrated. This avoided slippage between the grips and the specimen. To measure the deformation over the gauge length of the unreinforced geotextile specimen, two steel rods of about 3 mm in diameter, were bonded onto each of the leading edges of the reinforced geotextile. The sample preparation steps are shown schematically in Figure 4.4.

#### 4.3.3 Test Procedure

Like clay soil, to determine the levels of loads at which repeated loading tests would be performed, a couple of specimens of the polyethylene geotextile was tested in a Universal Testing Machine upto failure load. From this test result three levels of load were chosen for performing repeated loading tests.

To perform repeated loading uniaxial tensile tests the following procedures were adopted.

- (1) The top clamp of the specimen was connected through a pin and shaddle mechanism to the top plate of the rig.
- (2) The bottom clamp of the specimen was connected through a pin

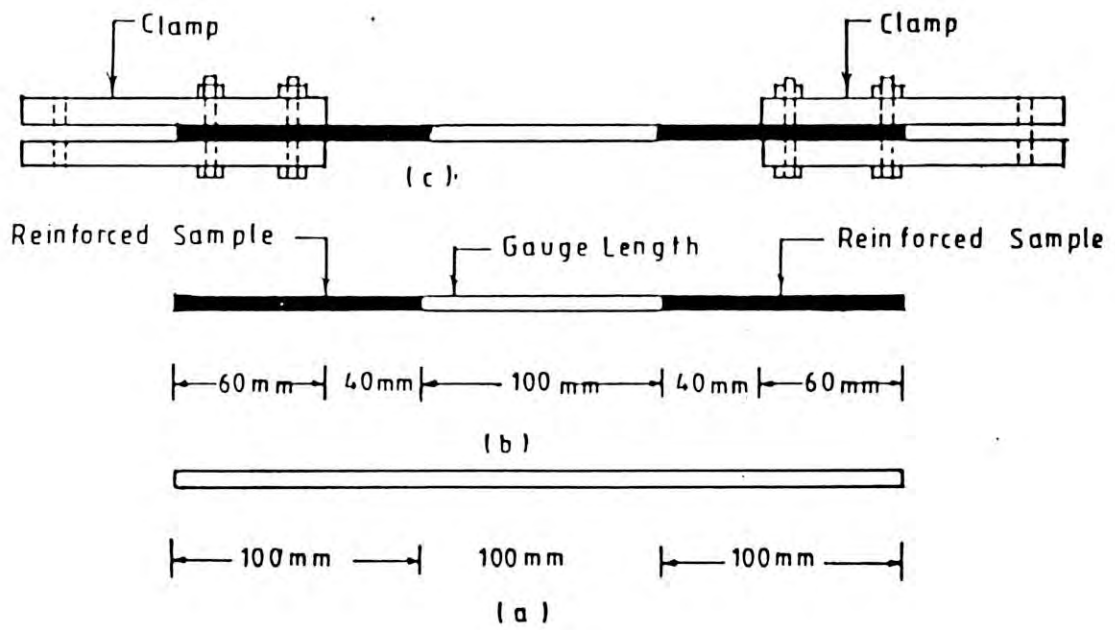


Figure 4.4 Schematic Diagram of Sample Preparation.



and shaddle mechanism to the direct loading hanger system.

(3) The weight of the hanger was preselected to provide the tare weight which is required to take away any slack in the specimen as well as the clamping mechanisms.

(4) Two deformation dial gauges were attached, each on either side of the specimen, between the gauge length and initial dial readings were taken.

(5) Predetermined load (combination of 10 kg and 5 kg dead weight) was placed on the seat of the hanger and the sample was loaded. After loading both dial gauges readings were taken.

(6) The sample was then unloaded and again both the dial gauges readings were recorded.

(7) Steps 5 and 6 were repeated upto 1000 times.

As in the case of repeated load tests on clay, the base frame of triaxial test apparatus was used to repeat application of loads (Figure 4.3 and Plate 4.1).

#### 4.3.4 Test Results

The results averaged from tests on twin samples are presented in Appendix II. Test results obtained from twin samples show a good agreement between them. The test results indicate that woven tape polyethylene geotextile is very susceptible degradation in load strain behaviour due to load repetitions as it losses its strength with load repetitions remarkably. In contrast, jute fabrics CANVAS 36X16 and CBC 72X12 (Kabir et.al., 1988) show good resistance against load repetitions. The test

results for the polyethylene geotextile are shown graphically in Figure 4.5. Those for CANVAS are also reproduced here in Figure 4.6. The relevant design parameters along with their physical properties are shown in Table 4.2.

#### 4.4 CHARACTERISATION OF DESIGN PARAMETERS

The steps those are followed in characterisation of design parameters from the test results, for both clay soil and geotextile reinforcing material, have been described in chapter three. To formulate the constitutive relation for the clay and the polyethylene geotextile, from the test results, Figures 4.7 and 4.8 have been produced following the recommended steps. The plots obtained from the newly developed constitutive relations for the clay and the polyethylene geotextile are compared with their respective test results, which are shown in Figures 4.9 and 4.10. These show a good agreement between the test results and the newly developed constitutive laws. This type of formulation is also applicable for jute fabrics. These are shown in Figures 4.11 and 4.12 for CANVAS and CBC respectively. A good agreement is also found between test results and constitutive relation.

The  $p_o - \delta$  plot for the clay soil is shown in Figure 4.13. This plot is produced using appropriate hyperbolic representation (Eqn. 3.6) and following the steps which have been described in chapter three and a computer program (Appendix III). The design parameters  $s_1$  (intercept on the ordinate axis of the hyperbolic plots of  $p_o - \delta$  relation) and  $s_2$  (slope of the hyperbolic plots of

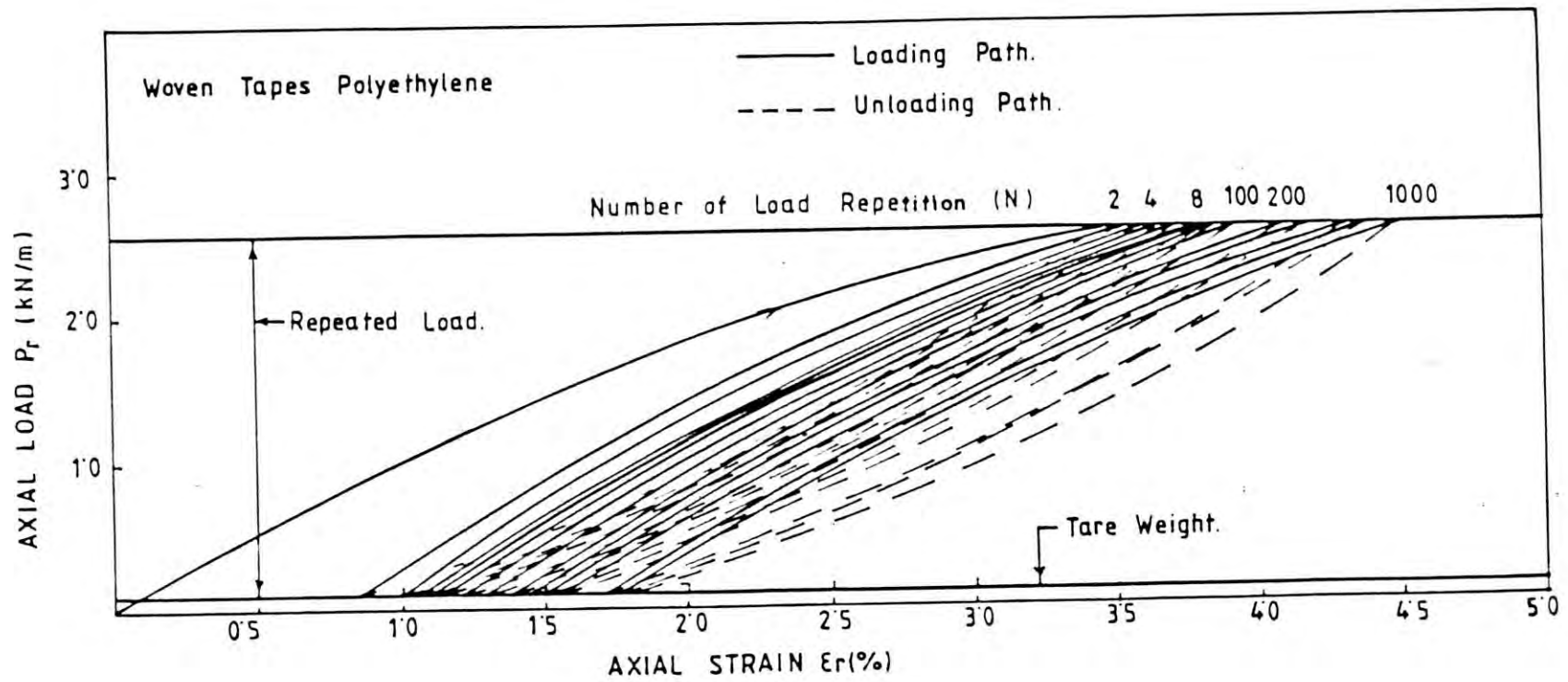


Figure 4.5 Graphical Representation of Test Results of Polyethylene.



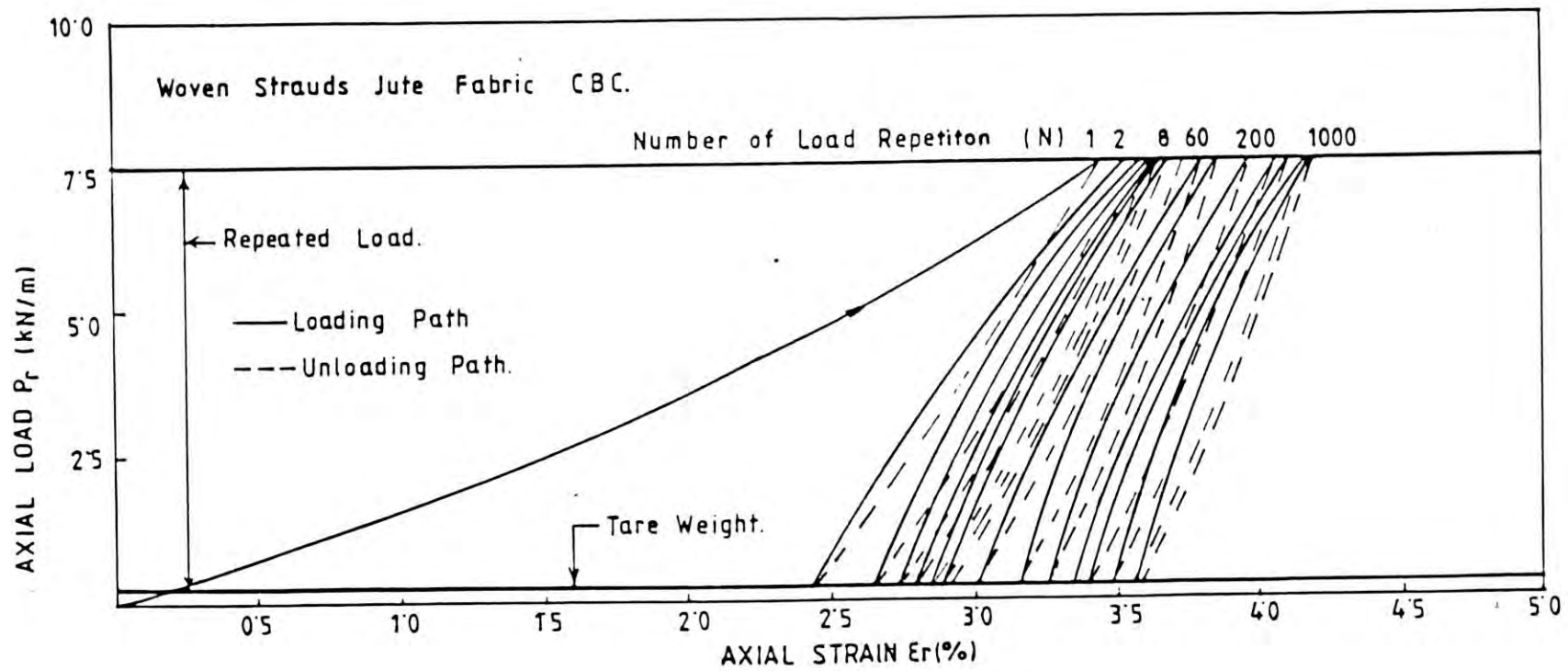


Figure 4.6 Graphical Representation of Test Results of CANVAS (after Kabir et.al. 1988)

Table 4.2 Properties of Reinforcing Materials

Reinforcement Type	Polyethylene Geotextile	CANVAS 36x16	CBC 72x12
Parameter			
Weight (gsm)	092	540	370
Thickness (mm)	0.33	1.30	1.41
$P_{r1}$ (kN/m)	3.30	8.00	7.44
$\epsilon_{r1}$ ( $10^{-2}$ )	5.00	4.89	3.45
$b_r$ (m/kN)	7.25	-	-
$r_1$ ( $10^{-1}$ )	7.20	2.53	2.50
$r_2$ ( $10^{-3}$ )	-	1.315	2.358
$r_3$ (m/kN)	1.125	-	-
$r_4$ ( $10^{-2}$ )	-	0.00	2.285

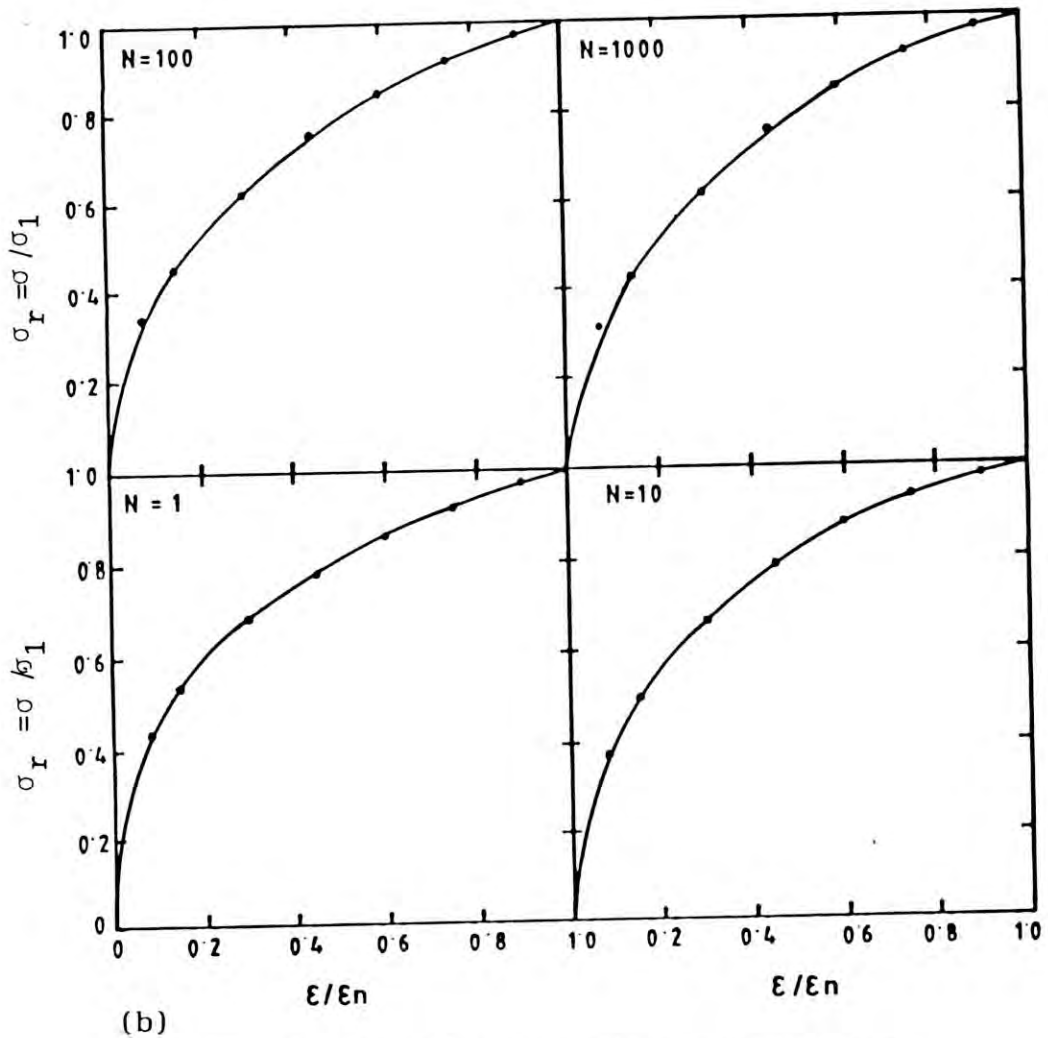
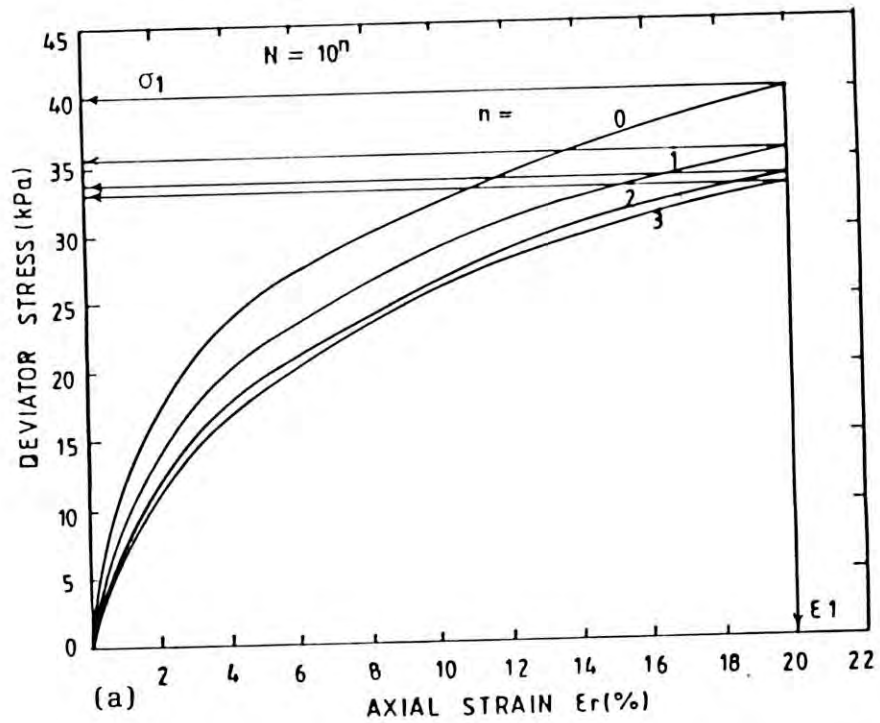


Figure 4.7 Constitutive Relation of Clay Soil



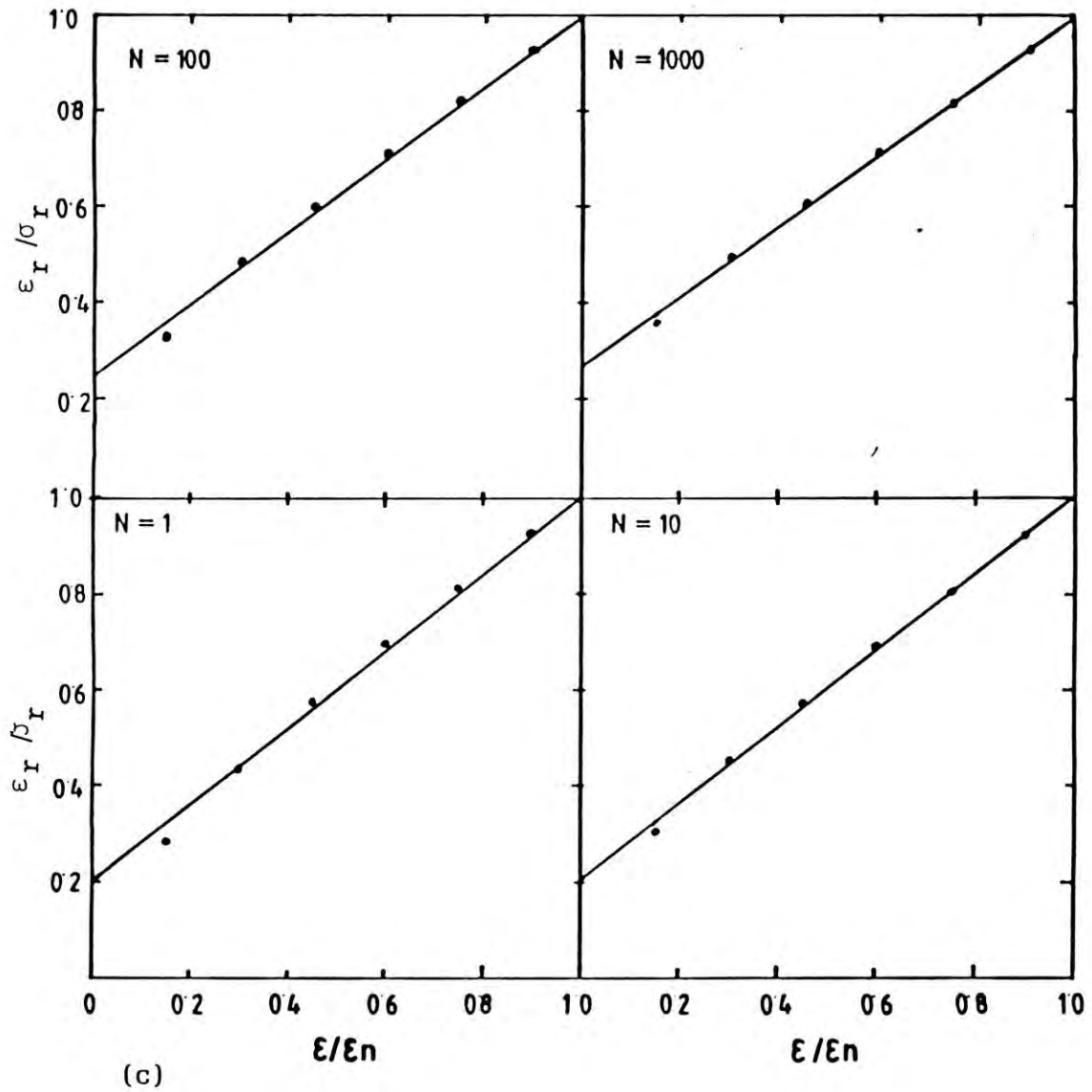
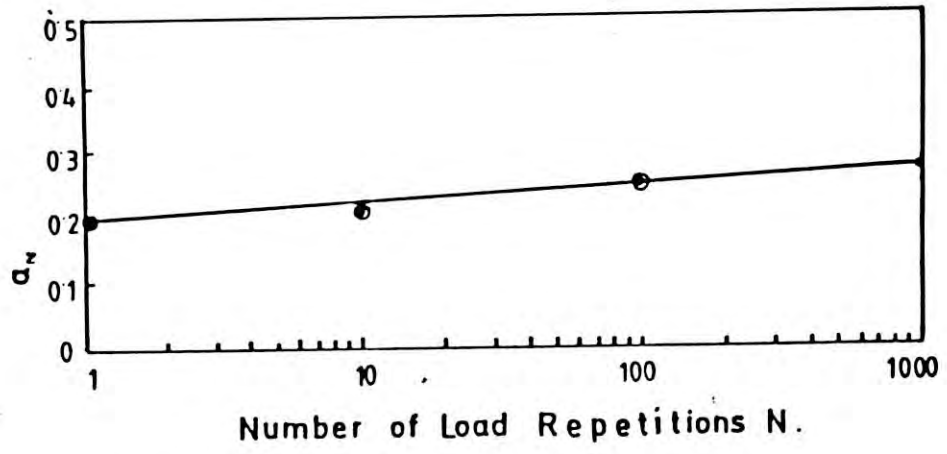
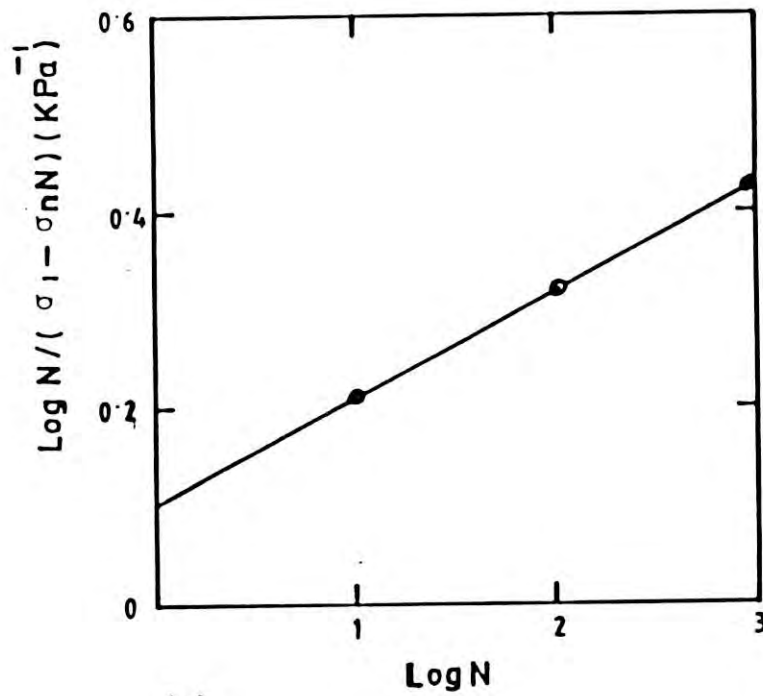


Figure 4.7 Constitutive Relation of Clay Soil



(d)



(e)

Figure 4.7 Constitutive Relation of Clay Soil

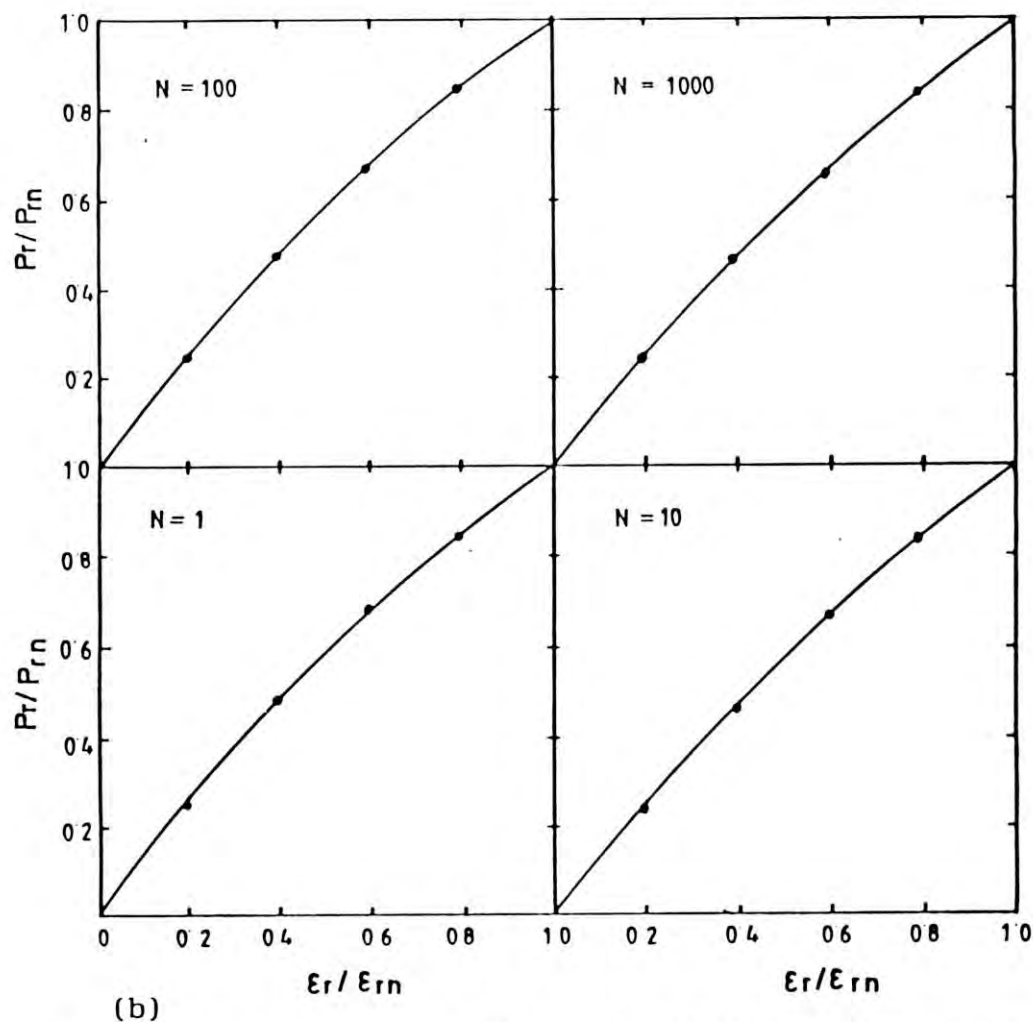
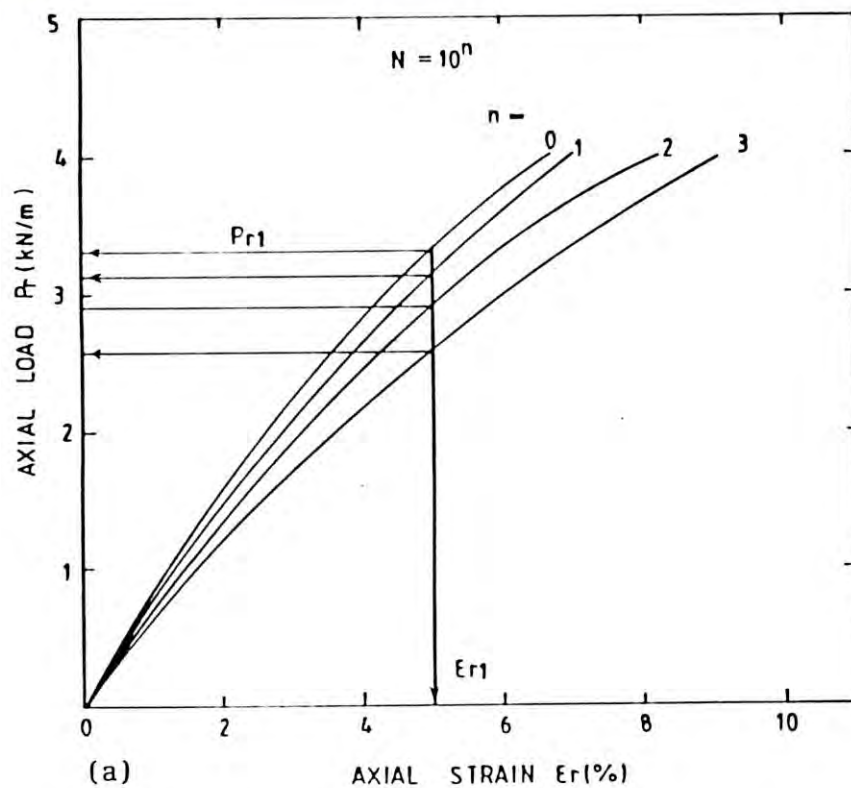
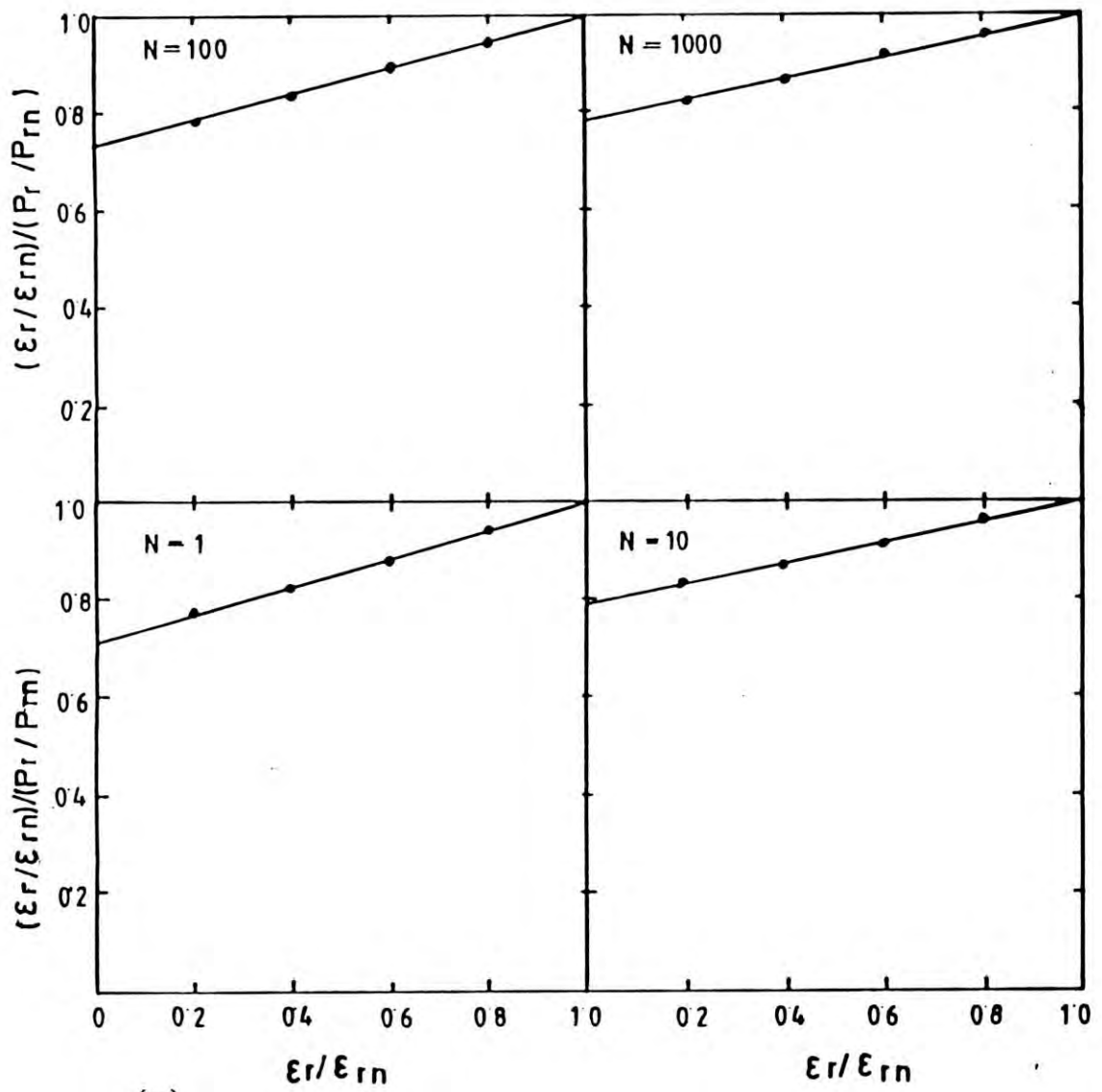


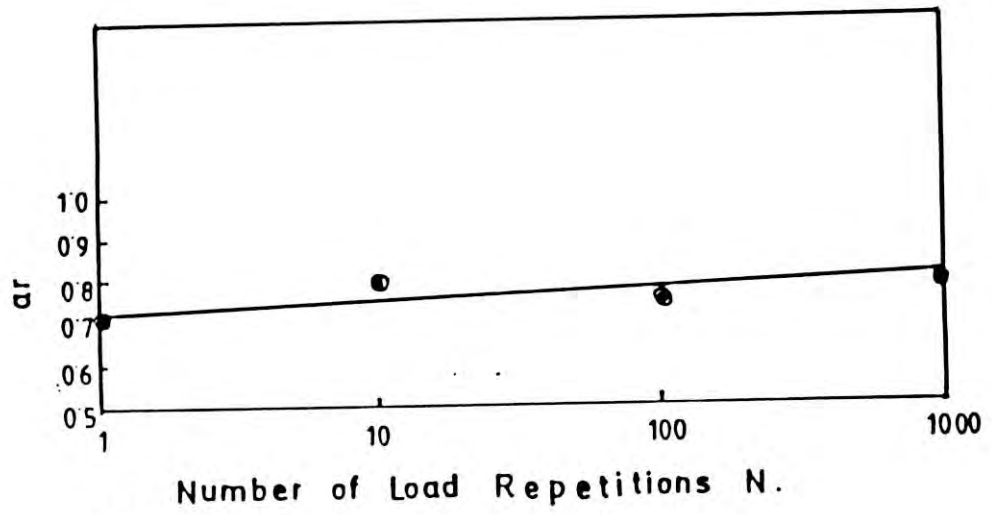
Figure 4.8 Constitutive Relation of Polyethylene Geotextile



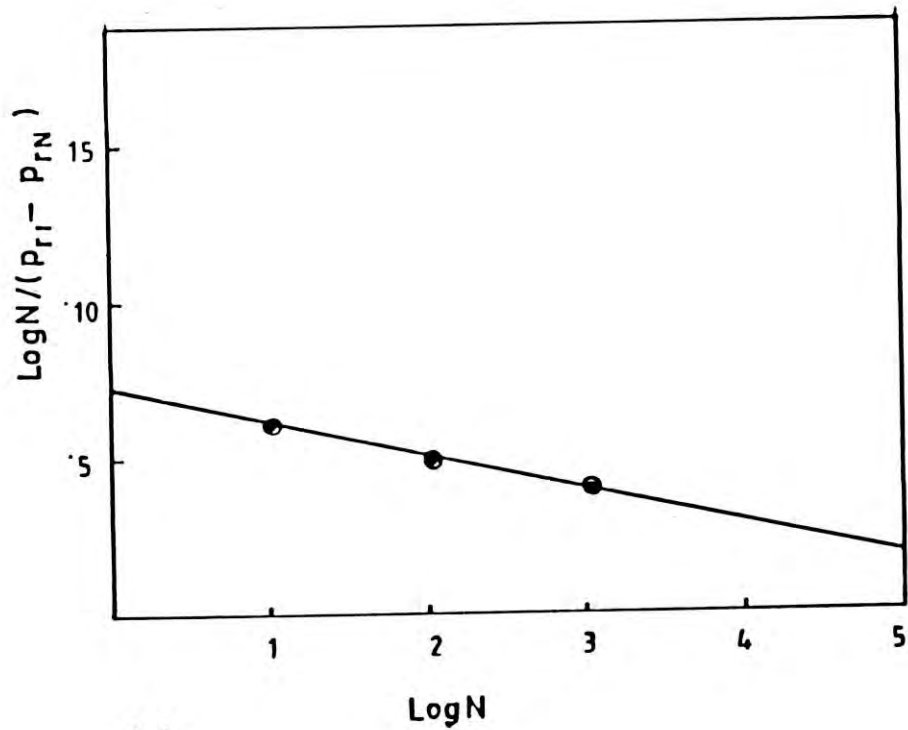


(c)

Figure 4.8 Constitutive Relation of Polyethylene Geotextile



(d)



(e)

Figure 4.8 Constitutive Relation of Polyethylene Geotextile

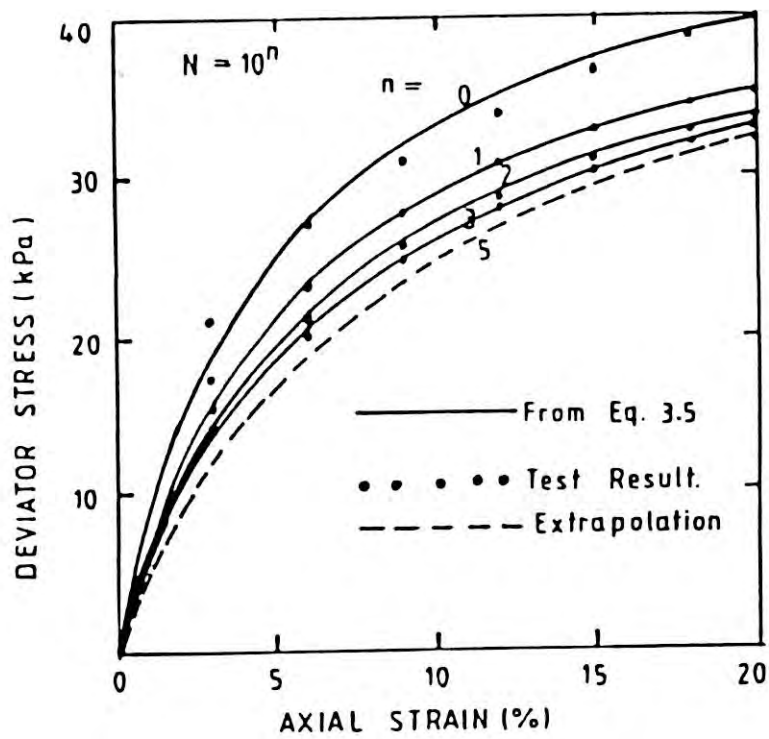


Figure 4.9 Mechanical Behaviour of Soil



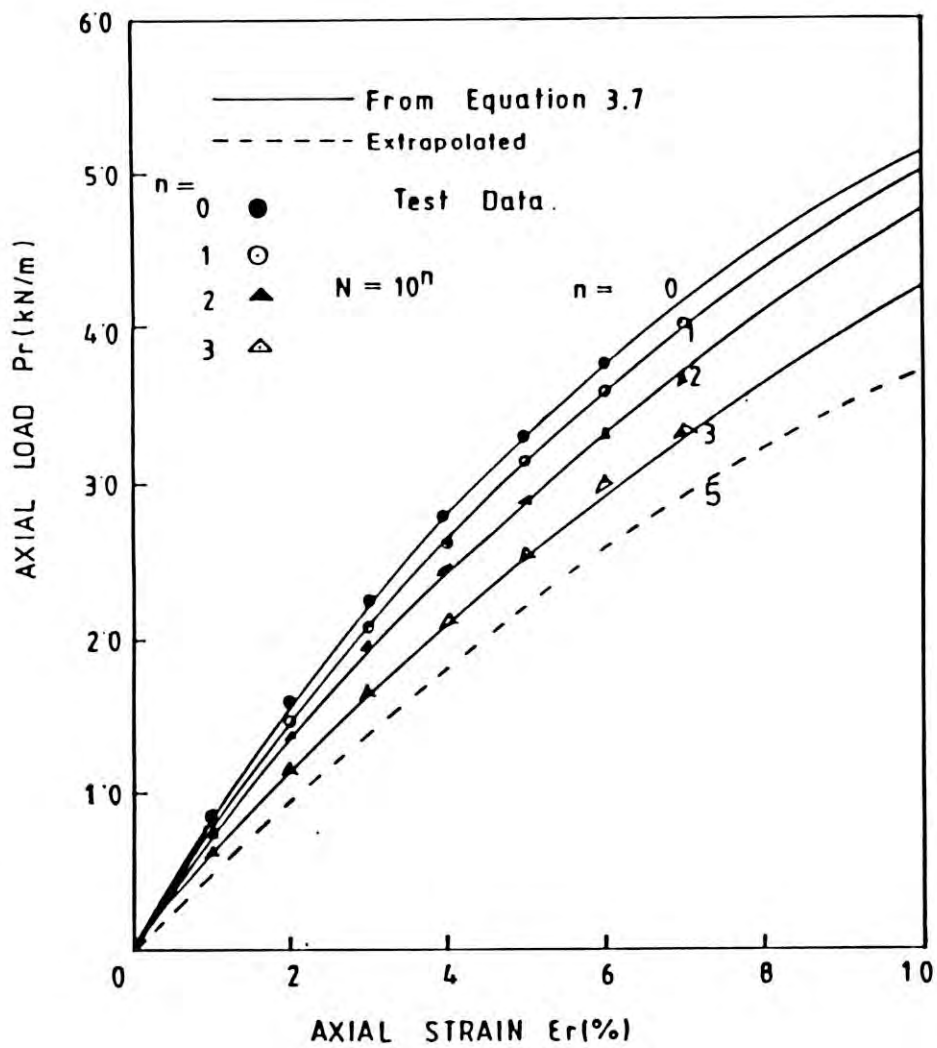


Figure 4.10 Mechanical Behaviour of Polyethylene Geotextile

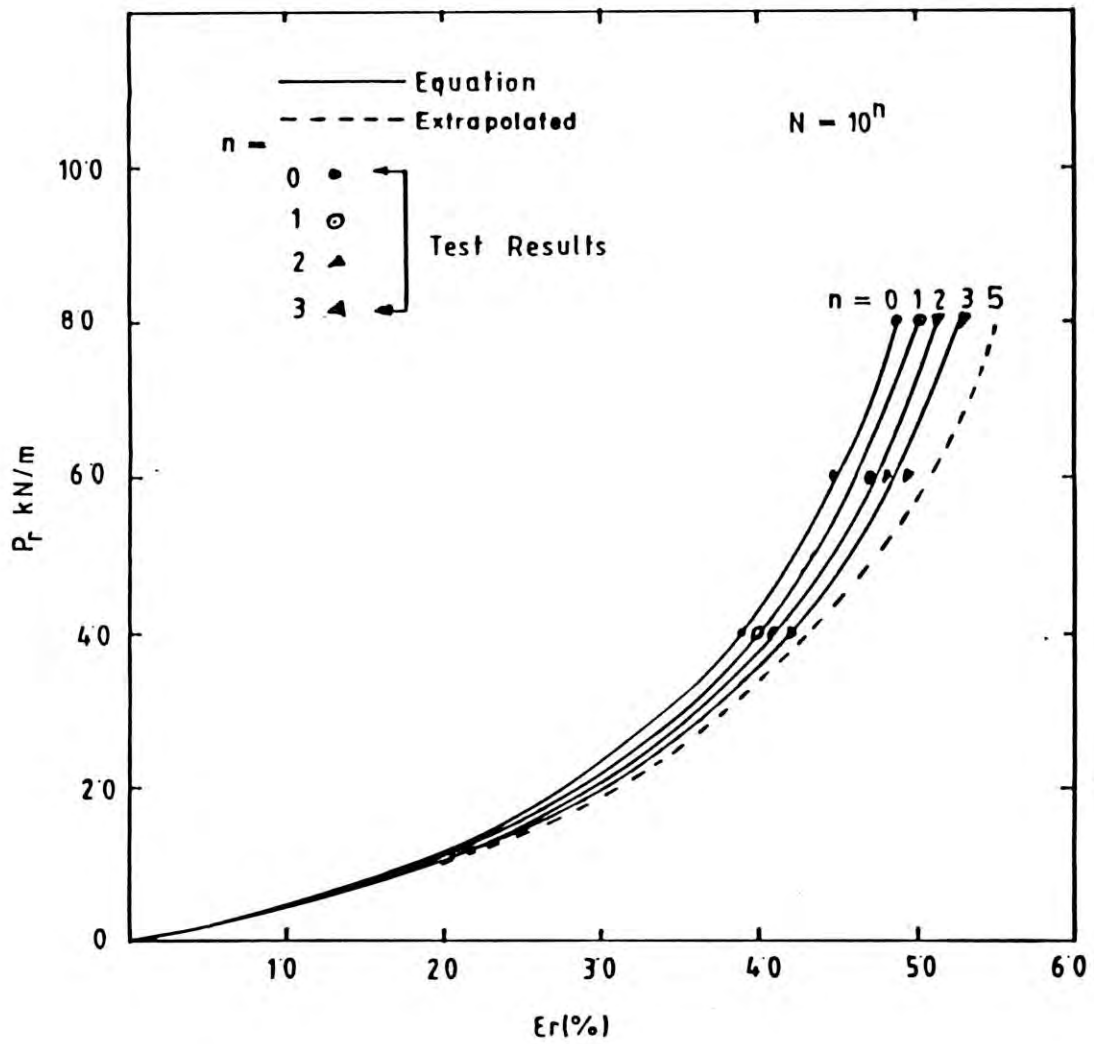


Figure 4.11 Mechanical Behaviour of Jute Fabric CANVAS (after Kabir et. al, 1988)

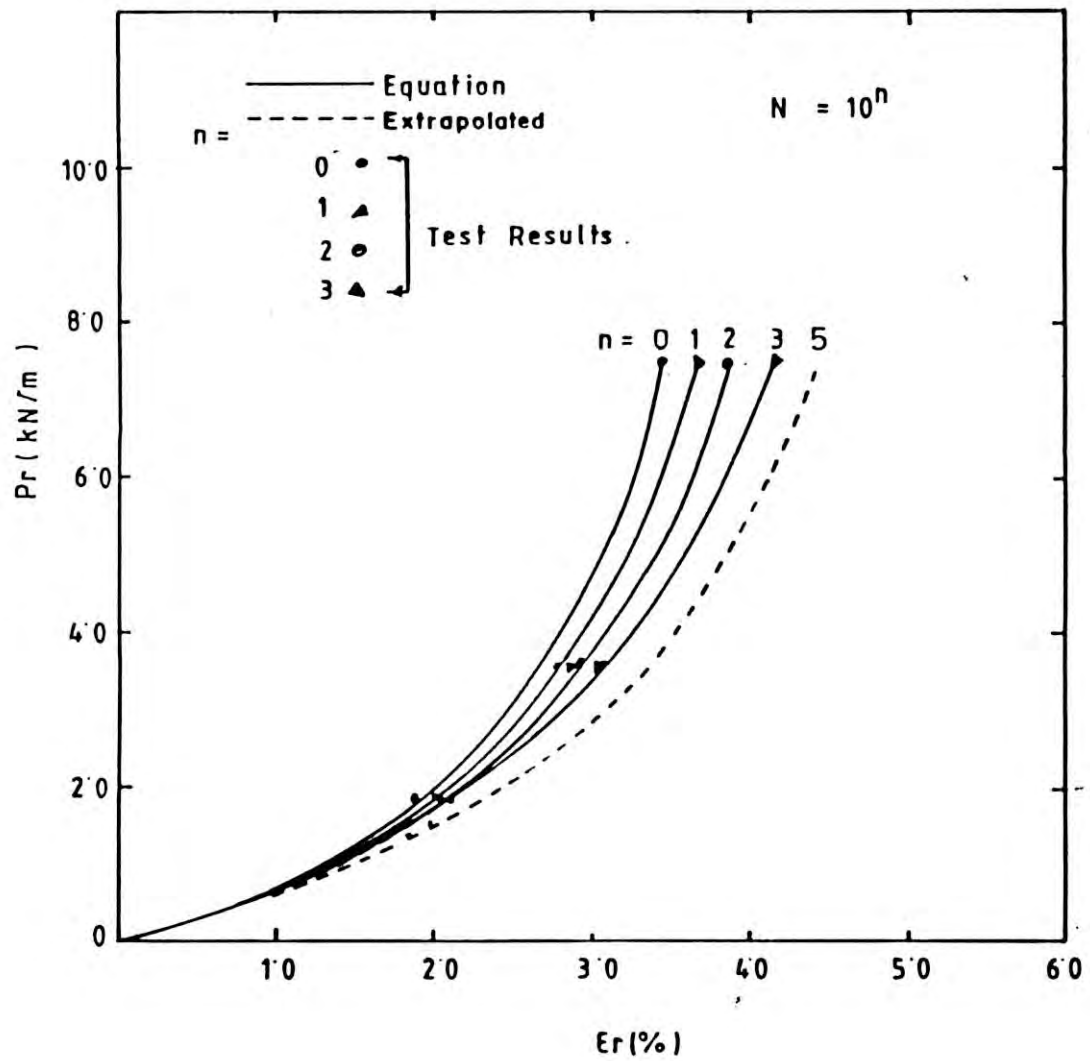


Figure 4.12 Mechanical Behaviour of Jute Fabric CBC (after Kabir et. al, 1988).

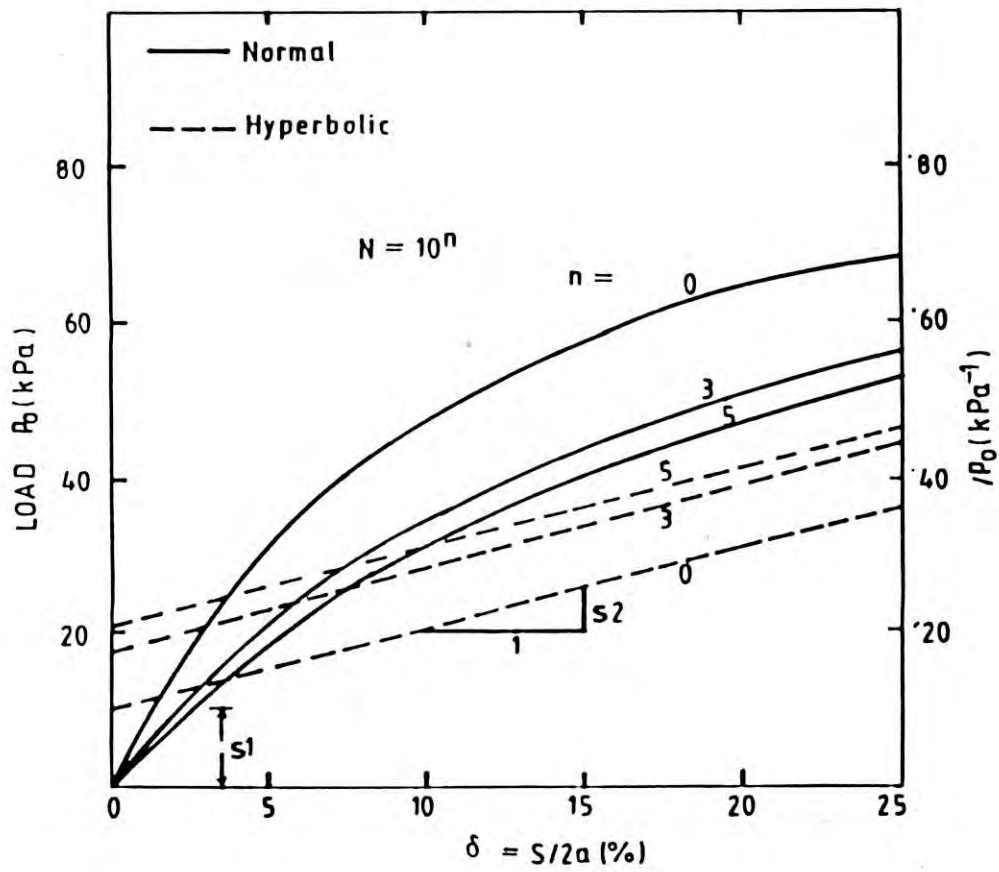


Figure 4.13  $p_0 - \delta$  Plots of Clay Soil



$p_o - \delta$  relation) used in the construction of design charts, are also shown in Figure 4.13. The design parameters  $b_1$  (intercept on the ordinate axis of hyperbolic plots of load strain behaviour) and  $b_2$  (slope of the hyperbolic plots of load strain behaviour) for the reinforcing materials may be obtained directly from Equation 3.16 using appropriate parameters.

**CHAPTER FIVE**

## CHAPTER FIVE

### DESIGN CHARTS

#### 5.1 GENERAL

To demonstrate the practical applicability of the characterisation and design method developed in this study, a number of design charts are presented in this chapter. The design charts produced here are used to calculate the required aggregate thicknesses ( $h_0$  and  $h$ ) and these are produced using newly developed design equations which have been described in chapter three. Load sharing diagrams for different rutting conditions are also presented.

#### 5.2 DESIGN CHARTS

Design charts for both unreinforced and reinforced unpaved roads are presented in this chapter are prepared using equations developed in this study and a main frame compatible computer program. The flow diagram of computer program is shown in Appendix III. In producing the design charts, a Silty Clay soil, three types of reinforcing elements, and three types of loading are considered. The reinforcements include a woven tape polyethylene geotextile and two grades of jute fabrics. The three types of loading include, axle loads from, trucks, minibuses and Light Cross Country Vehicle. The relevant design parameters of clay soils and reinforcing materials are shown in Table 5.1. The wheel loading parameters are shown in Table 5.2. The relevant

Table 5.1 Design Parameters

Number of Load Cycle (N)	Clay Subgrade			Reinforcement								
				Polyethylene			CANVAS			CBC		
	$s_1(10^{-3})$ $xm^2/kN$	$s_2(10^{-3})$ $xm^2/kN$	$p_o(kPa)$	$b_1(10^{-3})$ $xm/kN$	$b_2(10^{-3})$ $xm/kN$	$\epsilon_{rf}$ (%)	$b_1(10^{-3})$ $xm/kN$	$b_2(10^{-2})$ $xm/kN$	$\epsilon_{rf}$ (%)	$b_1(10^{-3})$ $xm/kN$	$b_2(10^{-2})$ $xm/kN$	$\epsilon_{rf}$ (%)
1	10.66	09.97	63.00	10.91	84.85	5.00	24.16	-36.64	10.00	18.55	-40.32	5.00
1000	17.30	10,91	56.00	16.11	73.68	5.00	26.11	-36.44	10.00	21.75	-38.89	5.00
100000	20.77	10.36	52.6	19.65	55.36	5.00	27.41	-36.44	10.00	23.80	-37.97	5.00



Table 5.2 Wheel Loading Parameters

Vehicle	Truck	Minibus	LCCV
Parameter			
Axle (Wheel)	Dual	Dual	Single
e (m)	1.88	1.64	1.20
B (m)	0.427	0.353	0.190
L (m)	0.214	0.249	0.226
BxL (m <sup>2</sup> )	0.0914	0.0879	0.0429
P (kN)	80	60	24
p <sub>c</sub> (kPa)	620	480	280

design charts are produced in Figures 5.1, 5.2, 5.3, 5.4. The method of use of the design charts are explained through a design example.

### 5.3 DESIGN EXAMPLE

To show the applicability of the proposed design method, the following design example is produced. A reinforced unpaved road should be designed for standard minibus with,  $P=60$  kN,  $p_c=480$  kPa,  $N=1000$  passages and  $r=190$  mm, on a silty clay subgrade and woven tape polyethylene geotextile as described in previous sections. Using Figures 5.1 and 5.2, for  $r=190$  mm and  $N=1000$ , the required thickness of aggregate layer,  $h_0$  and  $h$ , obtained as 0.55 m and 0.50 m, for unreinforced and reinforced condition respectively.

### 5.4 LOAD SHARING OF CONSTITUENT MATERIALS

The load (pressure) sharing mechanism of the constituent materials in a reinforced unpaved road system may be compared with the principle of "Effective Stress" which is very well known in conventional soil mechanics.

In the saturated soil the total imposed loading is shared by the soil skeleton and the pore fluid in a manner which can be represented by Equation 5.1.

$$\sigma = \bar{\sigma} + u \quad \dots \quad 5.1$$

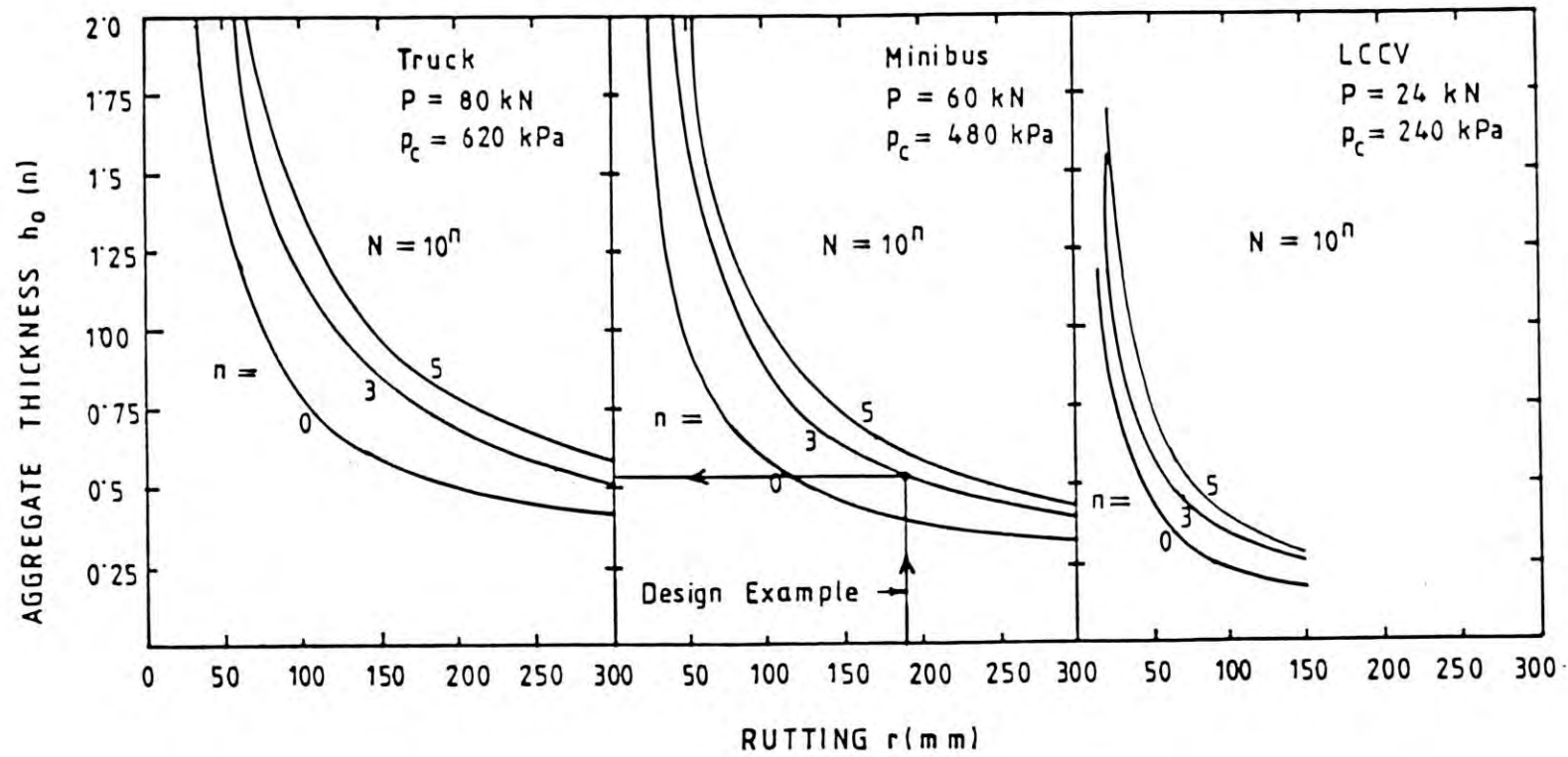


Figure 5.1 Design Chart for Unreinforced Road

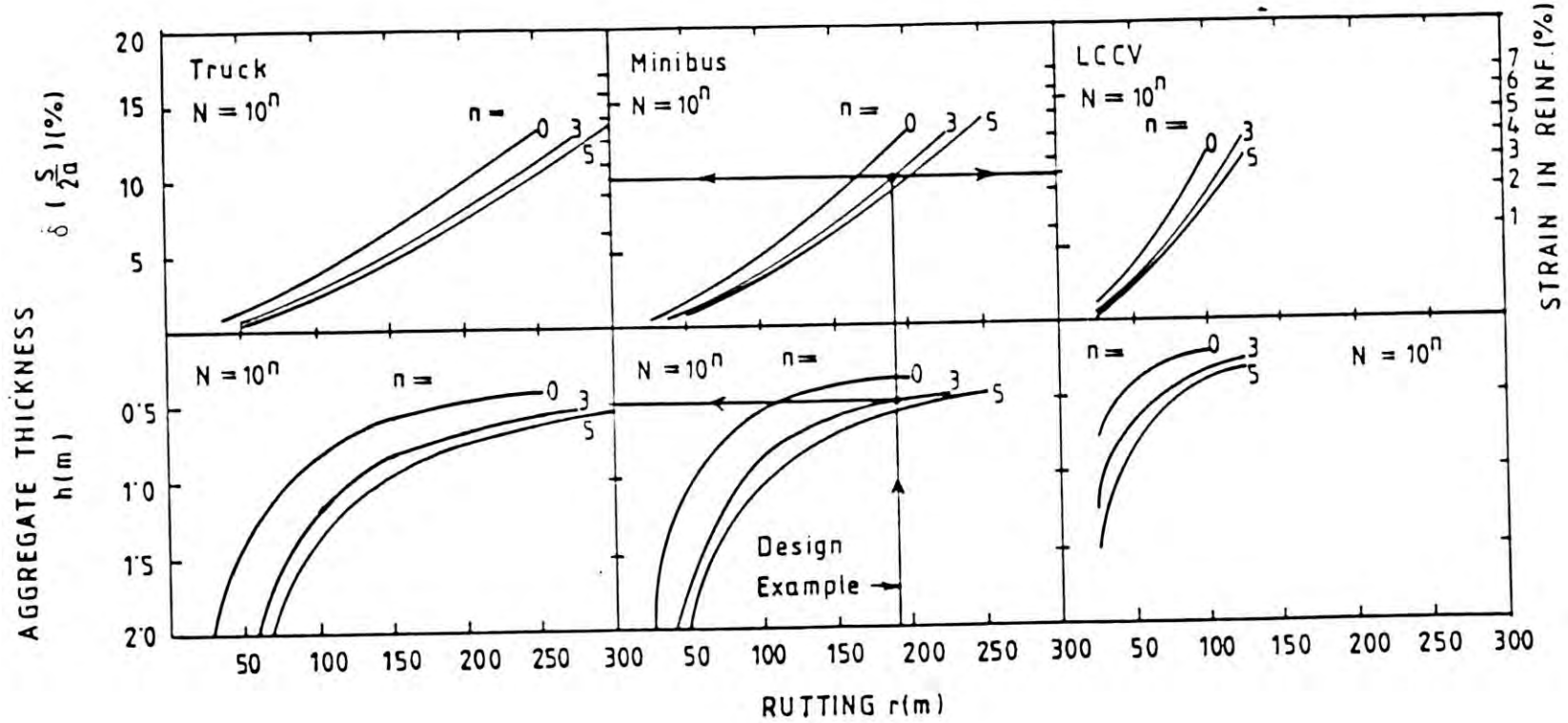


Figure 5.2 Design Chart for Reinforced Road with Polyethylene Geotextile



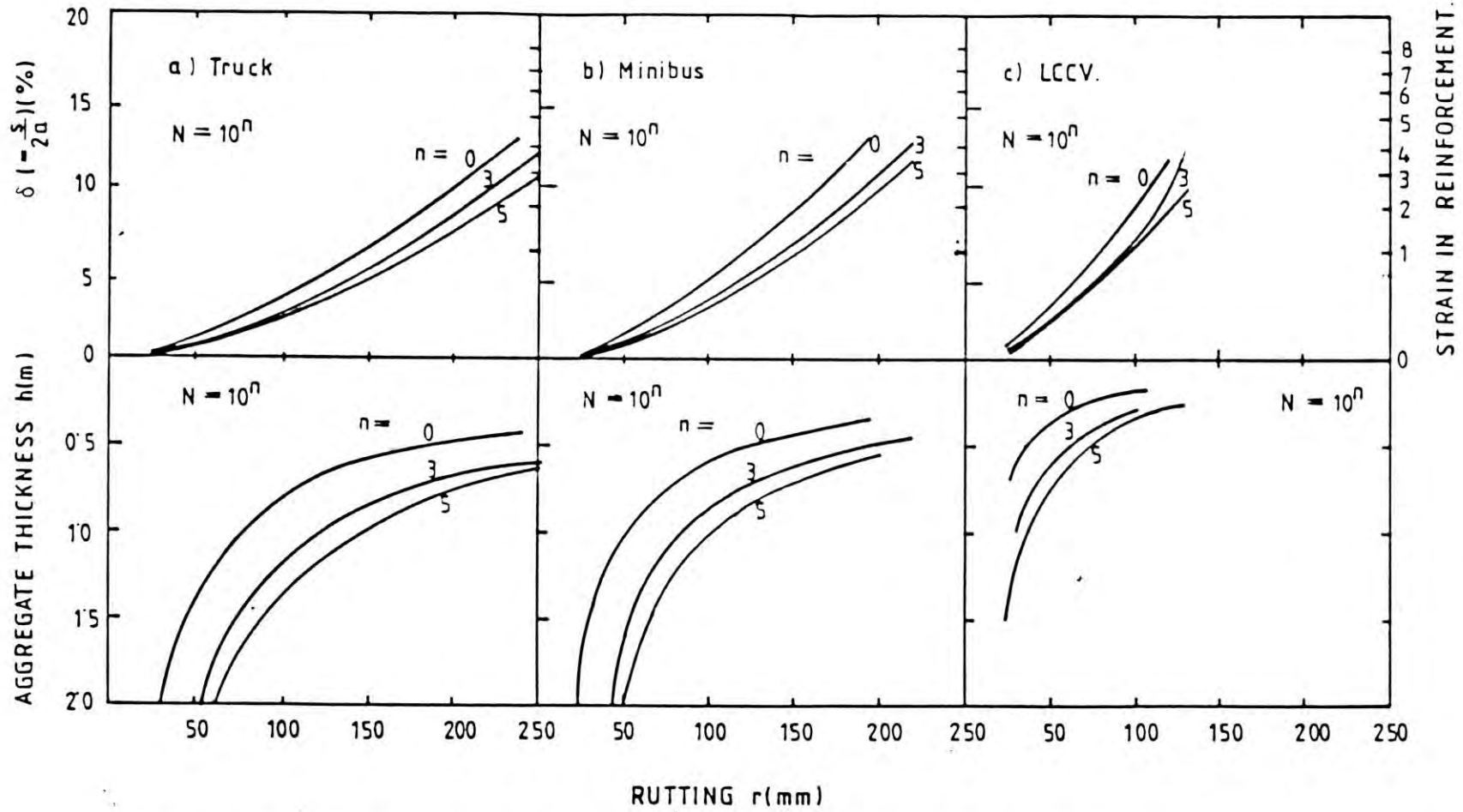


Figure 5.3 Design Chart for Reinforced Road with CANVAS (after Kabir, et.al, 1988)

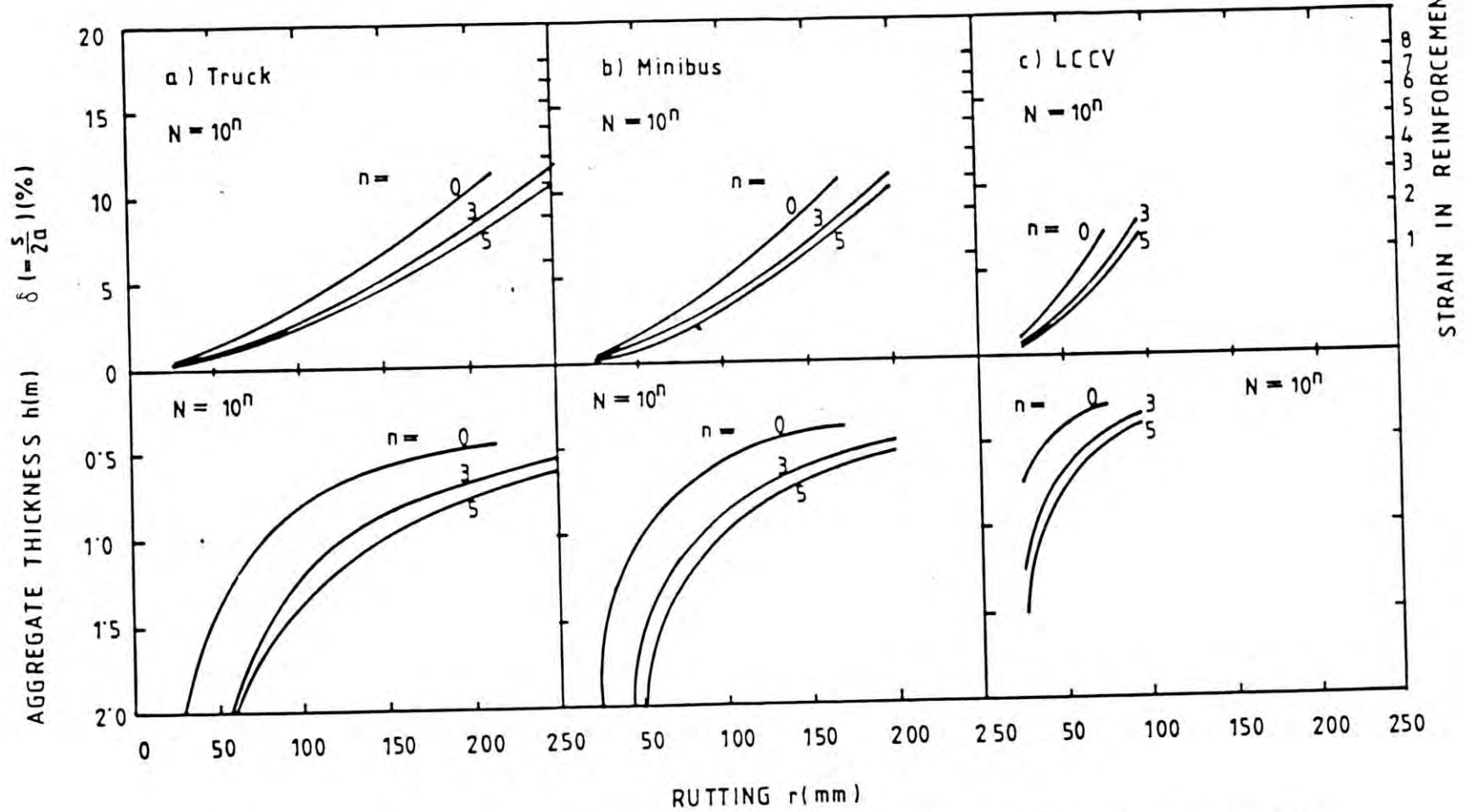


Figure 5.4 Design Chart for Reinforced Road with CBC (after Kabir et.al, 1988)

where  $\sigma$  is the total stress,  $\bar{\sigma}$  is the effective stress carried by the soil skeleton and  $u$  is the pore water pressure. Under drained condition the pore water pressure dissipate gradually and this stress is transferred to the soil skeleton and the effective stress increases with time. In case of a reinforced unpaved road the imposed loading is carried as stress shared by the reinforcement and the soil as depicted in Equation 5.2(r).

$$p = p_s + p_r \quad \dots \quad 5.2(r)$$

where  $p$  is the total stress (load) at the base of the aggregate layer which is transmitted from the wheel through the aggregate layer,  $p_s$  and  $p_r$  are stresses shared by the soil and reinforcement respectively. Under repeated loading, transfer of stress from one component to the other will occur depending on the relative degradation of mechanical behaviour due to load repetitions. This phenomena is shown here for the cases of polyethylene geotextile and jute fabric CANVAS reinforcing layer and the soft silty clay soil in Figures 5.5 and 5.6 respectively. Figures 5.5(a) and 5.6(a) show the imposed loading (pressure) of the reinforced road system, the load (pressure) shared by the clay subgrade is shown in Figures 5.5(b) and 5.6(b). Figures 5.5(c) and 5.6(c) show the load (pressure) shared by the respective reinforcing element. These show the clay subgrade to loose load slightly and the reinforcement to gain it, relative to their respective initial values.

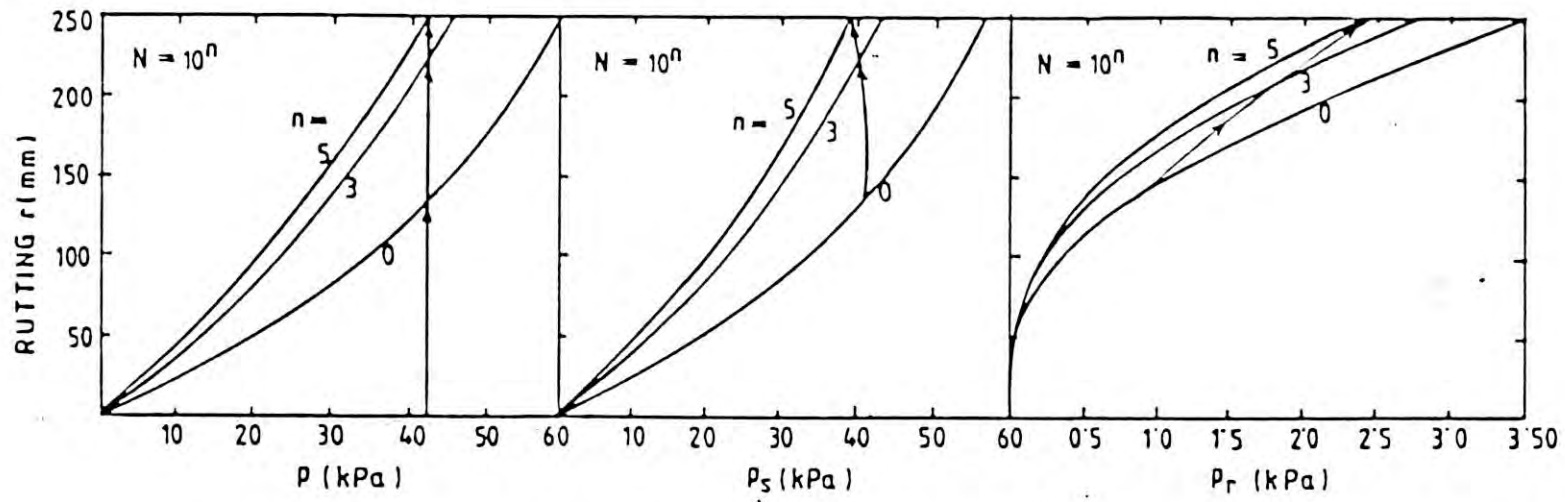


Figure 5.5 Load Sharing by Clay Subgrade and Polyethylene Geotextile.



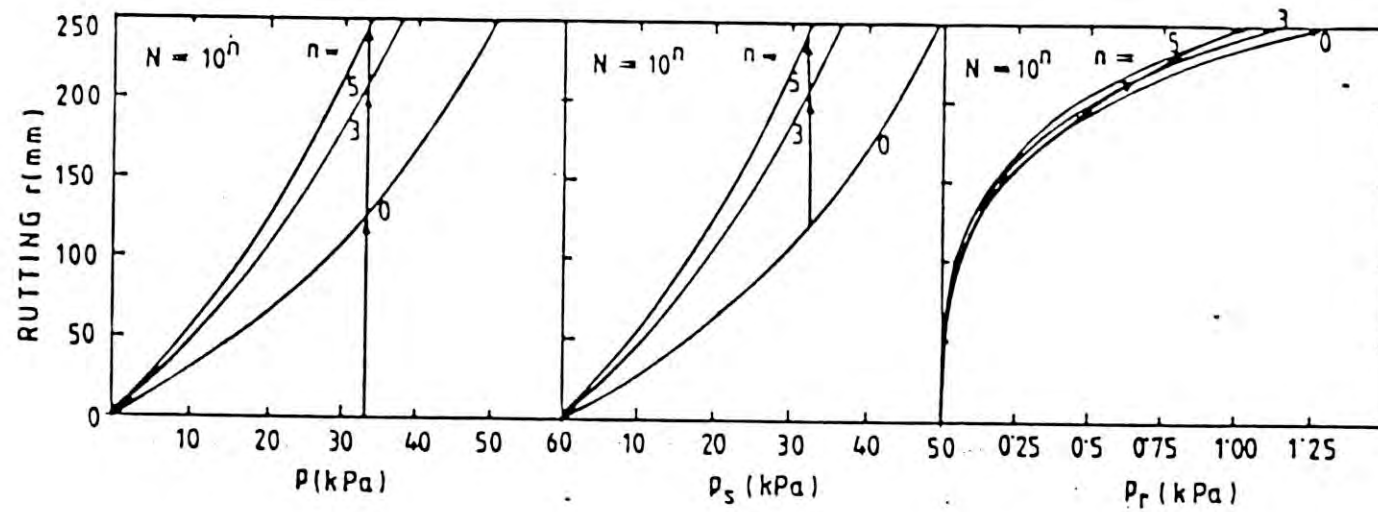


Figure 5.6 Load Sharing by Clay Subgrade and Reinforcement Jute Fabric CBC (after Kabir et. al, 1988).

CHAPTER SIX

## CHAPTER SIX

### DISCUSSION AND CONCLUSION

#### 6.1 GENERAL

In this chapter a general comparative discussion on the existing design and characterisation methods and the method proposed in this study is presented. As the Giroud and Noiray method is popularly used now, a detailed comparison between the proposed method and the method by Giroud and Noiray, in graphical and tabular form is produced here. Finally general conclusions which may be drawn from this study as well as from the review of the relevant literature are produced.

#### 6.2 MATERIAL BEHAVIOUR

Proper characterisation of materials behaviour concerned, is of paramount importance in any type of design. Therefore, new constitutive relation has been developed as part of this study which is based on tests simulating real field operational conditions. This constitutive relation portrays the load deformation behaviour under repeated loading conditions. A unified approach was followed for establishing the constitutive relations for the clay subgrade material as well as the reinforcing element. This relations enables portrayal of behaviour in very generalised form which may be used for the so called quasi static as well as repeated loading conditions.

### 6.3 DESIGN METHOD

The new design method developed in this research is based on realistic material behaviour and fundamental operational mechanisms. In discussion on the original paper (Giroud and Noiray, 1981), Giroud (1982) stated that the work presented in that paper is a starting point for the researchers to develop improved and realistic methods of design. Indeed, there is a lot of scope in improving that method and this study presents such a method. A detailed comparison between Giroud and Noiray method and the proposed method in tabular form is described later under the section 6.4. A graphical comparison of the Giroud and Noiray method and the proposed method show (Figure 6.1) the former method to calculate lower values of aggregates thickness under low rutting conditions, which may lead to unsafe design.

Giroud and Noiray assumed full mobilisation of resistances, the elastic resistance ( $\pi c_u$ ) for unreinforced condition and the plastic resistances ( $(\pi + 2)c_u$ ) for reinforced condition and linear load strain behaviour of reinforcing materials. Resistances offered by the reinforcing element don't vary significantly whether calculated by Giroud and Noiray method or the proposed method, as the operating range of strain in the reinforcement lies within 5%. The difference between Giroud and Noiray method and the new method results from the values of mobilised subgrade resistances. The resistances offered by the clay subgrade and reinforcement (polyethylene) are shown in Figures 6.2 and 6.3 respectively. Figure 6.2 shows that at low



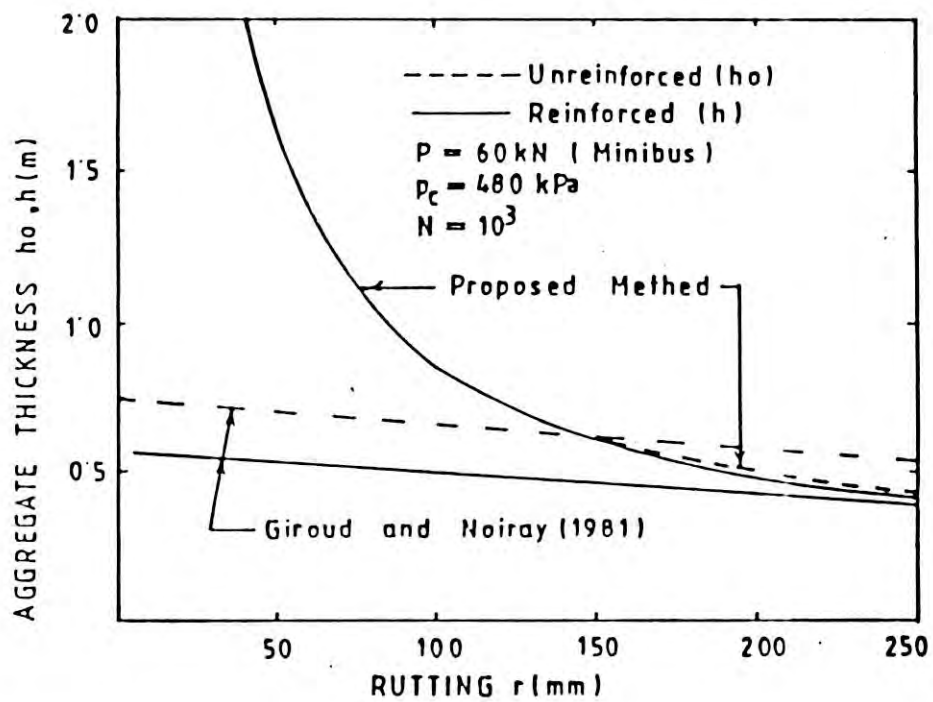


Figure 6.1 Design by Proposed Method and Giroud and Noiray (1981) method.

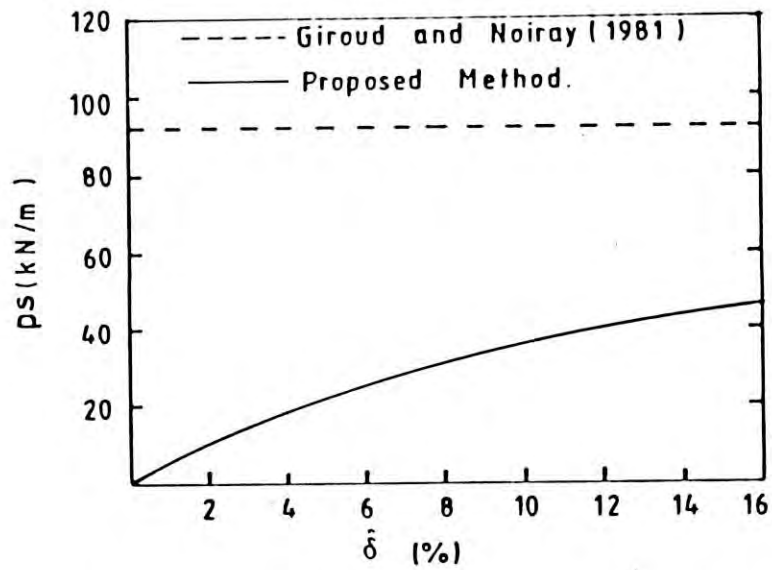


Figure 6.2 Resistance Offered by Clay Subgrade

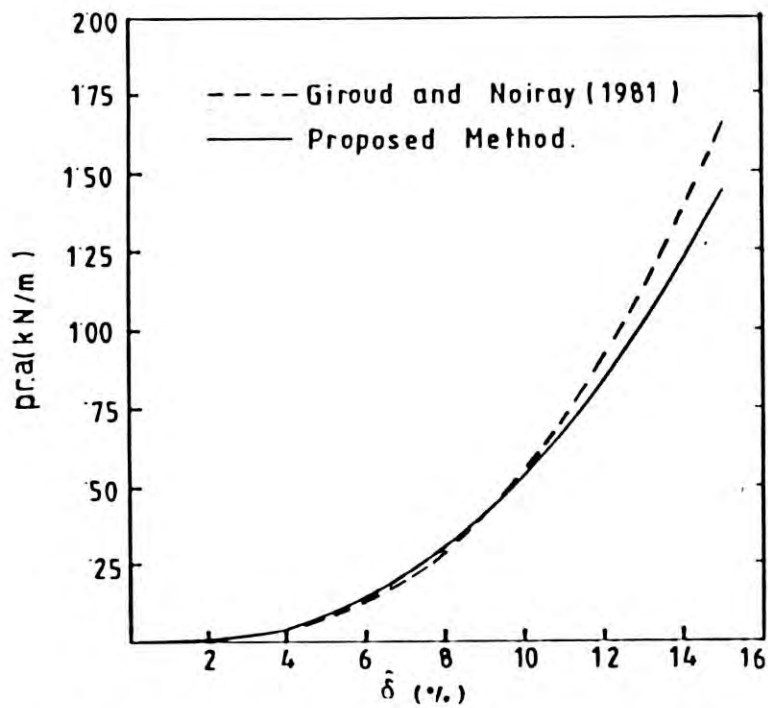


Figure 6.3 Resistance Offered by Reinforcement

degrees of rutting Giroud and Noiray method assumed high resistances for clay subgrade.

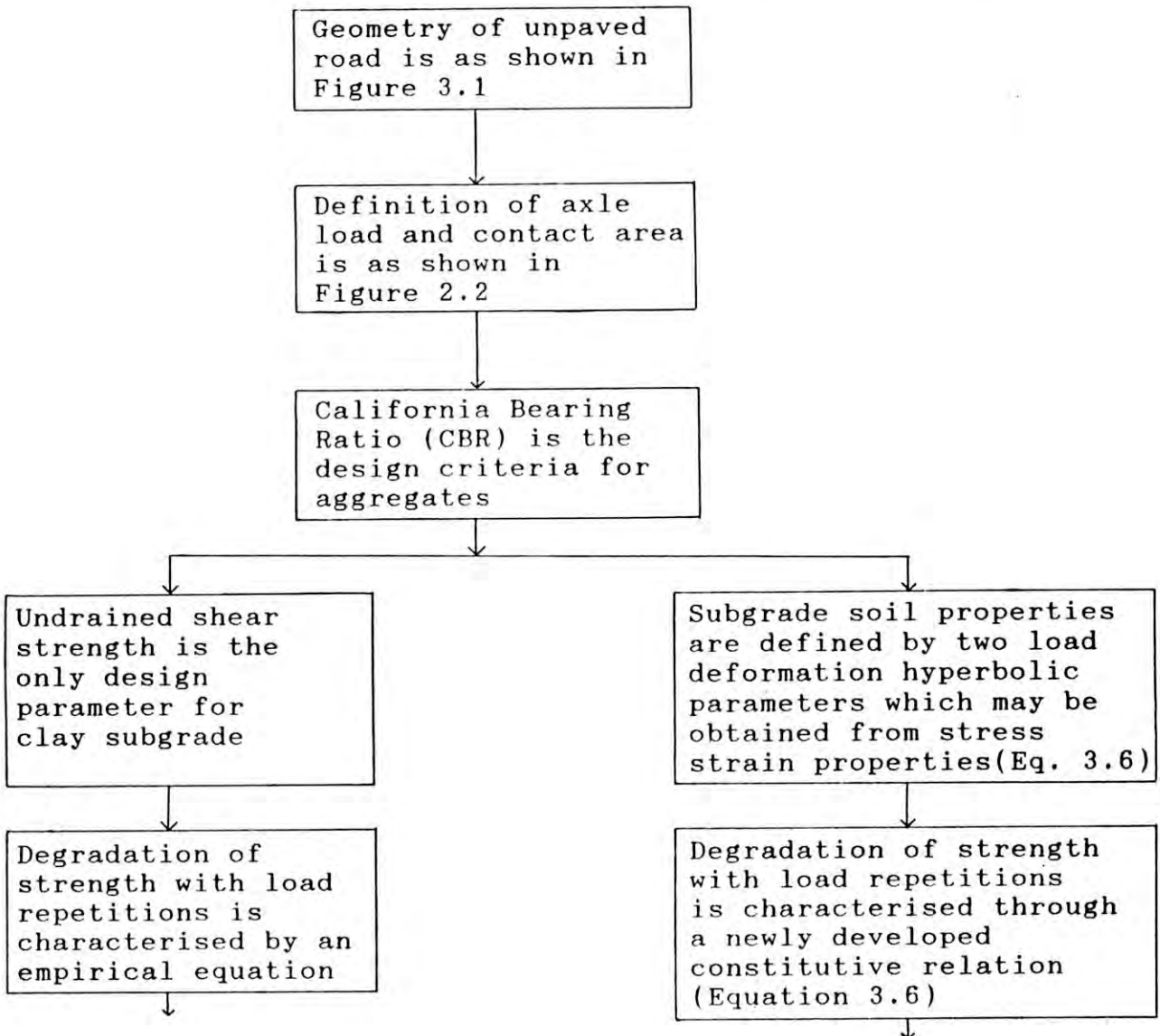
#### 6.4 COMPARISON

In this section a detailed comparison between the Giroud and Noiray method and the proposed method is produced in a tabular form.

Giroud and Noiray

Common

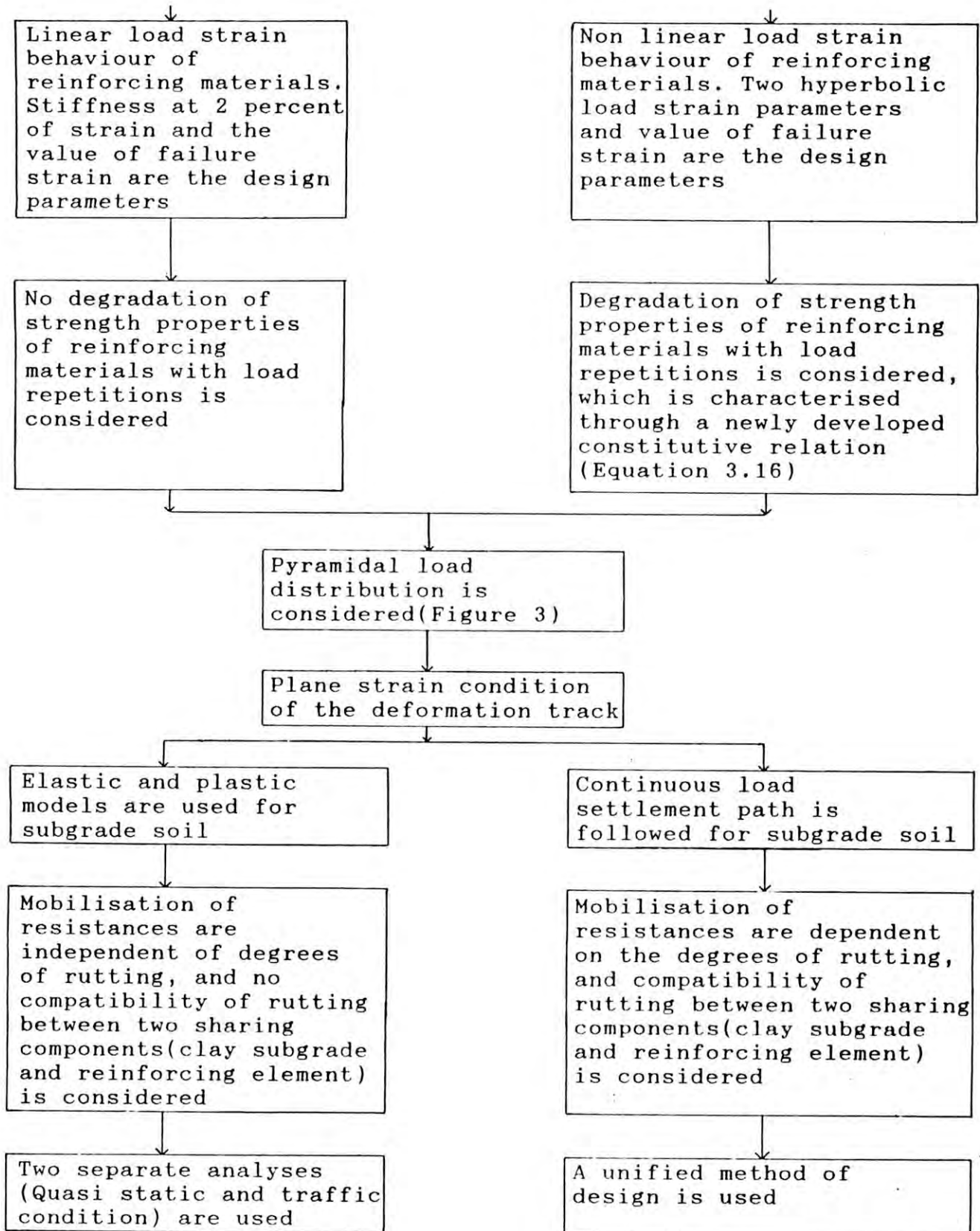
Proposed Method



Giroud and Noiray

Common

Proposed Method





Tabular comparison are shown in Table 6.1.

## 6.5 CONCLUSIONS

From the research work reported in this thesis the following conclusions could be made:

### 6.5.1 Existing Design Method

- (1) In all the design methods, materials behaviour are represented by single parameters. For clay subgrade soil undrained shear strength or modulus of subgrade reaction is used. Modulus of stiffness value at two percent of strain is used for reinforcing elements. This is unrealistic and inadequate.
- (2) Giroud and Noiray's design method is based on so called limit state theory of subgrade clay and thereby didn't take into account the mobilisation of resistances corresponding to the degrees of deformation. Van den Berg and Kenter considered the mobilisation of resistances in elastic phase only.
- (3) Giroud and Noiray didn't consider the compatibility of deformation between the constituent materials. Van den Berg and Kenter considered the compatibility of deformation under assumed elastic condition only.
- (4) For traffic loading condition Giroud and Noiray used an empirical relation established from extensive field tests for a particular condition of rutting. Van den Berg and Kenter considered it by reducing the bearing capacity factor, which could not represent the realistic degradation of mechanical behaviour of the constituent materials.

Table 6.1 Refinements of Proposed Design Method over Giroud and Noiray (1981)

Area of Refinement	Basic Design Parameter		Quasi Static Analysis			Analysis under Traffic Loading	
	Subgrade	Reint.	Unreinforced	Reinforced		Unreint.	Reinf.
				Subgrade	Reinf.		
Giroud and Noiray (1981)	Undrained Shear Strength $c_u$	K (modulus at $\epsilon_r = 2\%$ )	$p_o = \pi c_u$ $= t(r)$	$p_s = (\pi + 2)c_u$ $= f(r)$	$p_r = t(K, r)$	$p_o, p_s, p_r$ from Q.S and Webster and Alford(1978) equation	
Proposed Method	New constitutive relation $f(\sigma - \epsilon - N)$	New constitutive relation $f(P_r - \epsilon_r - N)$	for clay: $p_o, p_s$ are function of $\sigma, \epsilon, N$ and $r$ which may be obtained from $p_o - \delta - N$ and $p_s - \epsilon - N$ relations, developed using Prakash, Sharan and Saran (1984) For reinforcement: $p_r$ is function of $P_r, \epsilon_r$ and $r$ which may be obtained from $P_r - \epsilon_r - N$ relation.				

### 6.5.2 Proposed Design Method

(1) The proposed design method considered the non linear mechanical behaviour of the constituent materials by developing a new constitutive relations using hyperbolic law. These newly developed constitutive relations may be used to represent the mechanical behaviour of clay subgrade and reinforcing element to more reasonable degree of accuracy.

(2) Mobilisation of resistances in the constituent materials and compatibility of deformation between them, is taken into account in the design equations.

(3) An unified approach using realistic material behaviour under one time as well as repeated traffic loading condition is suggested.

### 6.5.3 Overall

The materials behaviour especially under repeated loading condition is represented more realistically by developing new constitutive relations. The design method based on realistic load sharing mechanism under traffic loading condition and mobilisation of respective resistances under compatible degrees of deformation (rutting) and therefore, should be adopted.

**RECOMMENDATION FOR FUTURE  
RESEARCH**



## RECOMMENDATION FOR FUTURE RESEARCH

Research in any field is a never ending process. Keeping in line with this philosophy, the author would like to recommend the following future research in this field.

### Materials

(1) Sufficient number of repeated loading test should be performed on different types of soils from different region of Bangladesh to establish relation amongst the constitutive design parameters and fundamental(index) properties of soils, so that the Design Engineers can use these in preliminary designs with least amount of effort.

(2) The repeated loading test of reinforcing materials should be done under in-soil, controlled temperature and humidity conditions as these factors may influence the load deformation behaviour significantly.

### Test Apparatus

Shopohisticated test apparatus should be installed for repeated loading tests on soil and reinforcing materials with automatic data logging, recording and plotting systems.

### Design Method

The proposed design method is applicable only for clay subgrade soils. Design method should be developed for other types of soils. Surcharge effect should be included in the design equation. Since the present study revealed that the function of

reinforcement is not much predominant in the load sharing, in the operational range of rutting, effect of prestretched and prerutted reinforcement may be studied. As the present study was limited to theoretical development of design method, sufficient number of laboratory model test as well as prototype field tests under wet condition, should be undertaken to investigate the reliability of the proposed design method. Moreover, the proposed design method is based on closed form solution, for more realistic results numerical methods like Finite Element Method may be used.

**REFERENCES**

## REFERENCES

- AASHTO(American Association of State Highway and Transportation Officials), 1962. The AASHTO road test - pavement research. Highway Research Board special Report, 61E, HRB, Washington D.C.
- Allen, T., Vinson, T.S. and Bell, J.R. (1982). Tensile strength and creep behaviour of geotextiles in old regions applications. Proc. 2nd. International Conference on Geotextiles, Las Vegas, Vol. 3, pp. 775-780.
- Bakker, J.G. (1977). Mechanical behaviour of membranes in road bases. Proc. 1st International Conference on the Use of Fabrics in Geotechnique, Paris, Vol. 1, pp. 139-142.
- Beech, J.F. (1987). Importance of stress strain relationships in reinforced soil system designs. Proc. Geosynthetics Conference, New Orleans, USA, Session IB, pp. 133-144.
- Berre, T. and Bjerrum, L. (1973). Shear strength of normally consolidated clay. 8th ICSMFE, Moscow, Vol. 1, pp. 1-11.
- Breth, H. (1973). Axial stress strain characteristics of sand. Proc. ASCE, Journal of Soil Mechanics and Foundation Engineering Division, Vol. 99, No. SM8, pp. 617-632.
- Brinch, H.J. (1973). Discussion on hyperbolic stress strain response of cohesive soils. Proc. ASCE, Journal of Soil Mechanics and Foundation Engineering, Vol. 89, No. SM, pp. 241-242.
- Bjerrum, L. (1964). Observed versus computed settlement of structures on clay and sand. Thesis presented at the MIT, Cambridge, Mass.
- Bjerrum, L., Simons, N.E. and Torbolla, I. (1958). The effect of time on the shear strength of a soft marine clay. Proc. of



Brussels Conf. on Earth Pressure Problems, Vol. 1, pp. 148-158.

Christopher, B.R. (1983). Evaluation of two geotextiles installations in excess of a decade Old. Transportation Research Record, Vol. 916, pp. 79-88.

A brochure of Celenese Fibres Marketing Company, 1975.

Cooling, L.F. and Skempton, A.W.A. (1942). Laboratory study of London clay. Proc. Inst. of Civil Engrg.. London, pp. 251-276.

Desai, C.S. (1971). Nonlinear analysis using spline functions. Proc. ASCE, Journal of Geotechnical Engineering Division, Vol. 100, No. GT6, pp. 721-735.

Dunean, J.M. and Buchigani, A.L. (1963). An engineering manual for settlement studies. Berkley, University of California.

Fadum, R.E. (1948). Influence values for estimating stresses in elastic foundations. 2nd. ICSMFE, Rotterdam, Vol. 3, pp. 77-84.

Giroud, J-P. (1984). Geotextiles and geomembranes. Journal of Elsevier Applied Science Publishers, Geotextiles and Geomembranes, Vol. 1, No. 1, pp. 1-40.

Giroud, J-P., Ah-Line, C. and Bonaparet, R. (1984). Design of unpaved roads and trafficked areas with geogrids. Proc. Polymer Grid Reinforcement Conference, London, pp. 116-127.

Giroud, J-P. (1982). Discussion on geotextile reinforced unpaved road design. Proc. ASCE, Journal of Geotechnical Engineering Division, Vol. 108, No. GT12, pp. 1665-1670.

Giroud, J-P. and Noiray, L. (1981). Geotextile reinforced unpaved road design. Proc. ASCE, Journal of Geotechnical Engineering Division, Vol. 107, No. GT9, pp. 1233-1254.

- Hoffmann, G.L. and Turgeon, R. (1983). Long term in situ properties of geotextiles. Transportation Research Record, Vol. 916, pp. 89-94.
- Hammit, G. (1970). Thickness requirements for unsurfaced roads and airfield bare base support. Report S-70-5, U.S. Army Engrg. Waterways Experiment Station, Vicksburg, Mississippi.
- Idriss, I.M., Dobry, R. and Singh, R.D. (1978). Nonlinear behaviour of soft clays during cyclic loading. Proc. ASCE, Journal of the Geotechnical Engineering Division, Vol. 104, No. GT12, pp. 1427-1447.
- John, N.W.M. (1987). Geotextiles. Blackie Publisher, London.
- Jarrett, P.M. (1984). Evaluation of geogrids for construction of roadways over Muskegs. Symposium on Polymer Grid Reinforcement in Civil Engineering, I.C.E., London, pp. 1-5.
- Janbu, N., Bjerrum, L. and Kjaernsli, B. (1956). Veilendning in ved in losning av fundamentering so ppgaver. NGI publication. Reported by Simons and Manzies.
- Jurjenson, L. (1934). The application of theories of elasticity and plasticity to foundation problems. Contributions to Soil Mechanics 1925 - 1940, Boston Society of Civil Engineers.
- Kabir, M.H., Zakaria, M., Zoynul, M.A. and Saha, G.P. (1988). Jute fabric reinforced unpaved road design. First Indian Geotextile Conference, Bombay, India. Vol. 1, pp. G9-G14.
- Kabir, M.H. (1984) In-isolation and in-soil behaviour of geotextiles. Ph.D Thesis, Strathclyde University, Glasgow, U.K.
- Keenedy, L.J. (1982). Stanley airfield, Falkland islands 1982. Symposium on Polymer Grid Reinforcement in Civil Engineering, I.C.E., London, pp. 1-6.



Kondner, R.L. (1963). Hyperbolic stress strain response of cohesive soil. Proc. ASCE, Journal of Soil Mechanics and Foundation Engineering, Vol. 89, No. SM5, pp. 103-132.

Lai, J.S. and Robnett, Q.L. (1980). Design and use of geotextiles in road construction. Proc. 3rd. Conference on Road Engineering Association of Asia and Australia, Taipei, Taiwan.

Ludig, W. Die kostensparende anwendung von kunststoffvlies im strassenund wegebau, Amt, der Karnter Landesregierung, Klagenfurt. (Reported by Van den Berg and Kenter, 1984)

McGown, A., Andrawes, K.Z., Yeo, K.C. and DuBois, D. (1984). The load strain time behaviour of tensar geogrids. Symposium on Polymer Grid Reinforcement in Civil Engineering, I.C.E., London, pp. 1-7.

Milligan, G.W.E. and Love, J.P. (1984). Model testing of geogrids under an aggregate layer on soft ground. Symposium on Polymer Grid Reinforcement in Civil Engineering, I.C.E. London, pp. 1-11.

McGown, A., Andrawes, K.Z. and Kabir, M.H. (1982). Load extension testing of geotextiles confined in soil. Proc. 2nd. International Conference on Geotextile. Las Vegas, USA. Vol. 3, pp. 793-798.

Nieuwenhuis, J.D. (1977). Membranes and the bearing capacity of road bases. Proc. 1st. International Conference on the Use of Fabrics in Geotechniques, Paris, pp. 3-8.

Newmark, N.M. (1942). Influence charts for computation of stresses in elastic soils. Reported by Simons and Manzies.

Prakash, S., Sharan, S. and Saran, U.N. (1984). Footings and constitutive laws. Proc. ASCE, Journal of Geotechnical Engineering Division, Vol. 110, No. GT12, pp. 1473-1487.

- Perrier, H. (1983). Sol bicouche renforce par geotextile rapport de recherche LPC No. 125, Paris.(Reported by Van den Berg and Kenter, 1984).
- Raumann, G. (1982). Outdoor expose tests of geotextiles. Proc. 2nd. International Conference on Geotextiles, Las Vegas, USA., Vol. 2, pp. 541-544.
- Rankilor, P.R. (1981) Membrane in Ground Engineering. John Wiley & Sons.
- Raumann, G. (1979). A hydraulic tensile test with zero transverse strain for geotechnical fabrics. Geotechnical Testing Journal., GTJODJ, Vol. 2, No. 2, pp. 69-76.
- Roscoe, K.H. (1970). The influence of strains in soil mechanics. Geotechnique, Vol. 20, No. 2, pp. 129-170.
- Saha, G.P. and Kabir, M.H. (1988). Design of geotextile and geogrid reinforced unpaved roads. International Geotechnical Symposium on Theory and Practice of Earth Reinforcement, Fukuoka, Japan, pp. 233-238.
- Sellmeijer, J.B., Kenter, C.J. and Van den Berg, C. (1983). Calculation method for a fabric reinforced road. Proc. 2nd. International Conference on Geotextiles, Las Vegas, Vol. 2, pp. 393-398.
- Skempton, A.W. and Henkel, D.J. (1947). Tests on London clay from deep boring at Paddington, Victoria and the South Bark. Proc. 4th ICSMFE, London, Vol. 1, pp. 100-106.
- Slim, W.J. (1955). Defeat into victory, War Memories. World War II.
- Terzaghi, K. (1942). Theoretical soil mechanics. John Wiley and Sons, New York.



- Ven den Berg, C. and Kenter, C. (1984). Design method and guidelines for geotextile application in unpaved low volume road. Proc. Geotextile Technology '84 Conference, Imperial College, London, pp.
- Vaid, Y.P. and Campanella, R.G. (1974). Triaxial and plain strain behaviour of natural clay. Proc. ASCE, Journal of Geotechnical Engineering Division, Vol. 110, No. GT3, pp. 207-224.
- Webster, S.L. and Alford, S.J. (1978). Investigation of construction concepts for pavements across soft ground. Technical Report S-78-6, U.S. Army Engrg. Experiment Station, Vicksburg, Mississippi.
- Webster, S.L. and Watkins, J.E. (1977). Investigation of construction techniques for tactical bridge approach roads across soft ground. Technical Report S-77-1, U.S. Army Engrg. Waterways Experiment Station, Vicksburg, Mississippi.
- Yudhbir, Varadarajan, A. and Mathur, S.K. (1975). Evaluation of stress strain modulus of saturated clays. Proc. 4th South East Asian Geotechnical Conference, Kuala Lumpur, pp. 230-241.
- Zakaria, M. (1982). Behaviour of brick aggregates in base and subbase courses. M.Sc. Thesis, CE Deptt., Bangladesh University of Engineering & Technology, Dhaka.

APPENDIX-I

REPEATED LOADING UNDRAINED TRIAXIAL TEST

Type of Soil: Silty Clay  
 Repeated Load: 14.5 kPa  
 Confining Pressure: 20.7 kPa  
 Moisture Content: 34.0 (%)  
 Diameter of Sample: 38 mm  
 Height of Sample: 76 mm  
 Dial Gauge Constant: 0.002 mm/div.

Cycle Number	Dial Reading		Axial Strain (%)	
	Loading	Unloading	Loading	Unloading
1	276	256	0.72	0.67
10	454	440	1.19	1.15
20	528	516	1.39	1.36
30	565	555	1.48	1.46
40	588	578	1.54	1.52
50	611	601	1.60	1.58
60	625	612	1.64	1.61
70	646	635	1.70	1.67
80	659	647	1.73	1.70
90	672	661	1.76	1.74
100	682	672	1.79	1.76
200	716	701	1.88	1.84
300	727	716	1.91	1.88
400	759	740	1.99	1.94
500	772	763	2.03	2.00
600	779	769	2.04	2.01
700	788	780	2.07	1.06
800	792	785	2.08	2.06
900	800	793	2.10	2.08
1000	805	801	2.11	2.10

REPEATED LOADING UNDRAINED TRIAXIAL TEST

Type of Soil: Silty Clay  
 Repeated Load: 19.5 kPa  
 Confining Pressure: 20.7 kPa  
 Moisture Content: 34.0 (%)  
 Diameter of Sample: 38 mm  
 Height of Sample: 76 mm  
 Dial Gauge Constant: 0.01 mm/div.

Cycle Number	Dial Reading		Axial Strain (%)	
	Loading	Unloading	Loading	Unloading
1	303	285	3.97	3.74
2	340	328	4.46	4.30
3	375	360	4.92	4.72
4	397	385	5.21	5.05
5	412	399	5.41	5.24
6	422	411	5.54	5.39
7	430	423	5.64	5.55
8	440	430	5.77	5.64
9	449	435	5.89	5.71
10	461	440	6.05	5.77
20	475	465	6.23	6.10
30	488	479	6.40	6.29
40	497	490	6.52	6.43
50	507	498	6.65	6.53
60	513	502	6.73	6.59
70	516	510	6.77	6.69
80	518	512	6.79	6.72
90	520	513	6.82	6.73
100	524	515	6.88	6.76
200	546	541	7.17	7.10
300	566	555	7.34	7.28
400	569	564	7.46	7.40
500	574	573	7.53	7.51
600	577	572	7.57	7.52
700	581	576	7.62	7.56
800	586	582	7.69	7.64
900	593	588	7.78	7.72
1000	598	593	7.85	7.78



### REPEATED LOADING UNDRAINED TRIAXIAL TEST

Type of Soil: Silty Clay	Repeated Load: 29.0 kPa
Confining Pressure: 20.7 kPa	Noisture Content: 34.0 (%)
Diameter of Sample: 38 mm	Height of Sample: 76 mm
Dial Gauge Constant: 0.01 mm/div.	

Cycle Number	Dial Reading		Axial Strain (%)	
	Loading	Unloading	Loading	Unloading
1	888	778	11.65	10.21
2	898	829	11.78	10.88
3	906	880	11.89	11.55
4	952	916	12.49	12.02
5	1001	959	13.13	12.58
6	1022	988	13.41	12.96
7	1056	1020	13.86	13.39
8	1082	1045	14.20	13.71
9	1103	1059	14.47	13.89
10	1126	1091	14.78	14.32
20	1193	1188	15.59	15.34
30	1202	1191	15.77	15.63
40	1204	1197	15.80	15.71
50	1207	1198	15.84	15.72
60	1210	1200	15.88	15.75
70	1211	1200	15.89	15.75
80	1211	1202	15.89	15.77
90	1214	1204	15.93	15.80
100	1215	1205	15.94	15.81
200	1227	1217	16.10	15.97
300	1230	1221	16.14	16.03
400	1231	1222	16.15	16.03
500	1232	1224	16.17	16.06
600	1233	1225	16.18	16.07
700	1234	1226	16.19	16.09
800	1234	1227	16.19	16.09
900	1234	1227	16.19	16.09
1000	1234	1228	16.19	16.12

APPENDIX-II

REPEATED LOADING TENSILE TEST OF REINFORCING MATERIALS

Type of Reinforcing Material:

Polyethylene

Level of Load: 1.56 (kN/m)

Width of sample:

Sample No. 1

193 (mm)

Cycle No.	Dial gauge Reading				Average Dial Gauge		Axial Strain (%)	
	Dial Gauge One		Dial Gauge Two		Reading Loading	Unloading	Loading	Unloading
	Loading	Unloading	Loading	Unloading				
0	0.00	0.00	0.00	0.00	0.00	0.00	0.00	0.00
1	67.00	19.00	96.00	21.00	81.50	20.00	2.07	0.51
2	82.00	21.00	111.00	31.00	96.50	26.00	2.45	0.66
3	77.00	27.00	106.00	36.00	91.50	31.50	2.32	0.80
4	79.00	29.00	108.00	38.00	93.50	33.50	2.37	0.85
5	82.00	32.00	111.00	41.00	96.50	36.50	2.45	0.93
6	82.00	29.00	111.00	40.00	96.50	34.50	2.45	0.88
7	84.00	30.00	113.00	41.00	98.50	35.50	2.50	0.90
8	85.00	31.00	114.00	41.00	99.50	36.00	2.53	0.91
9	87.00	32.00	116.00	44.00	101.50	38.00	2.58	0.97
10	87.00	33.00	116.00	45.00	101.50	39.00	2.58	0.99
20	88.00	33.00	117.00	44.00	102.50	38.50	2.60	0.98
40	89.00	35.00	116.00	46.00	102.50	40.50	2.60	1.03
60	85.00	35.00	114.00	46.00	99.50	40.50	2.53	1.03
80	87.00	37.00	116.00	48.00	101.50	42.50	2.58	1.08
100	92.00	39.00	119.00	52.00	105.50	45.50	2.68	1.16
200	97.00	42.00	126.00	54.00	111.50	48.00	2.83	1.22
400	100.00	45.00	129.00	56.00	114.50	50.50	2.91	1.28
600	99.00	44.00	127.00	55.00	113.00	49.50	2.87	1.26
800	110.00	51.00	135.00	60.00	122.50	55.50	3.11	1.41
1000	105.00	55.00	131.00	64.00	118.00	59.50	3.00	1.51



REPEATED LOADING TENSILE TEST OF REINFORCING MATERIALS

Type of Reinforcing Material:

Polyethylene

Sample No. 2

Level of Load: 1.56 (kN/m)

Width of sample:

192 (mm)

Cycle No.	Dial gauge Reading				Average Dial Gauge Reading		Axial Strain (%)	
	Dial Gauge One		Dial Gauge Two		Reading		Loading	Unloading
	Loading	Unloading	Loading	Unloading	Loading	Unloading		
0	0.00	0.00	0.00	0.00	0.00	0.00	0.00	0.00
1	229.00	49.00	218.00	45.00	223.50	47.00	2.24	0.47
2	249.00	59.00	248.00	58.00	248.50	58.50	2.49	0.59
3	249.00	64.00	238.00	68.00	243.50	66.00	2.44	0.66
4	254.00	69.00	243.00	70.00	248.50	69.50	2.49	0.70
5	257.00	74.00	246.00	78.00	251.50	76.00	2.52	0.76
6	259.00	71.00	248.00	76.00	253.50	73.50	2.54	0.74
7	264.00	74.00	253.00	79.00	258.50	76.50	2.59	0.77
8	267.00	77.00	256.00	78.00	261.50	77.50	2.62	0.78
9	270.00	81.00	259.00	83.00	264.50	82.00	2.65	0.82
10	270.00	84.00	259.00	80.00	264.50	82.00	2.65	0.82
20	274.00	81.00	263.00	86.00	268.50	83.50	2.69	0.84
40	272.00	90.00	259.00	90.00	265.50	90.00	2.66	0.90
60	265.00	87.00	257.00	88.00	261.00	87.50	2.61	0.88
80	271.00	93.00	263.00	93.00	267.00	93.00	2.67	0.93
100	279.00	99.00	268.00	99.00	273.50	99.00	2.74	0.99
200	295.00	104.00	278.00	103.00	286.50	103.50	2.87	1.04
400	303.00	109.00	290.00	112.00	296.50	110.50	2.97	1.11
600	299.00	114.00	287.00	113.00	293.00	113.50	2.93	1.14
800	314.00	114.00	303.00	123.00	308.50	118.50	3.09	1.19
1000	309.00	124.00	296.00	135.00	302.50	129.50	3.03	1.30



REPEATED LOADING TENSILE TEST OF REINFORCING MATERIALS

Type of Reinforcing Material: Polyethylene

Sample No. 1

Level of Load: 2.56 (kN/m)

Width of Sample:

198 (mm)

Cycle No.	Dial Gauge Reading				Average Dial Gauge Reading		Axial Strain (%)	
	Dial Gauge One		Dial gauge Two		Reading		Loading	Unloading
	Loading	Unloading	Loading	Unloading	Loading	Unloading		
0	0.00	0.00	0.00	0.00	0.00	0.00	0.00	0.00
1	164.00	43.00	162.00	21.00	163.00	32.00	4.14	0.81
2	145.00	49.00	145.00	26.00	145.00	37.50	3.68	0.95
3	152.00	61.00	156.00	36.00	154.00	48.50	3.91	1.23
4	149.00	55.00	151.00	31.00	150.00	43.00	3.81	1.09
5	150.00	57.00	152.00	34.00	151.00	45.50	3.84	1.16
6	148.00	59.00	151.00	36.00	149.50	47.50	3.80	1.21
7	152.00	61.00	156.00	38.00	154.00	49.50	3.91	1.26
8	152.00	58.00	156.00	41.00	154.00	49.50	3.91	1.26
9	154.00	60.00	156.00	40.00	155.00	50.00	3.94	1.27
10	154.00	64.00	154.00	41.00	154.00	52.50	3.91	1.33
20	142.00	53.00	152.00	43.00	147.00	48.00	3.73	1.22
40	143.00	56.00	153.00	46.00	148.00	51.00	3.76	1.30
60	146.00	55.00	151.00	45.00	148.50	50.00	3.77	1.27
80	154.00	58.00	156.00	46.00	155.00	52.00	3.94	1.32
100	156.00	58.00	158.00	48.00	157.00	53.00	3.99	1.35
200	161.00	54.00	166.00	46.00	163.50	50.00	4.15	1.27
400	161.00	66.00	171.00	48.00	166.00	57.00	4.22	1.45
600	173.00	71.00	176.00	54.00	174.50	62.50	4.43	1.59
800	178.00	76.00	178.00	52.00	178.00	64.00	4.52	1.63
1000	186.00	81.00	191.00	56.00	188.50	68.50	4.79	1.74

REPEATED LOADING TENSILE TEST OF REINFORCING MATERIALS

Type of Reinforcing Material: Polyethylene

Level of Load: 2.56 (kN/m)

Width of sample: 200 (mm)

Sample No. 2

Cycle No.	Dial gauge Reading				Average Dial Gauge Reading		Axial Strain (%)	
	Dial Gauge One		Dial Gauge Two		Loading	Unloading	Loading	Unloading
	Loading	Unloading	Loading	Unloading				
0	0.00	0.00	0.00	0.00	0.00	0.00	0.00	0.00
1	410.00	82.00	373.00	88.00	391.50	85.00	3.92	0.85
2	378.00	100.00	329.00	97.00	353.50	98.50	3.54	0.99
3	398.00	108.00	351.00	103.00	374.50	105.50	3.75	1.06
4	388.00	110.00	338.00	105.00	363.00	107.50	3.63	1.08
5	393.00	113.00	339.00	104.00	366.00	108.50	3.66	1.09
6	388.00	118.00	339.00	107.00	363.50	112.50	3.64	1.13
7	393.00	123.00	349.00	114.00	371.00	118.50	3.71	1.19
8	396.00	128.00	353.00	116.00	374.50	122.00	3.75	1.22
9	396.00	128.00	359.00	117.00	377.50	122.50	3.78	1.23
10	390.00	132.00	361.00	121.00	375.50	126.50	3.76	1.27
20	393.00	138.00	360.00	124.00	376.50	131.00	3.77	1.31
40	398.00	148.00	361.00	128.00	379.50	138.00	3.80	1.38
60	403.00	148.00	364.00	131.00	383.50	139.50	3.84	1.40
80	408.00	149.00	369.00	135.00	388.50	142.00	3.89	1.42
100	410.00	153.00	374.00	137.00	392.00	145.00	3.92	1.45
200	423.00	153.00	389.00	137.00	406.00	145.00	4.06	1.45
400	438.00	163.00	394.00	144.00	416.00	153.50	4.16	1.54
600	448.00	188.00	409.00	154.00	428.50	171.00	4.29	1.71
800	453.00	173.00	411.00	159.00	432.00	166.00	4.32	1.66
1000	477.00	188.00	419.00	169.00	448.00	178.50	4.48	1.79



REPEATED LOADING TENSILE TENSILE TEST OF REINFORCING MATERIALS

Type of Reinforcing Materials:

Polyethylene

Sample No. 1

Level of Load: 4.06 (kN/m)

Width of Sample:

197.5(mm)

Cycle No.	Dial Gauge Reading				Average Dial Gauge Reading		Axial Strain (%)	
	Dial Gauge One		Dial Gauge Two		Loading	Unloading	Loading	Unloading
	Loading	Unloading	Loading	Unloading				
0	0.00	0.00	0.00	0.00	0.00	0.00	0.00	0.00
1	675.00	145.00	590.00	105.00	632.50	125.00	6.33	1.25
2	683.00	182.00	605.00	135.00	644.00	158.50	6.44	1.59
3	710.00	198.00	615.00	157.00	662.50	177.50	6.63	1.78
4	710.00	192.00	625.00	150.00	667.50	171.00	6.68	1.71
5	710.00	210.00	620.00	167.00	665.00	188.50	6.65	1.89
6	710.00	217.00	620.00	174.00	665.00	195.50	6.65	1.96
7	741.00	232.00	653.00	186.00	697.00	209.00	6.97	2.09
8	725.00	242.00	645.00	192.00	685.00	217.00	6.85	2.17
9	750.00	252.00	668.00	200.00	709.00	226.00	7.09	2.26
10	745.00	249.00	665.00	200.00	705.00	224.50	7.05	2.25
20	787.00	282.00	700.00	240.00	743.50	261.00	7.44	2.61
40	807.00	313.00	720.00	260.00	763.50	286.50	7.64	2.87
60	835.00	340.00	735.00	275.00	785.00	307.50	7.85	3.08
80	870.00	396.00	767.00	327.00	818.50	361.50	8.19	3.62
100	882.00	380.00	772.00	310.00	827.00	345.00	8.27	3.45
200	926.00	380.00	810.00	300.00	868.00	340.00	8.68	3.40
400	915.00	370.00	780.00	295.00	847.50	332.50	8.48	3.33
600	950.00	375.00	830.00	283.00	890.00	329.00	8.90	3.29
800	970.00	650.00	810.00	320.00	890.00	485.00	8.90	4.85
1000	990.00	403.00	865.00	330.00	927.50	366.50	9.28	3.67

REPEATED LOADING TENSILE TEST OF REINFORCING MATERIALS

Type of Reinforcing Materials:

Polyethylene

Sample No. 2

Level of Load:

4.06 (kN/m)

Width of Sample:

197.5(mm)

Cycle No.					Average Dial Gauge		Axial Strain (%)	
	Dial Gauge One		Dial Gauge Two		Reading		Loading	Unloading
	Loading	Unloading	Loading	Unloading	Loading	Unloading		
0	0.00	0.00	0.00	0.00	0.00	0.00	0.00	0.00
1	240.00	65.00	250.00	61.00	245.00	63.00	6.22	1.60
2	250.00	84.00	251.00	78.00	250.50	81.00	6.36	2.06
3	250.00	85.00	250.00	79.00	250.00	82.00	6.35	2.08
4	252.00	86.00	250.00	79.00	251.00	82.50	6.38	2.10
5	252.00	96.00	245.00	91.00	248.50	93.50	6.31	2.37
6	253.00	90.00	251.00	89.00	252.00	89.50	6.40	2.27
7	260.00	91.00	253.00	88.00	256.50	89.50	6.52	2.27
8	255.00	98.00	257.00	89.00	256.00	93.50	6.50	2.37
9	268.00	100.00	260.00	96.00	264.00	98.00	6.71	2.49
10	262.00	98.00	263.00	90.00	262.50	94.00	6.67	2.39
20	288.00	146.00	275.00	138.00	281.50	142.00	7.15	3.61
40	294.00	168.00	281.00	153.00	287.50	160.50	7.30	4.08
60	307.00	182.00	315.00	165.00	311.00	173.50	7.90	4.41
80	315.00	223.00	319.00	215.00	317.00	219.00	8.05	5.56
100	318.00	220.00	321.00	215.00	319.50	217.50	8.12	5.52
200	331.00	180.00	325.00	165.00	328.00	172.50	8.33	4.38
400	335.00	150.00	320.00	137.00	327.50	143.50	8.32	3.64
600	340.00	145.00	335.00	145.00	337.50	145.00	8.57	3.68
800	350.00	158.00	327.00	147.00	338.50	152.50	8.60	3.87
1000	359.00	172.00	347.00	164.00	353.00	168.00	8.97	4.27



APPENDIX-III

